PHARMACOLOGICAL AND BIOCHEMICAL STUDIES ON THE CONTRIBUTION OF NADPH OXIDASE TO OXIDATIVE STRESS IN THE AORTA OF SPONTANEOUSLY HYPERTENSIVE RATS

Dissertation
zur
Erlangung des Doktorgrades
der Naturwissenschaften
(Dr. rer. nat.)

dem

Fachbereich Pharmazie
der Philipps-Universität Marburg
vorgelegt von
Sven Wind
aus Dillenburg

Marburg/Lahn 2006

Vom
Fachbereich Pharmazie
der Philipps-Universität Marburg als Dissertation

am _____angenommen.

Erstgutachter: Prof. Dr. Harald H. H. W. Schmidt

Zweitgutachter: Prof. Dr. Dr. Josef Krieglstein

Tag der mündlichen Prüfung: _____

für Alexandra

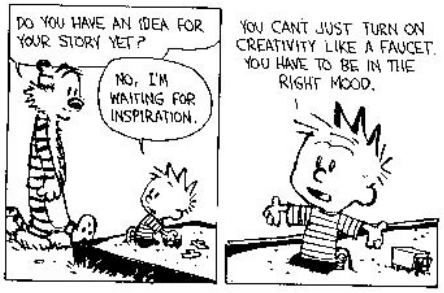

CONTENT

ABBREVIATIONS

ACh	Acetylcholine
AEBSF	4-(2-Aminoethyl)-benzenesulfonyl fluoride
ANOVA	Analysis of variance
Apocynin	4'-Hydroxy-3'-methoxyacetophenone
APS	Ammonium peroxodisulfate
BH_4	Tetrahydrobiopterine
BSA	Bovine serum albumine
CAT	Catalase
cDNA	Complementary desoxyribonucleic acid
cGMP	Cyclic guanosine monophosphate
CRC	Concentration response curve
DHE	Dihydroethidium
DM	Diabetes mellitus
DMSO	Dimethyl sulfoxide
DNA	Desoxyribonucleic acid
DPI	Diphenylene iodonium
ds	Docking sequence
Duox	Dual oxidase
e.g.	For example, *abbr. of latin 'exempli gratia'*
EC	Endothelial cells
ECL	Enhanced chemiluminescence
EDRF	Endothelium-derived relaxing factor
EDTA	Ethylenediamintetraacetic acid
E_{max}	Maximal efficacy
eNOS	Endothelial nitric oxide synthase
FAD	flavin adenine dinucleotide
FMN	Flavin mononucleotide
$gp91^{phox}$	Glycoprotein running in SDS pages at 91 kD (former synonyme for Nox2)
GSH	Glutathione

H_2O_2	hydrogen peroxide
HEPES	4-(2-hydroxyethyl)-1-piperazineethansulfonic acid
HIV	Human immunodeficiency virus
HL60	Human promyelocytic leukemia cell line
HUVEC	Human umbilical vein endothelial cells
IC_{50}	Half-maximal inhibitory concentration
IF	Immunofluorescence
IL-β	Interleukin-β
kb	Kilobase
kD	Kilodalton
L-NAME	NG-nitro-L-arginine methyl ester
Lucigenin	N,N-dimethyl-9,9-biacridinium dinitrate
MALDI-TOF	Matrix-assisted laser desorption/ionization – time of flight
mM	Millimolar
mRNA	Messenger ribonucleic acid
NADPH	Nicotineamide adenine dinucleotide phosphate
NO	Nitric oxide
NOS	Nitric oxide synthase
Nox	Catalytic subunit of the NADPH oxidase complex
O_2^-	Superoxide
$ONOO^-$	Peroxynitrite
oxLDL	Oxidized low density lipoprotein
PAGE	Polyacrylamide gel electrophoresis
PAO	Phenylarsine oxide
PDGF	Platelet-derived growth factor
PE	Phenylephrine
PEG-SOD	Polyethylene-glycol SOD
phox	Phagocytic oxidase
PKC	Protein kinase C
PMA	Phorbol-myristate-acetate
PMSF	Phenylmethylsulfonylfluoride
PNGase F	Peptide-N-glycosidase F

RECA-1	Rat endothelial cell antibody
ROS	Reactive oxygen species
RT	Room temperature
RT-PCR	Reverse transcriptase polymerase chain reaction
SDS	Sodium dodecyl sulfate
SEM	Standard error of mean
SHR	Spontaneously hypertensive rats
SHR-SP	SHR stroke prone rats
SOD	Superoxide dismutase
TEMED	N,N,N,N-Tetramethyl-ethylendiamine
Tempol	4-hydroxy-2,2,6,6-tetramethylpiperidinoxyl
Tiron	4,5-Dihydroxy-1,3-benzene-disulfonic acid
TNF-α	Tumor necrosis factor α
Tris	2-Amino-2-hydroxymethyl-1,3-propanediol
VAS2870	3-Benzyl-7-(2-benzoxazolyl)thio-1,2,3-triazolo[4,5-d]pyrimidine
VSMC	Vascular smooth muscle cell
WKY	Wistar rats from the Kyoto school of medicine
XDH	Xanthine dehydrogenase
XOD	Xanthine oxidase
µM	Micromolar

1 INTRODUCTION

Vascular oxidative stress is accompanied by an endothelium-dependent dysfunction. Reactive oxygen species (ROS) are described as proatherogenic stimuli which mediate angiogenesis, inflammation and vascular smooth muscle cell (VSMC) proliferation. In addition, inactivation of nitric oxide (NO) by superoxide (O_2^-) and other ROS appears to be a fundamental event occuring under conditions such as diabetes mellitus, hypercholesterolemia, cigarette smoking or arterial hypertension - common risk factors for cardiovascular diseases. Xanthine oxidase (XOD), uncoupled endothelial nitric oxide synthase (eNOS) and NADPH oxidases are described as relevant origins of oxidative stress in the vasculature. The vascular NADPH oxidase complex contains one of three different catalytic subunits termed Nox1, Nox2 and Nox4, and has been recently suggested as being the major source of ROS in blood vessels. Nevertheless, the relative contribution of both the Nox isoforms as well as the other above mentioned sources of ROS to oxidative stress still remains to be determined. Therefore, keeping this in mind, one major aim of the present work was to investigate the activity of XOD, eNOS and NADPH oxidases as well as the expression of Nox1, Nox2 and Nox4 in the aorta of 12-14 month old spontaneously hypertensive rats (SHR) which exhibit increased oxidative stress in comparison to age-matched normotensive Wistar Kyoto rats (WKY). Based on the findings evaluated in this model and taking into account that the modulation of vascular NADPH oxidases promises to have therapeutic potential in the treatment of oxidative stress-related vascular diseases, the present study also focussed on the investigation of the novel NAPDH oxidase inhibitor VAS2870 (3-Benzyl-7-(2-benzoxazolyl)thio-1,2,3-triazolo[4,5-d]pyrimidine) on aortic ROS formation and endothelium-dependent relaxation in SHR.

2 SCIENTIFIC BACKGROUND

2.1 Oxidative stress and the biology of reactive oxygen species

Oxygen metabolism, although essential for life, imposes a potential threat to cells because of the formation of ROS, such as O_2^-, hydrogen peroxide (H_2O_2), hydroxyl radicals and a variety of other reaction products (Fridovich, 1998). ROS can oxidize biological macromolecules such as DNA, proteins, lipids and carbohydrates. To avoid this damage, organisms developed antioxidant defense systems consisting of ROS catabolizing enzymes and antioxidants, such as ascorbate and the tocopherols. Oxidative stress can therefore be defined as the pathogenic outcome of an oxidant production that overwhelms the endogenous antioxidant defense system. This condition has been linked to the origin and progression of chronic degenerative diseases (e.g. cancer, diabetes, atherosclerosis as well as neurodegenerative diseases like Alzheimer's and Parkinsons's disease) (Droge, 2002). Nevertheless, when studying oxidative stress, one should keep in mind that ROS are not solely harmful and are accidentally generated as a consequence of an aerobic lifestyle. Organisms deliberately produce ROS for host defense. Furthermore, moderate physiological concentrations of ROS are implicated in signal transduction of biological processes including cell growth, apoptosis and cell migration (Taniyama & Griendling, 2003). This suggests that normal cellular homeostasis is an outcome of a delicate balance between the rate of ROS formation and elimination.

Reduction of oxygen by one electron leads to the formation of O_2^-, a process that is mediated by a variety of enzyme systems such as the mitochondrial respiratory chain, cytochrome P_{450} monoxygenases, lipoxygenases, xanthine oxidases and NADPH oxidases. O_2^- itself exerts effects in biological tissues and is also pivotal in generating other ROS. It reacts readily with NO to form peroxynitrite ($ONOO^-$), which is a strong oxidant and nitrating agent (Ischiropoulos et al., 1992). Under physiological conditions, superoxide dismutase (SOD) minimizes this reaction by converting O_2^- enzymatically into a more stable compound, H_2O_2. The importance of SODs in antioxidant

defense is illustrated by a study in SOD2-deficient mice, which developed cardiomyopathy and neurodegeneration (Melov et al., 2001). However, while H_2O_2, which diffuses through cell membranes (Krotz et al., 2004) is assumed to be involved in intracellular signaling pathways, at higher concentrations it is found to be toxic (Rhee, 2006) and can react with reduced transition metals to form the highly reactive hydroxyl radical. Thus, enzymatic defense against H_2O_2 provided by catalase and glutathione peroxidase which convert H_2O_2 into water is crucial. In phagocytes, myeloperoxidase converts H_2O_2 into the very reactive hypochlorous acid (HOCl). **Figure 2.1** shows an overview of ROS production and their removal as it occurs in biological systems.

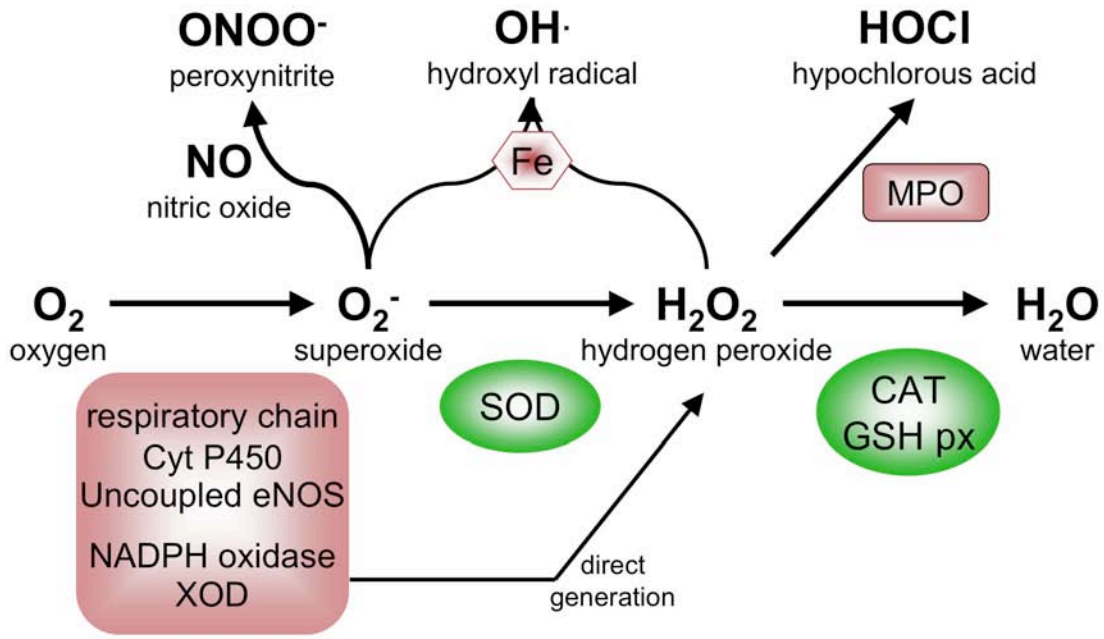

Figure 2.1: Production and clearance of reactive oxygen species. XOD= xanthine oxidase, eNOS = endothelial nitric oxide synthse, SOD = superoxide dismutase, CAT = catalase, GSH px = glutathione peroxidase, MPO = myeloperoxidase, Fe = iron / transition metals.

2.2 Effects of ROS in the vasculature

Virtually all types of vascular cells produce O_2^- and H_2O_2. ROS have distinct functional effects on each vascular cell type and can play both physiological and pathophysiological roles. In endothelial cells, ROS have been shown to induce signaling processes like apoptosis, expression of adhesion molecules and angiogenesis (Taniyama & Griendling, 2003). In smooth muscle cells and fibroblasts, promotion of proliferation and migration are mediated by ROS (Rey & Pagano, 2002). All these processes are fundamental in the homeostasis of the vasculature, but oxidative stress followed by an overstimulation of the pathways leads to events such as inflammation, hypertrophy, remodeling and angiogenesis, which are hallmarks of many cardiovascular diseases.

Moreover, increased production and release of ROS is considered to be the key event in the pathogenesis of endothelial dysfunction. The endothelium-derived relaxing factor (EDRF) NO plays an essential vasoprotective role by dilating blood vessels, preventing thrombus formation, reducing endothelial cell permeability and, in the long run, reducing vascular smooth muscle cell proliferation (Schmidt & Walter, 1994). The term endothelial dysfunction has been used to refer to several pathological conditions which are caused by a decline in the bioavailability of NO (Kojda & Harrison, 1999). This pathophysiological state is characterized by the impairment of the protective functions of NO leading to a loss of vasodilation, platelet aggregation, inflammation, smooth muscle cell growth and remodeling (Cai & Harrison, 2000). A loss of the NO bioavailability may be caused either by a decreased expression of eNOS (Wilcox et al., 1997), a lack of substrate or cofactors for eNOS (Pou et al., 1992) or accelerated NO scavenging by ROS (Harrison, 1997). Gryglewski et al. (Gryglewski et al., 1986) discovered that O_2^- inactivates and SOD stabilizes EDRF, even before it was known to be NO. The second order rate constant of the reaction between O_2^- and NO was found to be 6.7×10^9 $M^{-1} \bullet s^{-1}$ (Thomson et al., 1995) which is three times faster than the reaction of O_2^- with SOD (2.9×10^9 $M^{-1} \bullet s^{-1}$) and nearly thirty times faster than the reaction of NO with heme proteins (Fridovich, 1998). Given this

rapid reaction rate, there is probably some O_2^- reacting with NO at any given time within the cells suggesting a tenuous balance between these molecules which is disturbed under pathological conditions (Cai & Harrison, 2000). Apart from superoxide, lipid radicals can also react with NO (O'Donnell & Freeman, 2001), and a recent study reported that hydroxyl radicals may react with NO, too (Pieper et al., 1997).

2.3 Sources of ROS in the vasculature

The potential enzymatic sources of ROS in the vasculature include mitochondrial respiration, lipoxygenases, cyclooxygenases, heme oxygenases, cytochrome P_{450} monoxygenases, peroxidases, NO synthases, xanthine oxidases and NADPH oxidases. However, considerable attention particularly with regard to oxidative stress was paid to XOD, endothelial NOS and NADPH oxidases (Cai & Harrison, 2000; Jiang et al., 2004).

2.3.1 Xanthine oxidase

Xanthine oxidoreductase is generally recognized as the terminal enzyme of purine catabolism in humans. This molybdoflavoenzyme, which catalyzes the oxidation of hypoxanthine and xanthine, exists in two interconvertible forms, xanthine dehydrogenase (XDH) and XOD (for a review, see Harrison (2002)). XOD is formed by reversible thiol oxidation or irreversible proteolytic cleavage of XDH which predominates in vivo (XDH: approx. 80%, XOD: approx. 20%) (Parks et al., 1988; Frederiks & Bosch, 1996). While XDH preferentially reduces NAD^+, XOD is not able to reduce NAD^+ but prefers molecular oxygen as its substrate leading to the generation of O_2^- and H_2O_2 (Cai & Harrison, 2000). A pathological role of XOD-derived ROS was first proposed by Granger and colleagues suggesting XOD as the key enzyme responsible for oxidative stress following ischemia reperfusion injury (Granger et al., 1981; McCord, 1985). Furthermore, several studies have thereafter reported the involvement of XOD-derived oxidative stress in diminishing NO bioavailability

under conditions such as hypertension (Nakazono et al., 1991; Miyamoto et al., 1996) and hypercholesterolemia (White et al., 1996; Cardillo et al., 1997). Most studies investigating the role of XOD in oxidative stress are based upon oxypurinol as well as allopurinol, which inhibit xanthine oxidoreductase by targeting the molybdenum site of the enzyme. However, studies using high concentrations of these inhibitors should be interpreted with caution, because allopurinol and oxypurinol have been described to possess free radical-scavenging properties in concentrations higher than 500 µM (Moorhouse et al., 1987). Due to the unavailability of a specific antibody for XOD (Cai & Harrison, 2000), its role in vascular oxidative stress is superficial and awaits further clarification.

2.3.2 Endothelial NO synthase

Endogenous NO is produced by NOS. There are three different NOS isoforms, namely endothelial NOS (eNOS, NOSIII), which is the predominant isoform in the vasculature, inducible NOS (iNOS, NOSII) and neuronal NOS (nNOS, NOSI). All NOS homologues form homodimers in which the two monomers are linked by a single zinc thiolate cluster. The monomer contains two functionally different domains: An N-terminal oxygenase where heme, tetrahydrobiopterin (BH_4) and L-arginine bind and a C-terminal reductase comprising binding sites for FMN, FAD and NADPH. Both domains are linked by a calmodulin binding site. Ca^{2+}-induced calmodulin binding enables electron transfer from NADPH via the flavins to the heme centre for oxidation of the substrate L-arginine. Binding of BH_4 close to the heme group is required for the transfer of the electrons to the guanidine nitrogen of L-arginine to form NO and L-citrulline (for a review, see Alderton et al. (2001); Bruckdorfer (2005)). Under certain conditions NOS becomes uncoupled and produces O_2^- and H_2O_2 instead of NO (Pou et al., 1992). This can occur, if concentrations of either L-arginine or the essential co-factor BH_4 are low or if the zinc thiolate complex is disrupted (for a review, see Förstermann (2006)). Oxidative stress is suggested to lead to eNOS uncoupling (Laursen et al., 2001; Landmesser et al., 2003). The hypothesis that BH_4 is depleted under conditions of

oxidative stress is founded by the observations that administration of BH_4 restores endothelial dysfunction (Cosentino & Luscher, 1998) and that peroxynitrite is able to oxidize BH_4 (Milstien & Katusic, 1999). Recently, Zou and colleagues (2002) have pointed out an alternative concept by showing that much lower levels of peroxynitrite than necessary for BH_4 oxidation lead to a disruption of the zinc thiolate cluster of the enzyme. Nevertheless, these studies suggest that uncoupled eNOS is relevant in amplifying ROS generation. Inhibition of NOS in its functional as well as unfunctional/uncoupled state can be achieved by using the L-arginine analogue L-NAME.

2.3.3 NADPH oxidases

NADPH oxidases are thought to be the predominant source of ROS in the vasculature (Griendling et al., 2000). Intriguingly, NADPH oxidases appear to be the only dedicated ROS forming enzymes, whereas ROS generation by XOD, eNOS or mitochondria appears to occur accidentally. The sole purpose of NADPH oxidases is the formation of ROS and that favours these enzymes as outstanding targets for the treatment of oxidative stress. Therefore, their structure, activation and pharmacology will be discussed in more detail in chapter 2.4.

2.3.4 The “kindling bonfire” hypothesis

Many studies support a critical role of the above-mentioned enzymes in the pathology of vascular diseases. Their individual contribution to oxidative stress appears to be dependent on the cellular and subcellular circumstances as well as the environment (e.g. eNOS uncoupling occurs if BH_4 levels are low) (Jiang et al., 2004). An interesting hypothesis is that NADPH oxidases initiate oxidative stress at early stages of vascular diseases and then trigger themselves (Li et al., 2001) as well as other ROS sources leading to progressed oxidative stress and endothelial dysfunction (Landmesser et al., 2003). Accordingly, NADPH oxidases, XOD and uncoupled eNOS appear to

be in a substantial interplay with each other leading to feed forward processes and augmented ROS generation (Mueller et al., 2005). The relative contribution of these sources of ROS to oxidative stress therefore seems to be dependent on the disease state and remains to be defined in the pathogenesis of vascular diseases. **Figure 2.2** shows an overview of the correlations between vascular diseases, ROS sources, oxidative stress and endothelial dysfunction.

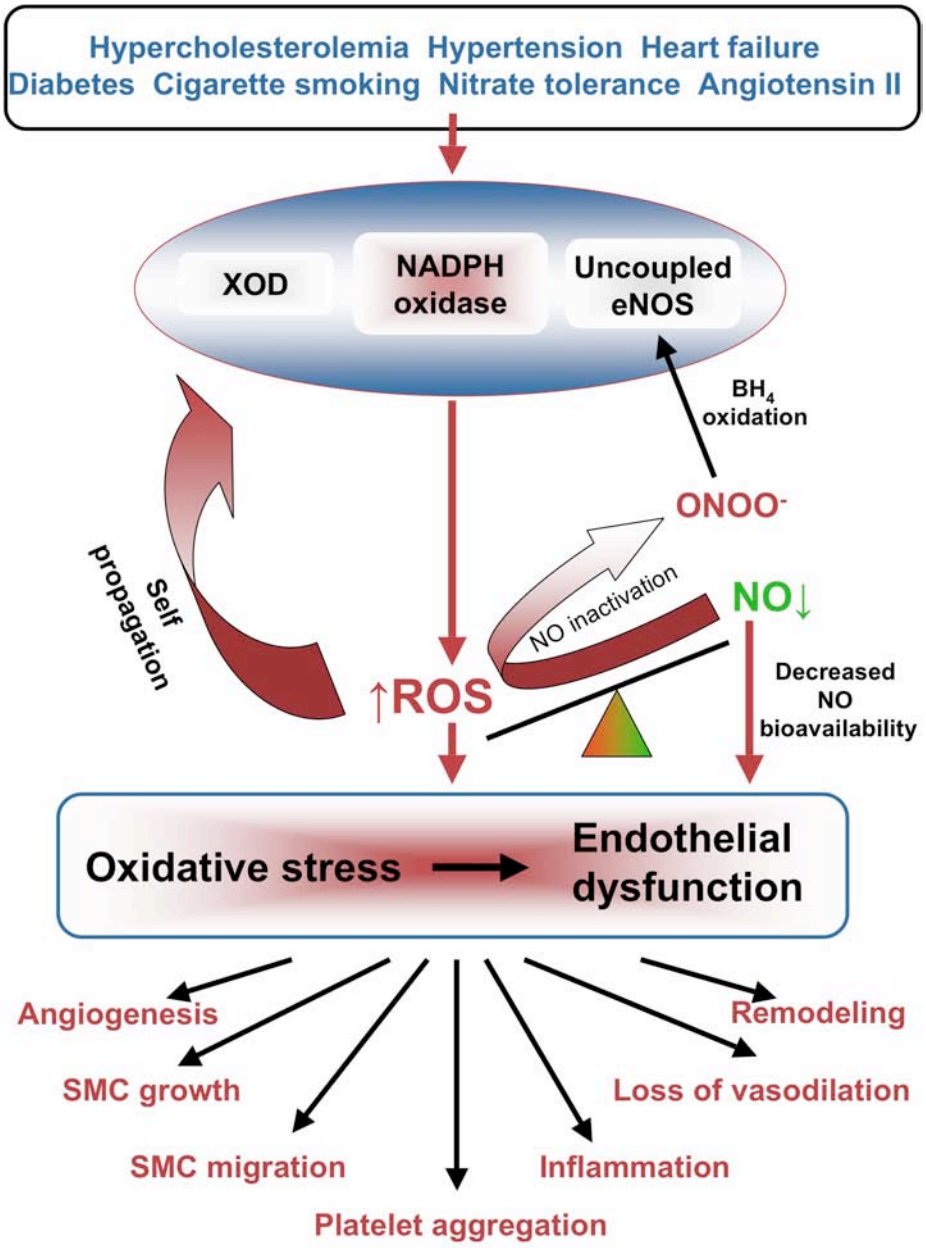

Figure 2.2: Oxidative stress and endothelial dysfunction in cardiovascular diseases. (Modified after Cai & Harrison (2000))

2.4 NADPH oxidases

2.4.1 Structure

NADPH oxidases are a group of membrane-associated enzymes that are expressed in various cells of mesodermal origin. The structure and function of NADPH oxidases are well characterized in phagocytic cells (neutrophils, macrophages and eosinophils) where these multimeric protein complexes produce large amounts of O_2^- (termed as *oxidative* or *respiratory burst*) for host defense (for a review, see Babior (1999); Vignais (2002); Groemping & Rittinger (2005)). NADPH oxidases generate O_2^- by catalyzing the one electron reduction of oxygen according to the following equation:

$$NADPH + 2\ O_2 \rightarrow 2\ O_2^- + NADP^+ + H^+$$

The leucocyte NADPH oxidase consists of two membrane components, a small α-subunit, $p22^{phox}$, and a larger catalytic β-subunit, $gp91^{phox}$ (termed Nox2 according to the new nomenclature and, will therefore be referred to as Nox2 in the following chapters). Nox2 is a highly glycosylated protein that has a molecular weight of 65.3 kD, but runs as a broad smear around 91 kD on SDS-PAGE gels. It possesses six transmembrane α-helices and contains binding sites for NADPH, molecular oxygen as well as flavin and heme groups to allow electron transport from NADPH to O_2. The small subunit $p22^{phox}$ associates with Nox2 in a 1:1 complex and contributes to its maturation and stabilization. These two components comprise the cytochrome b_{558} complex (heme absorbance peak at 558 nm in the reduced state). Furthermore, the complex contains four cytoplasmic subunits: $p47^{phox}$, $p67^{phox}$, $p40^{phox}$ and the guanine nucleotide-binding protein Rac1 or 2, which upon stimulation translocates to cytochrome b_{558}. This assembly is required for activation of the oxidase and facilitates electron transfer from NADPH to oxygen (see **Figure 2.3**)

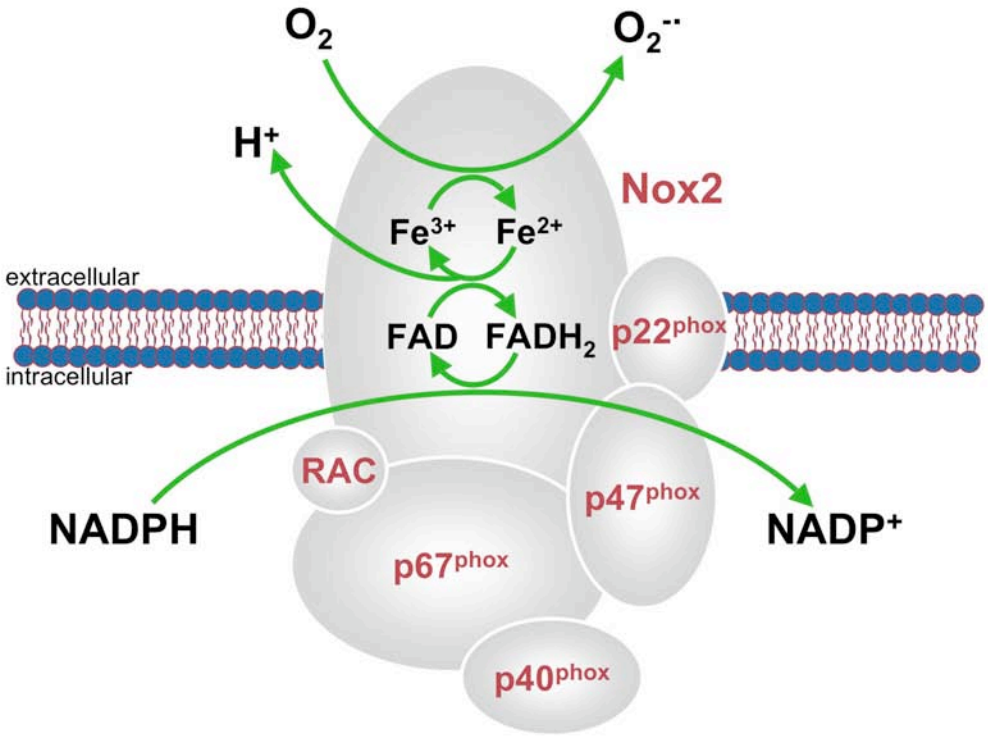

Figure 2.3: Assembly of the phagocytic NADPH oxidase (modified after Jiang et al. (2004))

Recently, homologues of the catalytic subunit Nox2 have been discovered. Starting with Nox1 (Suh et al., 1999) this new enzyme family has to date seven members, which are structured into three groups according to the presence of specific domains (Lambeth, 2002). The first group includes Nox1, primarily expressed in colon epithelial cells (Suh et al., 1999), Nox2, the isoform of the leucocytic oxidase, Nox3, found in the inner ear and required for otoconia formation (Paffenholz et al., 2004) and finally Nox4, first described as Renox due to its prominant expression in the kidney (Geiszt et al., 2000). In contrast to this group of Nox2 homologues, which are calcium-independent, Nox5 contains EF-hand calcium binding motifs and is activated by increased calcium levels. This isoform is essentially found in lymphoid tissues and testis (Banfi et al., 2001). The third group of homologues – Duox1 and 2 - further extends the Nox5 structure by a peroxidase homology domain (De Deken et al., 2000). Both enzymes are expressed in the thyroid gland and are involved in thyroid hormone synthesis (Moreno et al., 2002).

Transmembrane topologies and domain structures for the Nox family are shown in **Figure 2.4**.

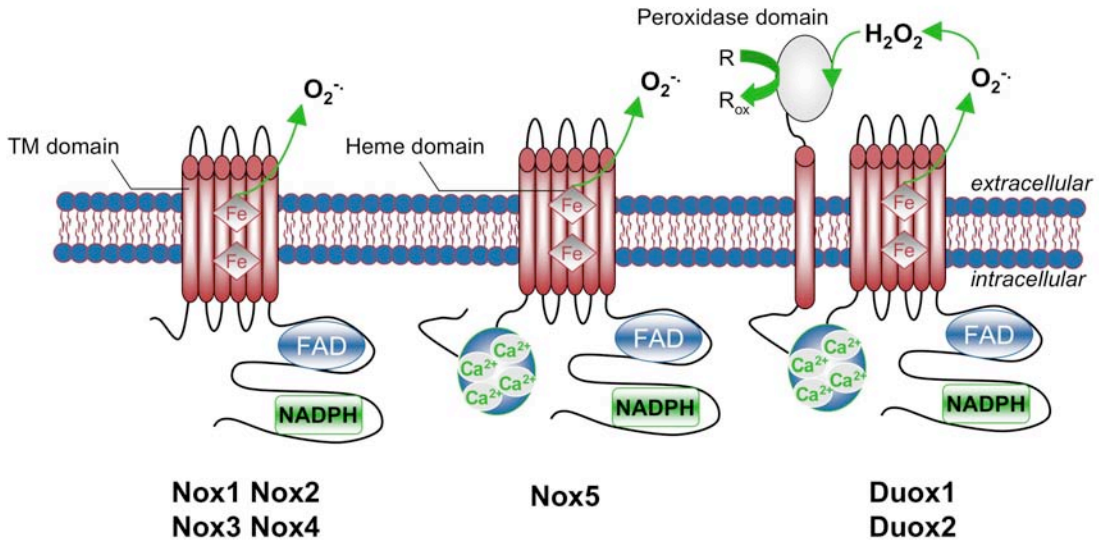

Figure 2.4: Transmembrane topology and domain structure of Nox family members. All homologues are predicted to form six transmembrane domains. This region also contains five conserved histidine residues providing binding sites for two heme goups. The carboxy-terminal part of the molecule contains a FAD as well as a NADPH binding domain. Nox5 and the Duox group have a cytosolic calcium binding EF hand. In addition, the Duox enzymes possess a further transmembrane domain followed by an extracellularly located peroxidase domain, which can use ROS produced by the catalytic core domains to oxidize extracellular substrates (R). (modified after Lambeth (2004))

Homologues of two cytosolic subunits have also been discovered: NoxO1 (O for organizer) is a homologue of $p47^{phox}$, and NoxA1 (A for activator) shares considerable similarity with $p67^{phox}$. Both subunits were recently cloned from colon epithelial cells and seem to be required for Nox1 activity (Banfi et al., 2003). Activation of Nox2 and Nox3 by the new cytosolic homologues has also been demonstrated (Cheng et al., 2004).

2.4.2 Expression of subunits in the vasculature

Vascular NADPH oxidases contain Nox1, Nox2 or Nox4 as catalytic subunit. In humans, Nox5 has also been found in vessels (Lassegue & Clempus, 2003), but this isoform is not present in the vasculature of rodents (Maru et al., 2005; Gavazzi et al., 2006). The expression profile of these Nox homologues varies in the vascular layers. Nox1 is expressed in low amounts in VSMC where its activity and expression can be stimulated by mitogenic substances such as angiotensin II and platelet-derived growth factor (PDGF) (Lassegue et al., 2001). Nox2 is present in endothelial cells (EC) (Meyer et al., 1999) and fibroblasts (Rey & Pagano, 2002) and seems to be expressed in VSMC of resistance arteries but not conduit vessels (Lassegue et al., 2001; Kalinina et al., 2002). In contrast to the relatively low levels of Nox1 and Nox2, Nox4 is abundantly expressed in all vascular cells (Sorescu et al., 2002; Ago et al., 2004; Brandes & Kreuzer, 2005). The small subunit $p22^{phox}$ is expressed in all layers of the vascular wall (Brandes & Kreuzer, 2005). Since it has been shown that this subunit stabilizes the Nox isoforms (Ambasta et al., 2004) and is important for the function of Nox1-4-based NADPH oxidases (Kawahara et al., 2005), such an abundant expression of p22phox is expected.

The cytosolic component $p47^{phox}$ has been detected in all vascular layers of conduit as well as resistance vessels and in vascular cell cultures, too (Lassegue & Clempus, 2003). In contrast, $p67^{phox}$ has only been found in the endothelium and adventitia (Jones et al., 1996; Pagano et al., 1998), but not in aortic smooth muscle cells (Patterson et al., 1999). Interestingly, $p67^{phox}$ similar to Nox2 has also been detected in VSMC of human resistance arteries (Touyz et al., 2002). The precise role of the new homologues NoxO1 and NoxA1 in the vasculature still remains to be determined. Recently, the expression of NoxA1 has been shown in VSMC of mouse carotid artery indicating that it replaces $p67^{phox}$ in the media of large vessels (Brandes & Kreuzer, 2005; Ambasta et al., 2006). Finally, Rac1 has been shown to be expressed in all vascular cells (Lassegue & Clempus, 2003).

2.4.3 Activation of the phagocytic NADPH oxidase

The process of NADPH oxidase activation has been well characterized in leucocytes. In the resting state, the subunits $p47^{phox}$, $p67^{phox}$ and $p40^{phox}$ are located in the cytosol and interact with each other in a trimeric (1:1:1) complex (Vignais, 2002). During this stage, $p47^{phox}$ is in an auto-inhibited conformation where two SH3 domains bind via an intramolecular interaction to a polybasic region (Groemping et al., 2003). Upon activation, $p47^{phox}$ becomes highly phosphorylated. This is required to abolish the auto-inhibition and allows its translocation to cytochrome b_{558} (Ago et al., 2003). Thereby $p47^{phox}$ organizes the assembly of the (p47-p67-$p40^{phox}$) triade to the membrane and docks via its SH3 domains to $p22^{phox}$ (Groemping et al., 2003). In addition, three interaction sites are reported between $p47^{phox}$ and Nox2 (DeLeo et al., 1995). The docking of $p47^{phox}$ to cytochrome b_{558} also facilitates the interaction between $p67^{phox}$ and Nox2 which is required for the activation of the catalytic subunit (Han et al., 1998). Another critical step in the activation process is the translocation of the activated GTPase Rac to cytochrome b_{558}. This binding is independent of $p47^{phox}$ since Rac-GTP anchors itself in the membrane via its prenylated tail (Brandes & Kreuzer, 2005). Finally, previous findings suggest that the presence of free fatty acids is required for the formation of the complex, at least under *in vivo* conditions (Dana et al., 1998).

Various stimulators can be used to target the phagocytic NADPH oxidase. Phorbol-myristate-acetate (PMA) activates protein kinase C (PKC), which phosphorylates $p47^{phox}$ and thereby induces a strong long-lasting oxidative burst. Other agonists of the phagocytic NADPH oxidase are opsonized zymosan and the chemoattractant formyl-methionyl-leucyl-phenylalanine. All these substances finally lead to the phosphorylation of $p47^{phox}$, activation of Rac and release of free fatty acids - the molecular triggers for the NADPH oxidase-derived oxidative burst (Lambeth, 2004).

2.4.4 Activation of vascular NADPH oxidases

The exact composition and assembly of vascular NADPH oxidases is poorly understood. While it is assumed that vascular Nox2 based oxidases follow a similar assembly mechanism as demonstrated for phagocytes, it has been shown that Nox1 activation requires NoxO1 and NoxA1. In contrast, Nox4 activity appears to be independent of the known cytosolic subunits.

In contrast to phagocytic cells, vascular cells exhibit a constitutively active oxidase which generates low amounts of ROS; the rate of O_2^- is thought to be 1-10% of that in leucocytes (Lassegue & Clempus, 2003). In line with this, a preassembled oxidase was found in endothelial cells, consisting of Nox2, $p22^{phox}$, $p47^{phox}$ and $p67^{phox}$ (Li & Shah, 2002). A constitutive activity is also suggested for Nox4 which was shown to produce ROS if coexpressed with $p22^{phox}$, however the cytosolic subunits $p47^{phox}$ and $p67^{phox}$ as well as the novel subunits NoxO1 and NoxA1 did not further increase its activity (Ago et al., 2004; Ambasta et al., 2004; Kawahara et al., 2005). NoxO1 and NoxA1 have not been investigated in vascular tissue so far. However, the lack of the autoinhibitory loop in NoxO1 in comparison to its homologue $p47^{phox}$ and the fact that it is prelocated at the membrane suggests an increased basal activity of NoxO1-based NADPH oxidases (Cheng & Lambeth, 2004).

NADPH oxidases in vascular cells can be activated by a number of stimuli such as angiotensin II, thrombin, PDGF, tumor necrosis factor-α (TNF-α), interleukin-1, vascular endothelial growth factor (VEGF) or mechanical forces like shear stress, although the resulting amounts of ROS are only a fraction of the phagocytic ROS generation (Stocker & Keaney, 2004). A key role for $p47^{phox}$ in mediating angiotensin II-induced NADPH oxidase activation has been demonstrated by use of $p47^{phox-/-}$ mice. Isolated EC and VSMC of these knockout mice did not produce $O_2^{-\cdot}$ in response to angiotensin II (Lavigne et al., 2001; Landmesser et al., 2002; Li & Shah, 2003). Furthermore, angiotensin II and PDGF upregulate Nox1 expression in rat VSMC, whereas transfection of these cells with antisense Nox1 mRNA inhibited superoxide production in response to these stimuli, but had no effect on basal ROS generation (Lassegue et al., 2001). This study by Lassegue et al. (2001)

indicates that Nox1 is essential for agonist-stimulated NADPH oxidase activity in VSMC. Nox2 has also been suggested to be responsive to agonists that promote ROS formation, since stimuli such as TNF-α, PMA or angiotensin II fail to generate ROS in EC and adventitial fibroblasts from $Nox2^{-/-}$ mice (Gorlach et al., 2000; Frey et al., 2002; Rey et al., 2002).

The constitutive and rather low activity of vascular NADPH oxidases suggests that they could play a role in signal transduction processes. The observation that ROS generation occurs mainly intracellularly provides another hint for their role in mediating signal transduction. However, under pathophysiological conditions, NADPH oxidases appear to be significantly involved in the oxidative stress found in a variety of cardiovascular diseases.

2.4.5 Pharmacology of NADPH oxidases

A number of inhibitors of NADPH oxidases have been used in experimental research. However, all of the currently available inhibitors have their drawbacks. They can be differentiated into peptide- and non-peptide-based inhibitors. Among the former, the antibiotic peptide PR-39 blocks leucocytic NADPH oxidase activity by binding $p47^{phox}$ and preventing its translocation to cytochrome b_{558} (Shi et al., 1996). This proline-arginine (PR) rich peptide, which is endogenously secreted by human and/or porcine intestine and neutrophils, interacts with SH3 domains of $p47^{phox}$ (Shi et al., 1996). PR-39 also inhibits non-phagocytic NADPH oxidases as observed in porcine pulmonary artery EC (Al-Mehdi et al., 1998) and decreases ROS production in ischemic reperfusion models of rat lungs (Al-Mehdi et al., 1998) and hearts (Ikeda et al., 2001). However, recent studies reveal non-specific effects of PR-39, because it binds to the SH3 domains of other proteins and interacts with membrane lipids (Chan et al., 2001; Tanaka et al., 2001). Rey et al. (2001) have developed a chimeric oligopeptide (“gp91-ds-tat”) consisting of 9 amino acids of Nox2 (formerly $gp91^{phox}$) known to interact with $p47^{phox}$ (docking sequence *ds*) and to inhibit NADPH oxidase activity (DeLeo et al., 1995). This peptide was attached to a 9-aa sequence derived from the HIV-coat protein (termed *tat*) that facilitates cellular internalization (Fawell et al., 1994). Gp91-

ds-tat competitively binds $p47^{phox}$ and thus prevents the assembly of NADPH oxidases (Rey et al., 2001). Multiple studies have been carried out with gp91-ds-tat in a variety of models, e.g. showing its *in vivo* effectiveness by inhibition of angiotensin II-induced hypertension (Rey et al., 2001) or neointima proliferation following balloon injury (Jacobson et al., 2003). Whether gp91-ds-tat is solely specific for Nox2 (Cai et al., 2003; Cifuentes & Pagano, 2006) or inhibits all vascular subunits (Brandes, 2003), is still a matter of debate and needs further clarifying studies. However, the tat portion alone appears to have effects, recommending control experiments using a peptide with a scrambled gp91 docking sequence.

Several non-peptide compounds have been used to inhibit NADPH oxidases; however, most of these are of dubious specificity. For example, Nox-catalyzed ROS production has traditionally been inhibited by the flavin antagonist diphenylene iodonium (DPI). This substance effectively inhibits all flavoenzymes (Majander et al., 1994), including NOS and cytochrome P_{450} and therefore little information on the specific role of NADPH oxidases is gained by using DPI, except exclusion of a role of all flavoenzymes in ROS production. Phenylarsine oxide (PAO) also directly targets the catalytic subunit Nox2 by forming ring complexes with vicinal or neighbouring thiols (Vignais, 2002). A similar mode of action is suggested to be partly responsible for the inhibition of NADPH oxidase by gliotoxin, a toxin derived from Aspergillus spp. and Candida spp. (Nishida et al., 2005). In addition, it has been shown that gliotoxin impedes the colocalization of PKC-β2 with $p47^{phox}$ and thereby prevents the essential phosphorylation of this organizing subunit (Tsunawaki et al., 2004). 4-(2-aminoethyl)-benzenesulfonyl fluoride (AEBSF) is able to block the $p47^{phox}$ organized assembly of the NADPH oxidase complex, but at the same time is also an irreversible serine protease inhibitor (Diatchuk et al., 1997). Other compounds that have been suggested to inhibit NADPH oxidases are neopterin (Kojima et al., 1993) and plumbagin (Ding et al., 2005); the mechanisms of action of both compounds are poorly understood. Recently, a novel flavonoid derivative, S17834, has been shown to inhibit TNF-stimulated NADPH oxidase activity in EC (Cayatte et al., 2001). In ApoE-deficient mice, it reduces aortic atherosclerosis by 60% (Cayatte et

al., 2001). However, its mechanism of action is also unknown and no other information about S17834 is currently available in the literature. Among all NADPH oxidase inhibitors the one of most frequently used is apocynin (4-hydroxy-3-methoxy-acetophenone). This natural compound, which was isolated from the roots of *Picrorhiza kurroa*, a plant used in Ayurvedic medicine for the treatment of asthma (Basu et al., 1971), inhibits NADPH oxidase activity in neutrophils (Simons et al., 1990) as well as non-phagocytic cells (Meyer et al., 1999). The proposed mechanism of action of apocynin is that it prevents the translocation of $p47^{phox}$ and $p67^{phox}$ to the membrane (Stolk et al., 1994; Meyer et al., 1999). It is suggested, that apocynin requires the presence of H_2O_2 and peroxidases to be converted into an active metabolite which was characterized as a 5'-5'-dimer called diapocynin (Stolk et al., 1994; Johnson et al., 2002; Vejrazka et al., 2005). Due to its high oral bioavailability, low toxicity and efficacy *in vivo* the compound seems to have a promising potential even for clinical therapeutics; for example, apocynin was able to prevent hypertension in rats (Beswick et al., 2001) and mice (Virdis et al., 2004). However, recent studies show that apocynin can even stimulate ROS production in non-phagocytic cells thereby questioning the specificity of this substance (Riganti et al., 2005; Vejrazka et al., 2005). Moreover, apocynin has to be applied in relatively high concentrations (< 500 µM) and it seems that the effect of apocynin varies depending on the inherent peroxidase activity of cells and tissues (Cifuentes & Pagano, 2006).

An overview of the mechanisms of action of NADPH oxidase inhibitors is shown in **Figure 2.5**. In conclusion, the pharmacology of NADPH oxidases is poorly developed. Most inhibitors appear to be either non-specific or their mechanism of action is unclear. In the quest for new compounds with high potency and specificity, a high-throughput screening was performed with PMA stimulated human leucocytes (DMSO differentiated HL60 cells) (Tegtmeier F et al., 2005). In this oxidative burst assay, a compound with a 1,2,3-triazolo[4,5-d]pyrimidine structure, namely VAS2870, was found to be highly effective. Flavoenzyme inhibition and antioxidative effects could be excluded by means of a xanthine/xanthine oxidase assay (Ten Freyhaus et al., 2006). However, the effects of VAS2870 on non-phagocytic NADPH oxidases *in vitro*

as well as *in vivo* remain to be elucidated. The structures of the above described NADPH oxidase inhibitors are shown in **Figure 2.6**.

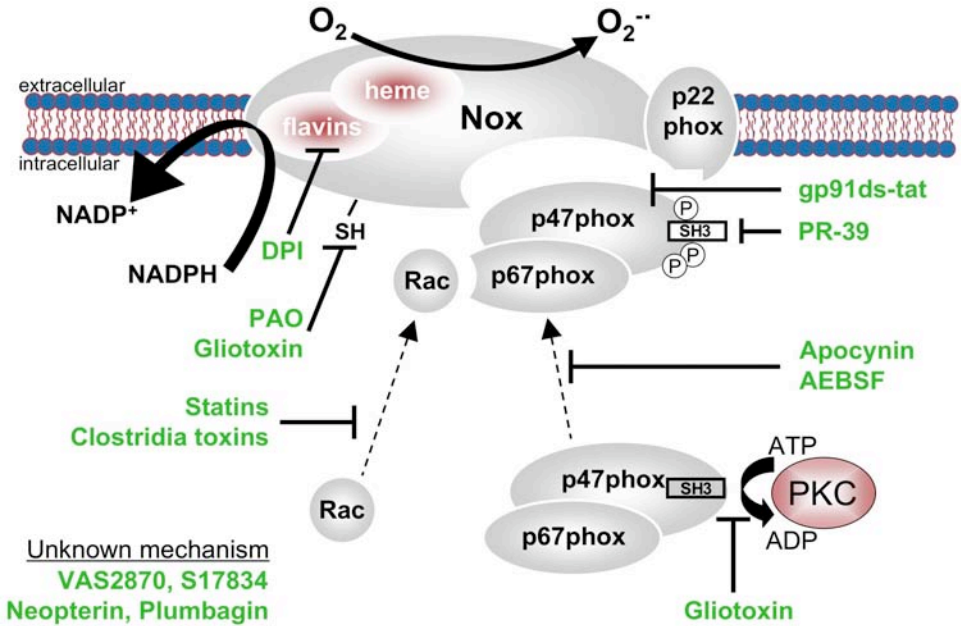

Figure 2.5: Mechanism of action of NADPH oxidase inhibitors. Modified scheme after Brandes (2003). For details, see text.

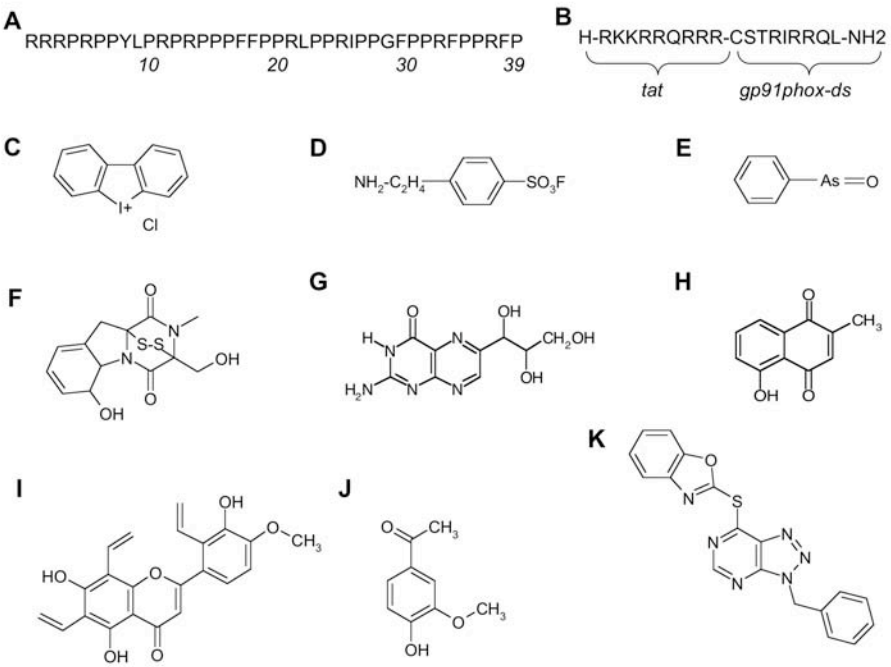

Figure 2.6: Structures of NADPH oxidase inhibitors. A. PR39. **B.** gp91phox-ds-tat peptide. **C.** DPI. **D.** AEBSF. **E.** PAO. **F.** Gliotoxin. **G.** Neopterine. **H.** Plumbagin. **I.** S17834. **J.** Apocynin. **K.** VAS2870.

2.5 ROS and vascular diseases

Animal as well as human studies support a fundamental role of ROS in cardiovascular diseases. In animal models of atherosclerosis, lesion formation is associated with an accumulation of lipid peroxidation products and an inactivation of NO resulting in endothelial dysfunction (for a review, see Griendling & FitzGerald (2003)). In rabbits fed with cholesterol, superoxide was increased in the aorta resulting in an impaired endothelial-dependent relaxation which could be reversed by treatment with PEG-SOD (Mugge et al., 1991). XOD seems to be involved in superoxide production associated with hypercholesterolemia, since oxypurinol normalized the increased ROS generation (Ohara et al., 1993) and improved the impaired vasodilation in hypercholesterolemic patients (Cardillo et al., 1997). A significant role of NADPH oxidases was demonstrated in apolipoprotein E and $p47^{phox}$ double-knockout mice ($ApoE^{-/-}/p47^{phox-/-}$) where a marked reduction of lesions was observed in the descending aorta (Barry-Lane et al., 2001). In human atherosclerotic arteries, Nox2 expression, mainly associated with intimal macrophages, showed a strong correlation with lesion severity, whereas Nox4 mRNA remained unchanged throughout most stages of atherosclerosis; however, the expression level of Nox4 was much lower in most advanced atherosclerotic lesions (Sorescu et al., 2002). Diabetes mellitus (DM) is another disorder associated with increased vascular ROS production. The resulting endothelial dysfuntion was demonstrated in streptozotocin-treated rats (a model of type-I-DM), in genetically diabetic rats (a model of type-II-DM) and human patients with type-II-DM (Griendling & FitzGerald, 2003). Pretreatment of the diabetic rat aorta with SOD significantly improved the endothelium-dependent relaxation (Langenstroer & Pieper, 1992), and NADPH oxidases as well as uncoupled eNOS have been identified as major sources of oxidative stress (Guzik et al., 2002). Other cardiovascular diseases including cardiac hypertrophy, heart failure, nitrate tolerance and restenosis after angioplasty are also accompanied by oxidative stress and increased NADPH oxidase activity (Griendling et al., 2000).

Vascular oxidative stress has been described in experimental hypertension such as angiotensin II-induced hypertension, Dahl salt-sensitive hypertension, DOCA-salt hypertension, or aldosterone-provoked hypertension (Touyz, 2004). NADPH oxidase, XOD and uncoupled eNOS have been identified as sources of amplified ROS generation in these models (Touyz, 2004). For example, several studies suggest a fundamental role of NADPH oxidase in angiotensin II-mediated oxidative stress and hypertension. Chronic infusion of angiotensin II in rats increased blood pressure and NADPH oxidase-derived O_2^- production which could be prevented by pretreating the animals with the AT1 receptor antagonist losartan (Rajagopalan et al., 1996). Concomitant with the increased NADPH oxidase activity, $p22^{phox}$ mRNA as well as $p67^{phox}$ and Nox2 protein levels were also elevated (Fukui et al., 1997; Cifuentes et al., 2000). Furthermore, $p47^{phox}$-deficient mice showed a markedly decreased pressure response and no increase in O_2^- generation after angiotensin II infusion in comparison to wildtype mice (Landmesser et al., 2002).

Genetic hypertension is also accompanied with pathophysiological levels of ROS. Spontaneously hypertensive rats (SHR) exhibit increased O_2^- production in venules as well as arterioles and heparin-binding SOD is able to normalize the blood pressure of these hypertensive animals (Nakazono et al., 1991; Suzuki et al., 1995). Zalba et al. (2000) have reported that enhanced NADPH oxidase activity is associated with endothelial dysfunction and vascular hypertrophy in the aorta of 30 week old SHR, whereas these parameters were unchanged in young SHR (16 weeks old) in comparison to their age-matched normotensive WKY controls. Additionaly, an age-dependent increase in NADPH oxidase activity and decreased NO bioavailability has been reported in a study using aorta from 3-4 and 9-12 month old stroke-prone SHR (Hamilton et al., 2001). Furthermore, increased NADPH oxidase activity in SHR is accompanied by an upregulation of $p22^{phox}$ mRNA and protein expression which has been suggested to be a consequence of an overactivity of the renin-angiotensin system as well as polymorphisms in the $p22^{phox}$ gene promoter (Hamilton et al., 2001; Zalba et al., 2001). However, the involvement of the individual vascular Nox homologues has not been clarified yet. Moreover, uncoupled eNOS has been

described as a critical source of vascular superoxide generation in stroke-prone SHR (Kerr et al., 1999). Treatment with either antioxidant vitamins, SOD mimetics, apocynin, BH_4 or AT_1 receptor blockers suppresses the vascular ROS generation and attenuates the development of hypertension in these models (Hamilton et al., 2002; Park et al., 2002; Rodriguez-Iturbe et al., 2003; Fortepiani & Reckelhoff, 2005). In summary, these data indicate that NADPH oxidases and a dysfunctional eNOS are involved in the generation of oxidative stress observed in genetic hypertension.

3 AIMS OF THE STUDY

The present study was carried out to identify the contribution of NADPH oxidases to vascular oxidative stress and endothelial dysfunction in essential hypertension using aortae of 12-14 month old male SHR and their respective WKY controls. Based on the achieved findings, the effectiveness of the novel NADPH oxidase inhibitor VAS2870 should be tested. The following experimental approaches were thus applied:

i. Investigating the enzymatic sources of ROS in aortae of SHR. XOD, uncoupled eNOS and especially vascular NADPH oxidases are suggested to promote oxidative stress in many cardiovascular diseases. Therefore, increased ROS production in SHR aorta in comparison to WKY should be investigated and the contribution of the individual ROS generating enzymes determined by using specific enzyme inhibitors.

ii. Investigating the contribution of vascular Nox isoforms to NADPH oxidase activity. The involvement of the vascular Nox homologues in increased NADPH oxidase activity of SHR has not yet been clarified. For this reason, protein expression of Nox1, Nox2 and Nox4 should be determined in SHR and WKY aortae.

iii. Investigating the localization of Nox isoforms within the aortic wall of SHR and WKY. The distribution of the Nox homologues in the aortic wall is poorly investigated at the protein level. Thus, possible differences of the Nox distribution between SHR and WKY aorta should be examined using immunohistochemistry.

iv. Investigating the effect of NADPH oxidase inhibition on endothelial function in SHR aorta. Oxidative stress decreases NO bioavailability thereby leading to impaired endothelium-dependent relaxation, a measure for endothelial function. Thus, the hypothesis that inhibition of NADPH oxidases by the novel inhibitor VAS2870 leads to improved endothelium-dependent relaxation should be investigated.

4 MATERIALS AND METHODS

4.1 Chemicals

Chemical	Producer
β-Mercaptoethanol	Carl Roth GmbH (Karlsruhe)
100 kb smart ladder (Marker/DNA)	Eurogentec (Seraing, Belgium)
Acetylcholine	Sigma (Deisenhofen)
Acrylamide (30%) with Bisacrylamide (0.8%)	Carl Roth GmbH (Karlsruhe)
Agaraose	Carl Roth GmbH (Karlsruhe)
Alcian blue 8GS	Carl Roth GmbH (Karlsruhe)
Ampicillin	Carl Roth GmbH (Karlsruhe)
Apocynin	Calbiochem (Darmstadt)
APS	Merck (Darmstadt)
Azophloxin	Fluka (Taufkirchen)
Bromphenol blue	Sigma (Deisenhofen)
BSA	Sigma (Deisenhofen)
$CaCl_2$	Merck (Darmstadt)
Casein-hydrolysate	Sigma (Deisenhofen)
Complete EDTA-free protease-inhibitor cocktail	Roche Molecular Biochemicals (Mannheim)
$CuSO_4 \cdot 5H_2O$	Merck (Darmstadt)
DHE	Molecular Probes (Eugene, USA)
DMSO	Carl Roth GmbH (Karlsruhe)
dNTPs	PeqLab Biotechnologie (Erlangen)
DPI	Sigma (Deisenhofen)
EDTA	Sigma (Deisenhofen)
Ethidium bromide	Carl Roth GmbH (Karlsruhe)
$FeCl_3$	Fluka (Taufkirchen)
Folin-Chiocalteu`s phenol agent	Merck (Darmstadt)
Glacial acetic acid	Merck (Darmstadt)

Glucose	Carl Roth GmbH (Karlsruhe)
Glycine	Carl Roth GmbH (Karlsruhe)
HBSS	PAA Laboratories (Pasching, Austria)
Hematoxylin	Merck (Darmstadt)
HEPES	Sigma (Deisenhofen)
Hoechst dye 33342	Molecular Probes (Eugene, USA)
IPTG	Carl Roth GmbH (Karlsruhe)
KCl	Carl Roth GmbH (Karlsruhe)
KH_2PO_4	Carl Roth GmbH (Karlsruhe)
Light green	Chroma (Köngen)
L-NAME	Sigma (Deisenhofen)
Lucigenin	Sigma (Deisenhofen)
Methanol	Merck (Darmstadt)
$MgCl_2$	Carl Roth GmbH (Karlsruhe)
$MgSO_4 \cdot 7H_2O$	Merck (Darmstadt)
NaCl	Merck (Darmstadt)
NADPH (reduced)	AppliChem (Darmstadt)
$NaHCO_3$	Merck (Darmstadt)
NaOH	Carl Roth GmbH (Karlsruhe)
Normal goat serum	DAKO (Hamburg)
Nuclear fast red	Merck (Darmstadt)
Orange G	Chroma (Köngen)
Orcein	Chroma (Köngen)
Oxypurinol	Sigma (Deisenhofen)
PEG-SOD	Sigma (Deisenhofen)
Phenylephrine hydrochloride	Sigma (Deisenhofen)
Phosphortungstic acid	Merck (Darmstadt)
Picric acid	Carl Roth GmbH (Karlsruhe)
Picroindigocarmin	Chroma (Köngen)
PNGase F from Flavobacterium meningosepticum	Roche Molecular Biochemicals (Mannheim)
Pure H_2O (RNase/DNase free)	Fluka (Taufkirchen)

Random Hexamer Primer	Invitrogen (Karlsruhe)
RNase away	Molecular Bioproducts (San Diego, USA)
Rotihistokit®	Carl Roth GmbH (Karlsruhe)
Rotihistol®	Carl Roth GmbH (Karlsruhe)
SDS	Carl Roth GmbH (Karlsruhe)
SOD from bovine erythrocytes	Sigma (Deisenhofen)
Sodium tartrate	Merck (Darmstadt)
TEMED	Sigma (Deisenhofen)
Tiron	Sigma (Deisenhofen)
Tissue Tek OCT Compound	Sakura Finetek (Torrance, USA)
Tris	Carl Roth GmbH (Karlsruhe)
VAS 2870	Vasopharm BIOTECH GmbH (Würzburg)
X-Gal	Carl Roth GmbH (Karlsruhe)
Yeast extract	Carl Roth GmbH (Karlsruhe)

4.2 Devices and software

4.2.1 Devices

Apparatus	**Type**	**Producer**
Analytical balance	AT 250	E. Mettler (Zürich, Switzerland)
Analytical balance	M5	E. Mettler (Zürich, Switzerland)
Camera system	EDAs 290	Kodak (New Haven, USA)
Centrifuge	5804	Eppendorf (Hamburg)
Centrifuge	Microfuge 22R	Beckman Coulter (Krefeld)
Chemluminescence microplate reader	Fluoroscan Ascent FL	Thermo labsystems (Vantaa, Finland)
CO_2 incubator	BB 6220	Heraeus instruments (Hanau)
Computer	iMac Power PC G4	Apple (Cupertino, USA)
Copy machine	DiAlta di 351	(Minolta, Hannover)

Cryostat	CM 1900	Leica Microsystems (Nussloch)
Electrophoresis chamber for agarose gels		Pharmacia Biotech (Piscataway, USA)
Fluorescence microscope	DM 6000 B	Leica (Wetzlar)
Image station	Kodak 440 CF	Rochester (NY, USA)
Isolated organ apparatus	IOA 5306	FMI Föhr Medical Instruments (Seeheim/Ober-Beerbach)
Microscope	CKX 41	Olympus (Hamburg)
Microwave		Sharp (Hamburg)
Mini SDS-PAGE system	Mini Protean 3 electrophoresis cell	Biorad (Munich)
Power supply	SX 250 mighty slim	Hoefer (San Francisco, USA)
Semi-Dry Transfer Cell	Trans Blot SD	Biorad (Munich)
Shaker	KS 10	Edmund Bühler (Tübingen)
Shaker	Vortex VF2	Janke und Kunkel IKA Labortechnik (Staufen)
Sterilizer	Varioclav Steam Sterilizer	H+P Labortechnik GmbH (Oberschleißheim)
Thermocycler	GeneAmp PCR System 2700	Applied Biosystems (Darmstadt)
Thermomixer	Thermomixer compact	Eppendorf (Hamburg)
Transilluminator	2UV^{TM}	MBT-Brand (Heidelberg)
Ultracentrifuge	CO TLX 120	Beckmann (Palo Alto, USA)
UV/VIS microplate reader	SPECTRAmax 340	Molecular devices (Sunnyvale, USA)
Water bath	Typ 1013	Gesellschaft für Labortechnik mbH (Burgwedel)

4.2.2 Software

Software	Version	Producer
Adobe Acrobat reader	6.0	Adobe system (San Jose, USA)
Adobe Photoshop	7.0	Adobe system (San Jose, USA)
Endnote	6.0	ISI research software (Berkley, USA)
Fluoroscan Ascent FL	2.4	Thermo labsystems (Vantaa, Finland)
IBJ-Amon vitro dat	3.4	Jaeckel (Hanau)
IBJ-Bemon vitro dat	3.4	Jaeckel (Hanau)
Isis Draw	2.5	MDL Information Systems (San Ramon, USA)
Kodak 1D Image Analysis	3.5	Eastman Kodak company (New Haven, USA)
Leica FW 4000	1.1	Leica (Wetzlar)
Mac OS	X 10.3.9	Apple (Cupertino, USA)
MacVektor	7.2	Accelrys (San Diego, USA)
Microsoft Office for Mac	2004	Microsoft Deutschland GmbH (Unterschleißheim)
Prism Graph Pad	4.0	Graph Pad Software (San Diego, USA)
Softmax Pro (SPECTRAmax)	1.2.0	Molecular devices (Sunnyvale, USA)

4.3 Animal models

Spontaneously hypertensive rats (SHR) developed at Okamato, Kyoto School of Medicine, in the 1960s by selective mating of hypertensive Wistar rats from the Kyoto School of Medicine (WKY rats) were used. SHR are a widely used animal model for essential hypertension. Inbred WKY rats have the same background and are thus the appropriate control for SHR.

Animals were purchased from Charles River Laboratories (Sulzfeld). They were maintained in the animal facilities of the Rudolf-Buchheim-Institute, Giessen and fed standard rodent chow and water ad libitum. Male SHR and WKY rats at the age of 12-14 month were used throughout the studies.

4.4 Organ preparation

Krebs Henseleit buffer

118 mM	NaCl
4.7 mM	KCl
2.5 mM	$CaCl_2 \bullet 2H_20$
1.18 mM	$MgSO_4 \bullet 7H_20$
1.18 mM	KH_2PO_4
24.9 mM	$NaHCO_3$
pH 7.4	

Rats were killed by CO_2 inhalation and thoracic aortae were carefully excised, dissected and placed in chilled Krebs-Henseleit buffer (pH 7.4). Adherent tissues as well as contaminating blood were carefully removed. Subsequently, organs were treated as specified in the individual method parts.

4.5 Cytomorphology

Alcian blue solution

1 g	Alcian blue 8GX
3 ml	Acetic acid
97 ml	Aqua dest.

Nuclear fast red solution

25 g	Aluminium sulfate
0.5 g	Nuclear fast red
500 ml	Aqua dest.

Weigert's iron hematoxylin solution

Sol. A:	1g	Hematoxylin in 100 ml 96% ethanol
Sol. B:	1,16g	$FeCl_3$
	99 ml	Aqua dest.
	1 ml	Conc. HCl

Azophloxin solution

0,5 g	Azophloxin
100 ml	Aqua dest.
0,2 ml	Acetic acid

Phosphotungstic acid/ orange G solution

3-5 g	Phosphotungstic acid
2 g	Orange G
100 ml	Aqua dest.

Light green solution

0,2 g	Light green
100 ml	Aqua dest.
0,2 ml	Acetic acid

Orcein solution

1 g	Orcein
100 ml	70% Ethanol
1 ml	HCl conc.

Picroindigocarmin solution

0,5 g	Picroindigocarmin
200 ml	Picric acid (saturated)

Aortic segments of SHR (n=6) and WKY (n=6) were fixed in 4% buffered formaldehyde for 24 h, dehydrated in a graded series of ethanols and embedded in paraffin wax (melting point 58°C). Tissue segments were cut into 7 µm sections using a microtome, dewaxed in Rotihistol® and rehydrated in a graded series of ethanols.

Alcian blue staining according to the method of Steedmann (Romeis, 1989) combined with nuclear fast red counterstaining was used for selective demonstration of acidic mucosubstances. The hydrated sections were bathed in 3% acetic acid for 3 min, stained with 1% Alcian blue solution (pH 3) for 30 min and rinsed for 1 min in 3% acetic acid. Subsequently, sections were counterstained with nuclear fast red solution for 5 min, washed, dehydrated, cleared and covered with Rotihistokit®.

Acidic mucins/mucosubstances:	blue
Nuclei:	reddish pink

Masson's trichrome staining, according to a slightly modified method of Goldner (Romeis, 1989), was performed to differentiate between muscle and collagen fibres. Hydrated slides were first stained with Weigert's iron hematoxylin solution (nuclei) for 3 min. After washing for 10-15 min, slides were stained with azophloxin for 5 min (cytoplasma) and rinsed in 1% acetic acid. Subsequently, aortic sections were bathed using phosphotungstic acid/ orange G for 20 min and rinsed again in 1% acetic acid. Finally, slides were incubated with light green for 5 min to stain collagen fibres. After rinsing with 1% acetic acid, slides were dehydrated, cleared and covered with Rotihistokit®.

Nuclei:	brownish black
Muscle fibres:	red
Collagen fibres:	green

Elastic fibres were visualized according to the method of Taenzer and Unna using orcein staining combined with picroindigocarmin counterstaining

(Romeis, 1989). Hydrated slides were stained with 1% orcein solution for 30 min, differentiated with 80% ethanol and counterstained with picroindigocarmin solution for 15 min. After rinsing with 3.5% acetic acid, slides were dehydrated, cleared and covered with Rotihistokit®.

Nuclei, elastic fibres:	brown-red
Muscle fibres:	yellow
Collagen fibres:	blue-green

Images were obtained with a Leica DM 6000B microscope equipped with a Leica DC 320 camera and the Leica FW4000 software was used for calculation of the aortic wall thickness.

4.6 *In situ* ROS detection using DHE fluorescence

Phosphate-buffered saline (PBS)

2.7 mM	KCl
1.5 mM	KH_2PO_4
137 mM	NaCl
8 mM	Na_2HPO_4
pH 7.4	

Thoracic aortae were embedded in Tissue Tek O.C.T. Compound. Non-fixed frozen cross sections (5 µm) were incubated with 5 µM DHE in a light-protected moist chamber at 37°C for 30 min. Serial sections were treated with the inhibitors indicated for 30 min before incubation with DHE. Images were obtained with a Leica DM 6000B fluorescence microscope using the same imaging settings in each case. For semi-quantitative analysis of superoxide production, three to six images were acquired from three sections per aortic ring and sampled for each experimental condition. Images were analyzed with the Leica FW4000 software and changes in total fluorescence intensity were calculated as percent of SHR control.

4.7 NADPH-derived lucigenin chemiluminescence

Krebs HEPES buffer

118 mM	NaCl
4.7 mM	KCl
2.5 mM	$CaCl_2 \bullet 2H_20$
1.18 mM	$MgSO_4 \bullet 7H_20$
1.18 mM	KH_2PO_4
24.9 mM	$NaHCO_3$
11 mM	Glucose
0.03 mM	EDTA
20 mM	HEPES
1x	Complete EDTA-free protease-inhibitor cocktail
pH 7.4	

NADPH-dependent O_2^- production was measured in aortic homogenates using a chemiluminescence based assay containing 5 μM lucigenin, a concentration that does not appear to be involved in redox cycling (Munzel et al., 2002). Aortae were snap frozen in liquid nitrogen and stored at -80°C. After mincing in liquid nitrogen, aortic homogenates were collected in 0.5 ml Krebs-HEPES buffer. The homogenates were centrifuged with 1000g (4°C, 10 min) to remove cell debris, and the protein contents of the supernatants were determined by means of Micro-Lowry (detailed later). 100 µl reaction mixture containing 50 µg protein and 5 µM lucigenin in Krebs-HEPES buffer were transferred to individual wells of an opaque white 96 well plate and incubated for 30 min in the dark. Following addition of the substrate NADPH (100 μM), NADPH oxidase activity was measured using a luminescence plate reader (Fluoroskan Ascent FL) in the absence and presence of the substances indicated. Changes in chemiluminescent signals were calculated as percent of SHR control.

4.8 RNA analysis

4.8.1 Reverse Transcriptase Polymerase Chain Reaction (RT-PCR)

Running buffer (TAE buffer)

40 mM Tris
20 mM Glacetic actic acid
0.05 mM EDTA
pH 8

Total RNA was isolated from aortic homogenates using the RNeasy Mini Kit (see **Table 4.1**) according to the manufacturer`s protocol. RNA (100 ng) was reverse transcribed using Superscript III (see **Table 4.2**) according to the manufacturer`s protocol using Random Hexamers (250 ng/µl). Subsequently, probes were treated with RNase H (see **Table 4.2**) for 20 min at 37°C. PCR was performed using specific primers for rat Nox1, 2 and 4 and β-actin as housekeeping gene. The sequences for the specific genes were obtained from GenBank (NIH genetic sequence data base) and are shown in **Table 4.3**. Amplification was carried out using a thermocycler with Platinum Taq-polymerase (see **Table 4.2**). PCR was performed using the following conditions: after initial denaturation for 5 min at 94°C, 35 cycles of 1 min at 94°C, 1 min at 59°C and 30 sec at 72°C were conducted followed by a final extension for 10 min at 72° C. Amplified PCR products were separated on a 1.2% agarose gel in TAE buffer, stained with ethidium bromide and visualized and photographed under ultraviolet light.

Method	Kit	Company
RNA isolation	RNeasy/ QIAshredder	Qiagen (Hilden)
Gel purification	SNAP Gel Purification Kit	Invitrogen (Karlsruhe)
Subcloning	TOPO TA Cloning Kit	Invitrogen (Karlsruhe)
Plasmid isolation	QIA prep Spin Miniprepkit	Qiagen (Hilden)

Table 4.1: Kits used for RT-PCR and subcloning of PCR products

Method	Enzyme	Company
RT-PCR	Superscript III	Invitrogen (Karlsruhe)
RNA digestion	RNase H	Invitrogen (Karlsruhe)
PCR	Platinum Taq Polymerase	Invitrogen (Karlsruhe)
Plasmid digestion	EcoRI	Roche (Mannheim)

Table 4.2: Enzymes used for RT-PCR and subcloning of PCR products

Gene	Primer sequence
Nox1	Fwd: 5‘ –CCT GCT CAT TTT GCA ACC AC - 3‘ Rev: 5‘ -CAT GAG AAC CAA AGC CAC AG -3‘
Nox2	Fwd: 5‘ -GAC AGA CTT CGG ACA GTT TG - 3‘ Rev: 5‘ -ACT CTA GCT TGG ATA CCT GG -3‘
Nox4	Fwd: 5‘ -GTG TTT GAG CAG AGC TTC TG – 3‘ Rev: 5‘ -GTG AAG AGA AGC TTT CTG GG -3‘
β-actin	Fwd: 5‘ -GAA GTA CCC CAT TGA ACA CG - 3‘ Rev: 5‘ -CGC GTA ACC CTC ATA GAT GG -3‘

Table 4.3: **Primers against rat Nox1, Nox2, Nox4 and β-actin used for RT-PCR**

4.8.2 Subcloning of Nox1, Nox2 and Nox4

XIA Agar

1.5%	Agar
1%	Casein-hydrolysate
0.5%	Yeast extract
0.5%	NaCl
200 µg/ml	Ampicillin
50 µg/ml	IPTG
40 µg/ml	X-Gal

LB medium

1%	Casein-hydrolysate
0.5%	Yeast extract
1%	NaCl
200 µg/ml	Ampicillin

PCR fragments were isolated from agarose gels and purified using the SNAP Gel Purification Kit (see **Table 4.1**) according to the manufacturers protocol. Subsequently, the purified PCR products were cloned by the TOPO TA Cloning Kit (see **Table 4.1**) into the pCR®2.1-TOPO®3.9kb vector according to the manufacturers protocol (bacteria strain: E. coli TOP10F'). Positive/negative selection of the subclones was carried out with XIA plates. Positive clones were incubated for 18h in liquid LB medium supplemented with ampicillin at 37°C and 220 rpm. Plasmids were isolated using the QIA Prep Spin Miniprepkit (see **Table 4.1**) according to the manufacturers protocol. Plasmids were digested with the restriction enzyme EcoRI **(**see **Table 4.2)** for 1h at 37°C and restriction products were visualized after agarose gel electrophoresis. Positive clones were outsourced for sequencing to GENterprise (Gesellschaft für Genanalyse und Biotechnologie mbH, Darmstadt.)

4.9 Protein analysis

4.9.1 Preparation of samples for Western blot analysis

Triton lysis buffer

20 mM	Tris
150 mM	NaCl
10 mM	Na-Pyrophosphat
1 %	Triton X 100
2 mM	Orthovanadat
10 nM	Okadeic acid
230 µM	PMSF
1x	Roche Protease Inhibitor Mix (Complete EDTA-free - tablet)
pH 7.5	

Aortae were snap frozen in liquid nitrogen and stored at -80°C. After mincing in liquid nitrogen, rat aortic tissue powder was lysed in 2x Triton lysis buffer with a protease inhibitor cocktail for 10 min on ice. Approximately 250 µl buffer was used for 30 mg frozen tissue. The mixture was vortexed and diluted 1:2 with SDS-containing Rotiload® 4x (1:2 diluted in aqua dest.). Samples were heated under these reducing conditions for 10 min at 95°C in an Eppendorf thermo-mixer. After centrifugation at 8000g for 10 min, the supernatants were further analyzed.

4.9.2 Protein determination (Micro-Lowry)

Rotiload® sample buffer (Rotiload® 4x)

62.5 mM	Phospate buffer (pH 6.8)
10% (v/v)	Glycerol
2% (w/v)	SDS
0.01% (w/v)	Bromophenol blue
5% (v/v)	β-Mercaptoethanol

Folin 1 solution

Folin 1 is a mixture of the solutions A to D in a ratio of 1:1:28:10.

Solution A:	1% (w/v)	$CuSO_4 \bullet 5H_20$
Solution B:	2% (w/v)	Di-sodium tartrate $\bullet 2H_20$
Solution C:	3.4% (w/v)	Na_2CO_3
	0.2 M	NaOH
Solution D:	10% (w/v)	SDS

Following precipitation of the Rotiload®-lysed proteins by trichloroacetic acid, protein content was determined using the protocol of Lowry et al. (Lowry et al., 1951; Peterson, 1977). Samples (10 µl) were diluted with 1 ml distilled water and 100 µl of 0.15% (w/V) deoxycholic acid was added. After 10 min incubation (all incubation steps were performed at room temperature on an Eppendorf shaker), 100 µl of 72% trichloroacetic acid was added followed by 15 min incubation. The samples were centrifuged at 16000g for 10 min, the supernatants were removed and the pellets resolved in 300 µl water and 300 µl Folin 1 solution. After an incubation step of 10 min, 150 µl of 25% Folin-Ciocalteu`s phenol reagent was added and samples were incubated for further 30 min. Subsequently, the optical density of the samples was measured at 595 nm with a UV/VIS microplate reader and the protein concentration was calculated using BSA protein standards.

4.9.3 PNGase F digestion

Protein (150 µg) of aortic homogenates lysed in Triton lysis buffer was denatured by heating at 95°C for 10 min. Subsequently, samples were cooled to RT, 0.5% N-octyl glucoside and 50 units PNGase F were added and this mixture was incubated overnight at 37°C. Finally, Rotiload® buffer was added to the samples and Western blot analysis was performed as described below.

4.9.4 SDS polyacrylamide gel electrophoresis (SDS-PAGE)

Electrophoresis buffer

25 mM Tris
120 mM Glycin
0.1% (w/v) SDS
pH 8.3

Equal amounts of protein (40 µg) were separated by SDS-PAGE using 9% polyacrylamide gels (for composition see **Table 4.4**) according to the method described by Laemmli (Laemmli, 1970). Gels of 1 mm thickness and a size of 8 x 9.5 cm were generated with a Biorad gel caster. After loading the samples, electrophoresis was performed at RT in a mini-SDS-PAGE system with a constant current of 15 mA/gel (stacking gel) and 20 mA/gel (resolving gel) using the power supply SX 250 mighty slim. Protein molecular weight standards were used as indicated under **Table 4.5**.

Stacking gel	Resolving gel 9%
5% (v/v) Rotiphorese® Gel 30	9% (v/v) Rotiphorese® Gel 30
80 mM Tris pH 6.8	375 mM Tris pH 8.8
0.1% (v/v) SDS	0.1% (v/v) SDS
0.05% (v/v) TEMED	0.05% (v/v) TEMED
0.07% (w/v) APS	0.05% (w/v) APS

Table 4.4: **Gel compositions for SDS-PAGE.**

Marker	Source
PeqGOLD protein marker IV	PeqLab Biotechnologie (Erlangen)
Prestained Protein marker	Biolabs (Frankfurt a.M.)

Table 4.5: **Protein markers used for Western blot anlysis.**

4.9.5 Western blotting

Blotting buffer

48 mM	Tris
39 mM	Glycin
0.1% (w/v)	SDS
20% (v/v)	Methanol
pH 8.5	

Ponceau S staining solution

0.1% (w/v)	Ponceau S
5% (v/v)	Acetic acid

Tris-buffered saline with Tween 20 (TBS-T)

20 mM	Tris
150 mM	NaCl
0.1% (w/v)	Tween 20
pH 7.5	

Proteins were transfered from resolving gels to a Hybond-ECL nitrocellulose membrane (Amersham Pharmacia Biotech, Freiburg) by semi-dry blotting (1.2 mA/cm^2 for 75 min). The transfer was performed in the Semi-Dry Transfer Cell Trans Blot SD using the blotting buffer mentioned above.

Equal rates of transfer were confirmed by reversible staining with Ponceau-S solution. Blots were washed in aqua dest., stained for 5 min at room temperature and washed again with aqua dest.. Imaging was performed using the DiAlta di 351 copy machine.

Non-specific binding to the membranes was blocked by incubation with 2.5% non-fat dry milk powder (Nestlé, Glandale, CA, USA) in Tris buffered saline containing Tween-20 (TBS-T) for 2 h at room temperature. Primary antibodies (see **Table 4.6**) were diluted in 2.5% milk/TBS-T and membranes were incubated at 4° C overnight. Subsequently, these membranes were washed 5

times for 8 min with TBS-T and incubated with horseradish peroxidase conjugated secondary antibody (diluted as indicated in **Table 4.7**) for 1 h in the dark at RT. After washing with TBS-T (5x for 8 min in the dark), membranes were incubated either with ECL or with ECL advanced (Amersham Pharmacia Biotech, Freiburg, Germany) for 1 min and 5 min, respectively. Immunoreactive chemiluminescence signals were captured using the Kodak Imager Station 440CF which has a much higher saturation level (64000 grey levels) than traditional films (256 grey levels). Quantification of the light signals was performed using the Kodak ID image analysis software.

Antibody	Species	Source	Method	Dilution
Anti-Nox1 (polyclonal)	Rabbit	Raised against Nox1-aa-545-561: RYSSLDPRKVQFYC	WB IF	1:25000 1:200
Anti-Nox2 (polyclonal)	Rabbit	Upstate biotechnology (Lake Placid, USA)	WB	1:2000
Anti-Nox2 (polyclonal)	Mouse	BD biosciences (Heidelberg, Germany)	IF	1:200
Anti-Nox4 (polyclonal)	Rabbit	Raised against Nox4-aa 84-101: RGSQKVPSRRTRRLLDKS	WB IF	1:10000 1:200
eNOS (monoclonal)	Mouse	Transduction Laboratories (Lexington, USA)	WB	1:2500
β-Actin (monoclonal)	Mouse	Oncogene (San Diego, USA)	WB	1:20000
α-SMC actin – FITC	Mouse	Sigma (Deisenhofen, Germany)	IF	1:400
RECA-1 (monoclonal)	Mouse	Serotec (Düsseldorf, Germany)	IF	1:100

Table 4.6: Primary antibodies used for Western blotting (WB) and immunofluorescence (IF). Nox1 and Nox4 antibodies were affinity-purified.

Antibody	Species	Conjugation	Source	Method	Dilution
Anti-rabbit	Goat	HRPO	Dako (Hamburg)	WB	1:2000-1:20000
Anti-mouse	Goat	HRPO	Dako (Hamburg)	WB	1:2000
Anti-rabbit	Donkey	Cy3	Chemicon (Hofheim)	IF	1:200
Anti-mouse	Donkey	Cy3	Chemicon (Hofeheim)	IF	1:200
Anti-rabbit	Goat	FITC	Sigma (Deisenhofen)	IF	1:100
Anti-mouse	Goat	FITC	Sigma (Deisenhofen)	IF	1:100

Table 4.7: Secondary antibodies used for Western blotting (WB) and immunofluorescence (IF).

Stripping buffer

62.5 mM Tris
2% (w/v) SDS
100 mM β-Mercaptoethanol
pH 6.8

”Stripping” is a method for re-using a Western blot: the nitrocellulose membrane was incubated with 10 ml of stripping buffer in a water bath at 60-70°C for 30 min to remove primary and secondary antibodies. After washing with TBS-T for 4 x 15 min, the membranes were ready for the next immunostaining as described above.

4.10 Immunohistochemistry

Aortic segments were embedded in Tissue Tec O.C.T. Compound (Sakura Finetek, Torrance, USA) and stored at -80°C until use. Tissues were sectioned to an average thickness of 7 µm with a Leica 1900 cryostat (Bensheim, Germany). After fixing with ice-cold acetone (10 min), sections were blocked with 10% normal goat serum (DAKO, Hamburg, Germany) containing 5% bovine serum albumine (Sigma, Deisenhofen, Germany). Incubations with the primary antibodies used in the concentrations indicated in **Table 4.6** (diluted in PBS (pH 7.4) containing 0.1 %Triton X-100) were performed at 4°C for 24 h. Incubations with the secondary antibodies used in the concentrations indicated in **Table 4.7** (diluted in PBS/Triton) were done at RT for 2 h. Immunoreactivity was visualized by fluorescence microscopy. In addition, double fluorescence labeling was performed with the FITC conjugated α-smooth muscle actin antibody and/or a RECA-1 antibody. For nuclear staining, the Hoechst dye 33342 was used. Serial sections were treated with the secondary antibodies alone as control for non-specific staining.

DHE staining combined with immunofluorescence was performed as follows: aortic sections were stained with DHE as described above (see **chapter 4.6**) and subsequently blocked with 50% normal goat serum in PBS/Triton. Incubations with the primary antibodies (see **Table 4.6**) were done at 4°C for 24 h in a moist chamber. Immunoreactivity was visualized by fluorescence microscopy using the secondary FITC conjugated antibodies (RT, 2 h) as described in **Table 4.7**. As controls the primary antibodies were omitted.

4.11 Isometric force measurement

Aortae were cut into rings (2-3 mm) and mounted on individual organ baths containing 5 ml of Krebs Henseleit buffer (pH 7.4). The solution was continuously oxygenated with a 95% O_2 – 5% CO_2 mixture and maintained at 37°C. Changes in isometric tension were detected by a force transducer and recorded via a 6-channel transducer data acquisition system. During an equilibration period of 90 min the resting tension was gradually increased to 20 mN and the buffer was exchanged every 15 min. The aortic rings were then challenged 1-2 times with 80 mM KCl to determine the viability of the rings and to activate them. After a regeneration phase of at least 45 min, rings were precontracted submaximally (60-80%) with 300-1000 nM phenylephrine. Concentration response curves (CRC) and E_{max} values were generated in the plateau phase of the phenylephrine contraction for the endothelium-dependent vasodilator acetylcholine (1 nM – 10 µM in semi-logarithmic steps) in the absence and presence of apocynin (100 µM) or VAS2870 (10 µM). After the generation of the first CRC, rings were washed 3 times and allowed to regenerate for at least 45 min before performing the second CRC.

4.12 Statistical analysis

Statistical differences between the means were analyzed by Student´s t-test. For multiple comparisons, one-way analysis of variance (ANOVA) followed by Bonferroni´s multiple range test was employed. A value of $p<0.05$ was considered significant. Asterisks represent significance as follows: * $p<0.05$, ** $p<0.01$, ***$p<0.001$. Data analysis was performed using Prism 4.0 for Macintosh.

5 RESULTS

5.1 Common characteristics of the animals

(body weights, cytomorphology and contractility of aortae)

In order to characterize the animal model investigated in this study, body weights were measured directly after sacrificing the animals. Surprisingly, 12-14 month old male SHR weighed significantly less than their age-matched WKY controls (SHR: 381.6 ± 3.9 g (n=11), WKY: 547.9 ± 10.8 g (n=11), $p<0.001$).

Chronic hypertension is supposed to be accompanied by a remodeling of vessels. Indeed, as shown in **Figure 5.1** all histological staining methods that were performed point to major structural changes in the aortic wall of SHR in comparison to WKY. Alcian blue staining for acidic mucosubstances revealed increased accumulation of extracellular matrix proteins in SHR. Masson´s trichrome staining confirmed these findings and demonstrated partially enriched inclusions of connective tissue in the aortic media indicating a discrepancy in the occurence of medial muscle and collagen fibres between SHR and WKY. Furthermore, elastica staining revealed reduced numbers as well as structural differences in the elastic fibres in the aortic wall of SHR in contrast to WKY. These findings, which suggest a pathological modification of the vessel by increased extracellular matrix deposition and stiffness, were finally supplemented by the evaluation of the thickness of aortic intima and media. Analysis of the images obtained from the individual stainings exhibited an increased wall thickness in SHR (133.8 ± 1.4 µm) in comparison to WKY (103.3 ± 1.8 µm; $p<0.001$) suggesting hypertrophy and remodeling in the hypertensive animals.

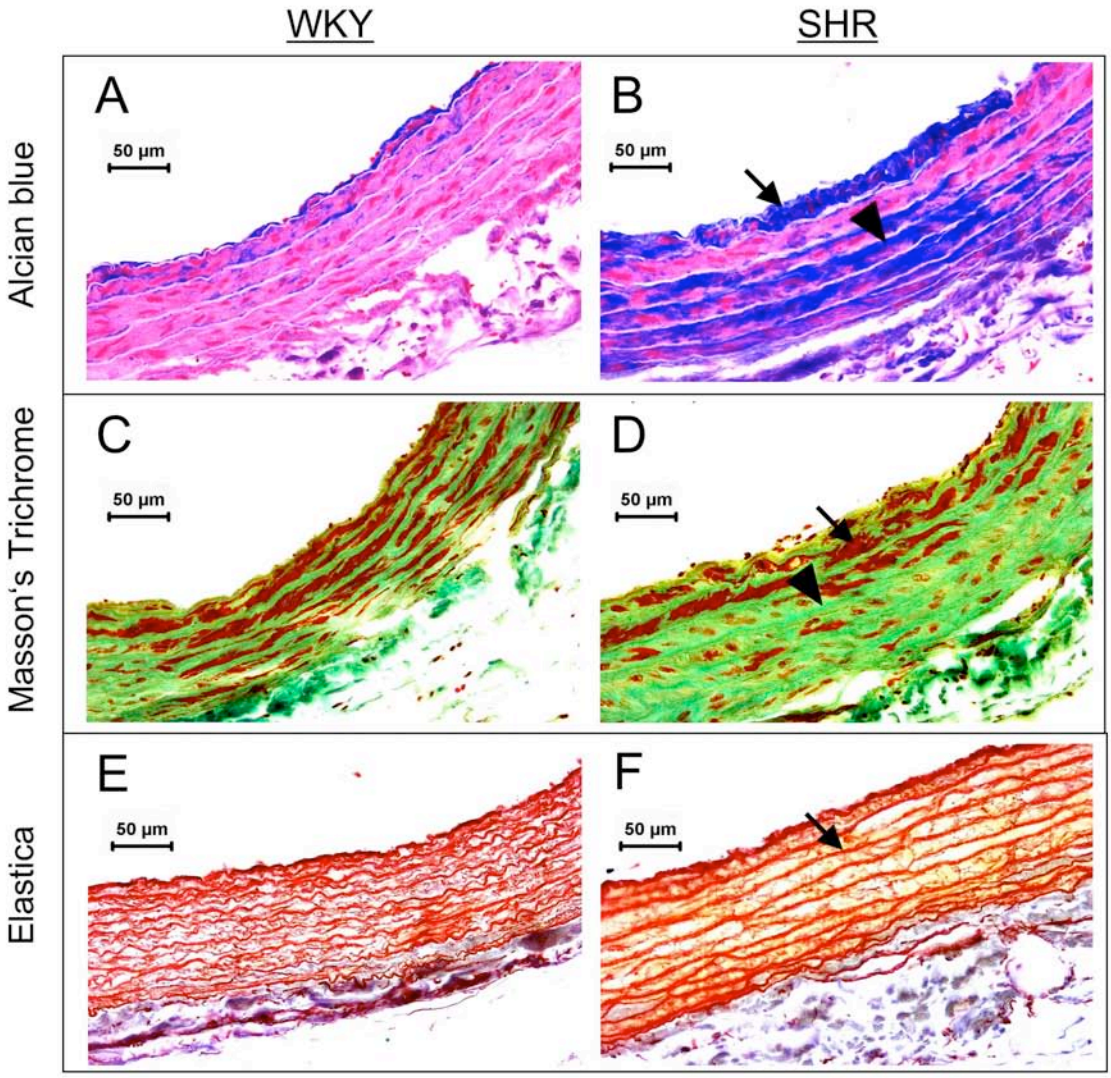

Figure 5.1: Structural changes in the aortic wall of SHR. In comparison to the aorta of WKY rats (**A**), alcian blue staining revealed an increased accumulation of ECM proteins (blue) in the intimal (arrow) as well as the medial layer (arrowhead) of SHR aorta (**B**). Nuclei were counterstained with nuclear fast red (red). The middle panels show Masson's trichrome staining. Compared to WKY aortae (**C**), the aortic media of SHR (**D**) displayed an increased amount of connective tissue and/or collagen fibres (green, arrowhead), whereas the amount of muscle fibres (red, arrow) was partially decreased. Elastica staining demonstrated a decline of elastic fibres (arrow) in SHR aorta (**F**) in comparison to WKY aorta (**E**). Images are representative for n = 6 observations for each staining method.

In line with these histological findings, the contractile response was decreased in SHR aortic rings in comparison to their WKY controls. Aortic rings were either challenged with potassium chloride or phenylephrine and the response

of the SHR aorta was diminished to 72% and 75% of the WKY contraction, respectively (**Table 5.1**).

Contractile agent	Response (mN) WKY	Response (mN) SHR	P value
120mM KCl (mN)	29.9 ± 2.2	21.4 ± 1.3	< 0.01
10µM PE (mN)	39.5 ± 2.9	29.5 ± 1.3	< 0.01

Table 5.1: Diminished contractility of SHR aortic rings. Contraction response to 120 mM KCl or 10 µM PE was significantly lower in SHR aortic rings in comparison to their normotensive WKY controls (results are expressed as mean ± SEM, n=18, unpaired Student's t-test)

5.2 ROS generation in SHR and WKY aortae

In order to investigate whether the essential hypertension is accompanied by oxidative stress, ROS production within the aortic wall was determined using dihydroethidium (DHE). In addition, the signal was specified and the main sources of ROS production were identified by preincubation with certain ROS scavengers or enzyme inhibitors. **Figure 5.2** shows representative images of the assay. SHR aortic tissue exhibited a clearly visible increase of fluorescence intensity in comparison to WKY indicating enhanced oxidative stress in these animals. Semi-quantitative analysis of the images revealed a 5.7 ± 1.3 fold higher signal intensity (**Figure 5.3**). The fluorescence, which is derived from the intercalation of oxidated DHE products with DNA, was enhanced in all layers of the SHR vessel. The superoxide scavenger tiron (1 mM) and the cell-permeable PEG-ylated superoxide dimutase (PEG-SOD, 250 U/ml) completely suppressed the increased fluorescence in SHR aortae indicating that superoxide is the predominant ROS responsible for oxidative stress in these animals.

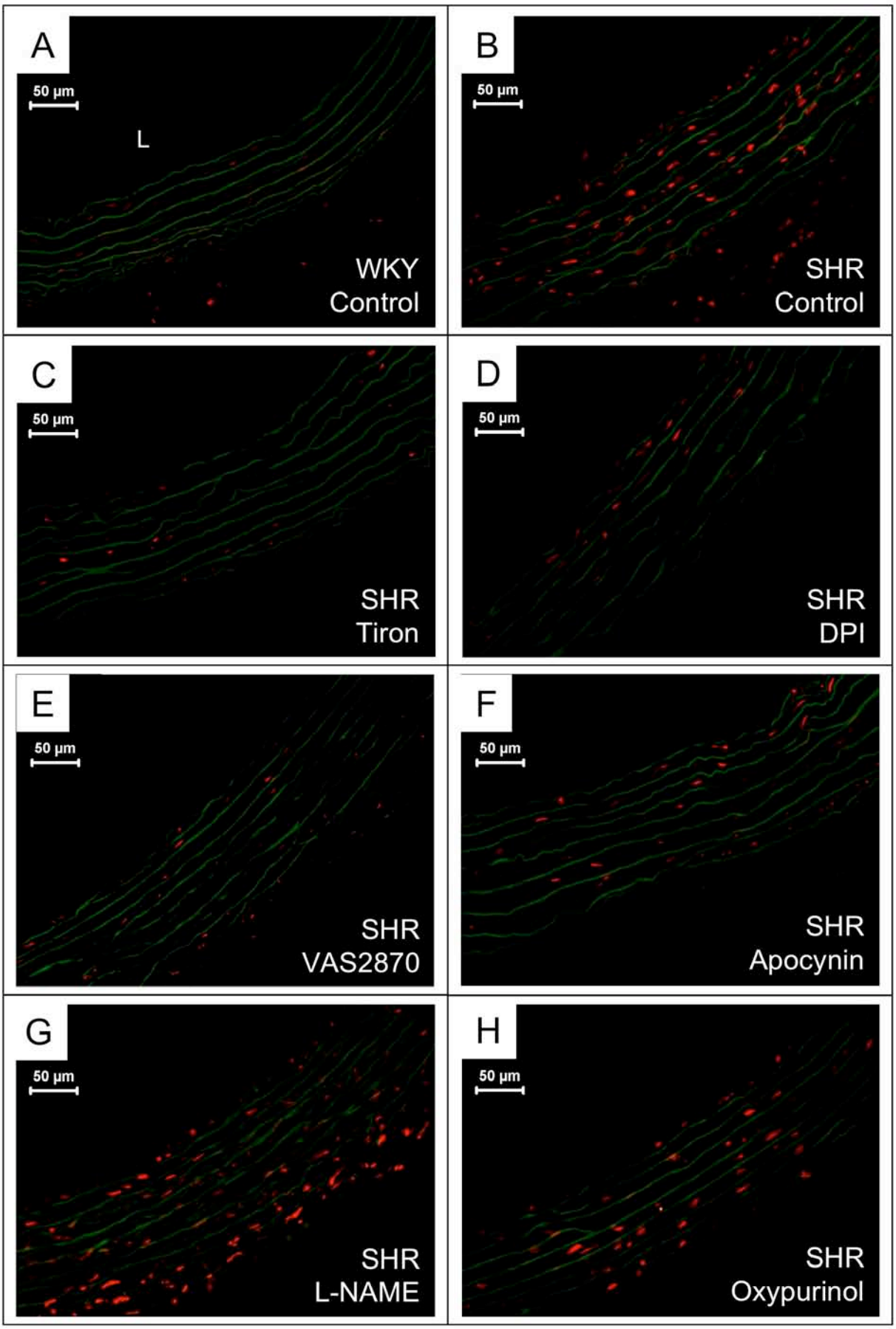
A
50 µm
L
WKY
Control
B
50 µm
SHR
Control
C
50 µm
SHR
Tiron
D
50 µm
SHR
DPI
E
50 µm
SHR
VAS2870
F
50 µm
SHR
Apocynin
G
50 µm
SHR
L-NAME
H
50 µm
SHR
Oxypurinol

Figure 5.2: Increased superoxide production in SHR aortic sections is prevented by NADPH oxidase inhibition. Aortic segments of WKY and SHR were incubated with DHE in the absence and presence of the substances indicated. In comparison to WKY (**A**), ROS production was significantly increased in SHR (**B**). Tiron (**C**, 1 mM), DPI (**D**, 10 µM) and the NADPH oxidase inhibitors VAS2870 (**E**, 10 µM) and apocynin (**F**, 1 mM) suppressed the ROS production in SHR aortae, whereas the NOS inhibitor L-NAME (**G**, 1 mM) and the XOD inhibitor oxypurinol (**H**, 100 µM) had no or rather weak effects on fluorescence intensity. Images are representative for n=6 observations.

Furthermore, this production of superoxide can be predominantly attributed to flavoenzymes, because DPI (10 µM) effectively inhibited the signal in SHR aortae. Incubation with the NADPH oxidase inhibitors VAS2870 (10 µM) and apocynin (1 mM) significantly suppressed the fluorescence intensity in all layers of the SHR aorta indicating NADPH oxidase as the predominant source of oxidative stress. The novel compound VAS2870 completely eliminated the increased ROS production in all vascular layers of SHR aortae, whereas apocynin partially inhibited the signal even with the relatively high concentration of 1 mM. In contrast to the NADPH oxidase inhibitors, the NOS inhibitor L-NAME did not suppress the ROS production but rather showed a slight upregulation of ROS generation in the adventitia. However, the semi-quantitative analysis of the images could not confirm this observation. Finally, the contribution of XOD was estimated by incubating aortic sections with oxypurinol. The fluorescence was slightly affected by this inhibitor, especially in the adventitia, but this suppression did not reach statistical significance with semi-quantitative analysis. All compounds were tested in parallel in WKY aortic segments, but did not exhibit any statistically significant effects, probably due to the weaker ROS production in the organs of these animals making it difficult to detect any effects on the fluorescence intensity (data not shown). In summary, these data suggest a major role of NADPH oxidase in increased ROS production in the aortae of 12-14 month old male SHR.

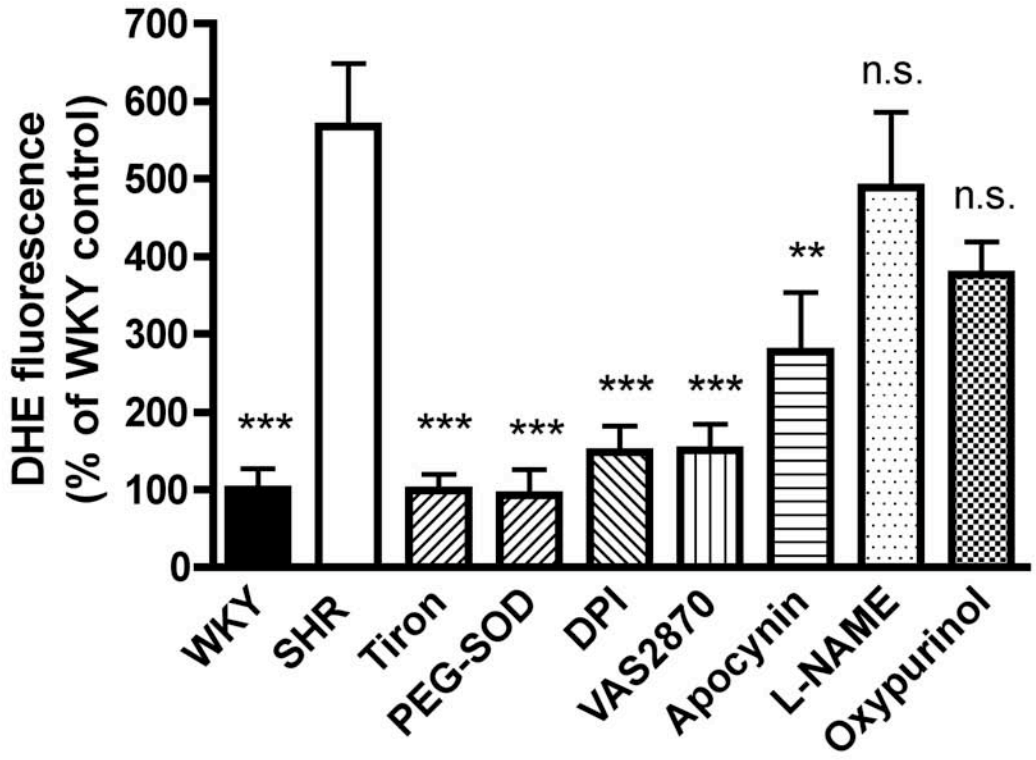

Figure 5.3: Semi-quantitative analysis of ROS production detected with DHE. Fluorescence intensity was quantified and shown as percent of the signal of untreated WKY aortic rings. ROS production in WKY was significantly lower than in SHR aorta. Tiron (1 mM), PEG-SOD (250 U/ml), DPI (10 µM), VAS2870 (10 µM) and apocynin (1 mM) significantly attenuated the signal in SHR segments, whereas L-NAME (1 mM) and oxypurinol (100 µM) had no significant effects. Values are mean ± SEM, n=6 (**p<0.01, ***p<0.001)

5.3 NADPH oxidase activity in SHR and WKY aortae

To verify the results obtained in the DHE assay, NADPH oxidase activity was measured in aortic homogenates of SHR and WKY rats. As shown in **Figure 5.4**, NADPH-derived lucigenin (5 µM) chemiluminescence was significantly higher in aortic homogenates of SHR compared to WKY. This signal was suppressed by tiron (1 mM) indicating that superoxide was the main ROS detected in this assay. Inhibition by the flavoenzyme antagonist DPI (10 µM) as well as by the NADPH oxidase inhibitors VAS2870 (10 µM) and apocynin (100 µM) confirmed NADPH oxidase as the source of enhanced aortic

superoxide production in SHR. As expected, neither the NOS inhibitor L-NAME nor the xanthine oxidase inhibitor oxypurinol interfered with the chemiluminescence signal ruling out a significant contribution of these putative ROS sources. None of the above mentioned substances showed a significant suppression of the signal in homogenates of WKY aortae (data not shown). In summary, these results demonstrated that NADPH oxidase activity was enhanced in the aortic homogenates of 12-14 month old male SHR.

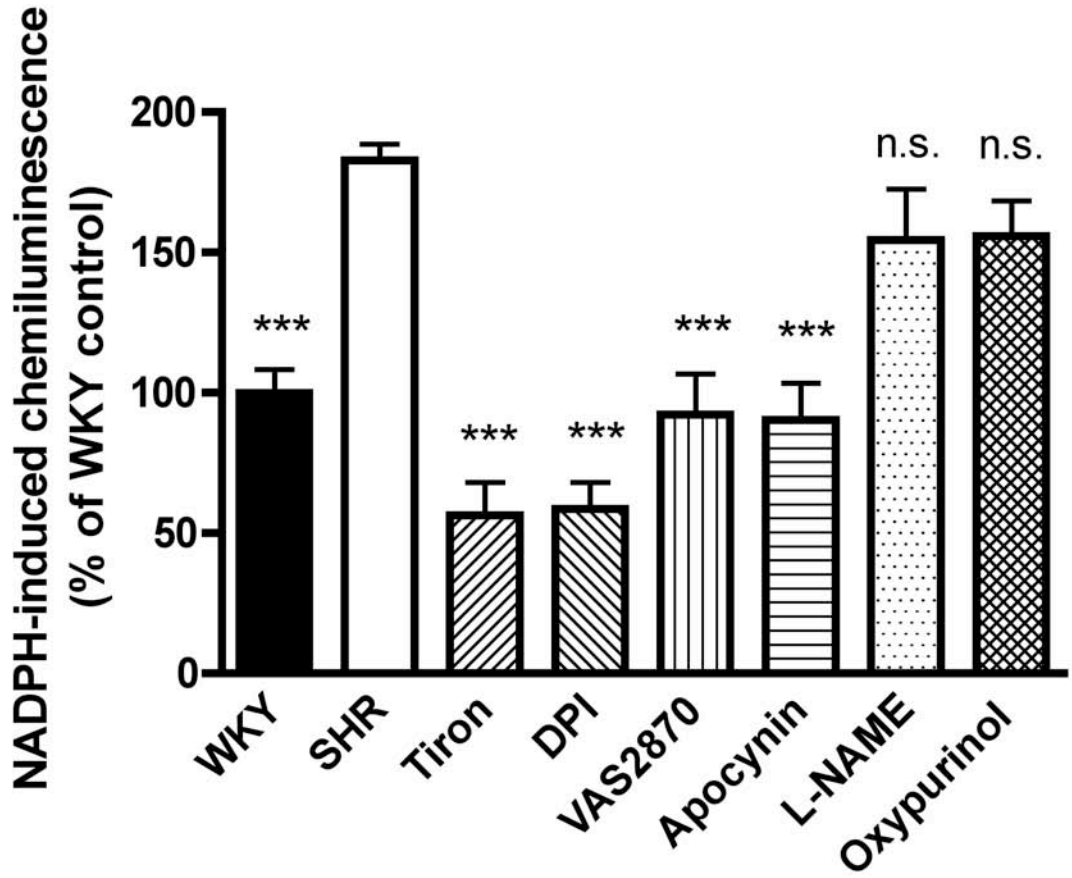

Figure 5.4: NADPH-derived lucigenin chemiluminescence. NADPH-derived ROS production was measured using 5 µM lucigenin and expressed as percent of the chemiluminescence signal generated in WKY aortic homogenates. ROS production was significantly lowered in WKY in comparison to SHR. Tiron (1 mM), DPI (10 µM), VAS2870 (10 µM) and apocynin (100 µM) suppressed the chemiluminescence signal in SHR homogenates, whereas L-NAME (1 mM) and oxypurinol (100 µM) had no effect. Values are means ± SEM (***$p<0.001$).

5.4 mRNA expression of Nox isoforms in aortic homogenates

Expression of Nox1, Nox2 and Nox4 mRNA was determined in aortic homogenates to investigate the occurence of the vascular Nox isoforms in 12-14 month old male SHR and WKY rats. Reverse transcriptase polymerase chain reaction (RT-PCR) was performed and confirmed the expression of Nox1, Nox2 and Nox4 in aortae of SHR as well as WKY (**Figure 5.5**).

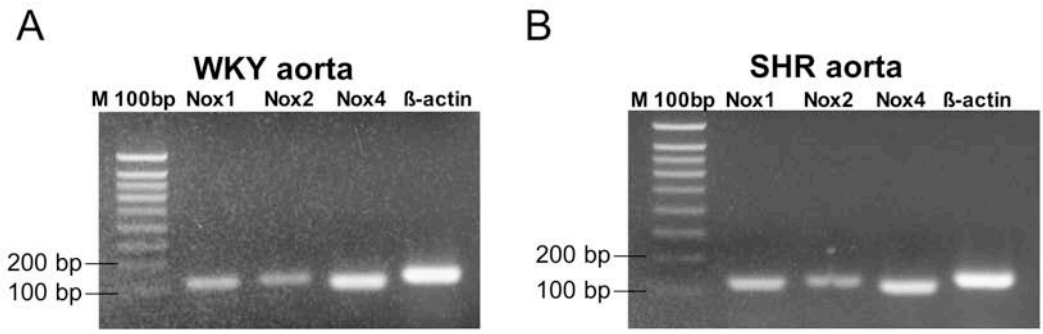

Figure 5.5: mRNA expression of Nox isoforms in SHR and WKY aorta. RT-PCR analysis indicated that Nox1, Nox2 and Nox4 are expressed in WKY aortae (**A**) and SHR aortae (**B**). In both strains Nox4 seemed to be higher expressed than Nox1 and Nox2. (Images are representative for n = 6 animals of both strains).

5.5 Distribution of Nox isoforms in the aortic wall of SHR and WKY

In order to visualize topographically in which layers of the vessel wall the Nox isoforms are located, aortae of SHR and WKY were investigated immunohistochemically.

As shown in **Figure 5.6,** Nox1 protein was mainly detected in the media of the aortic wall with strong signals in the luminal situated cell layers of the media. Remarkably, the intima of SHR aortae showed a strong Nox1 immunofluorescence, whereas no or at least very weak signals were found in the corresponding cell layer in WKY.

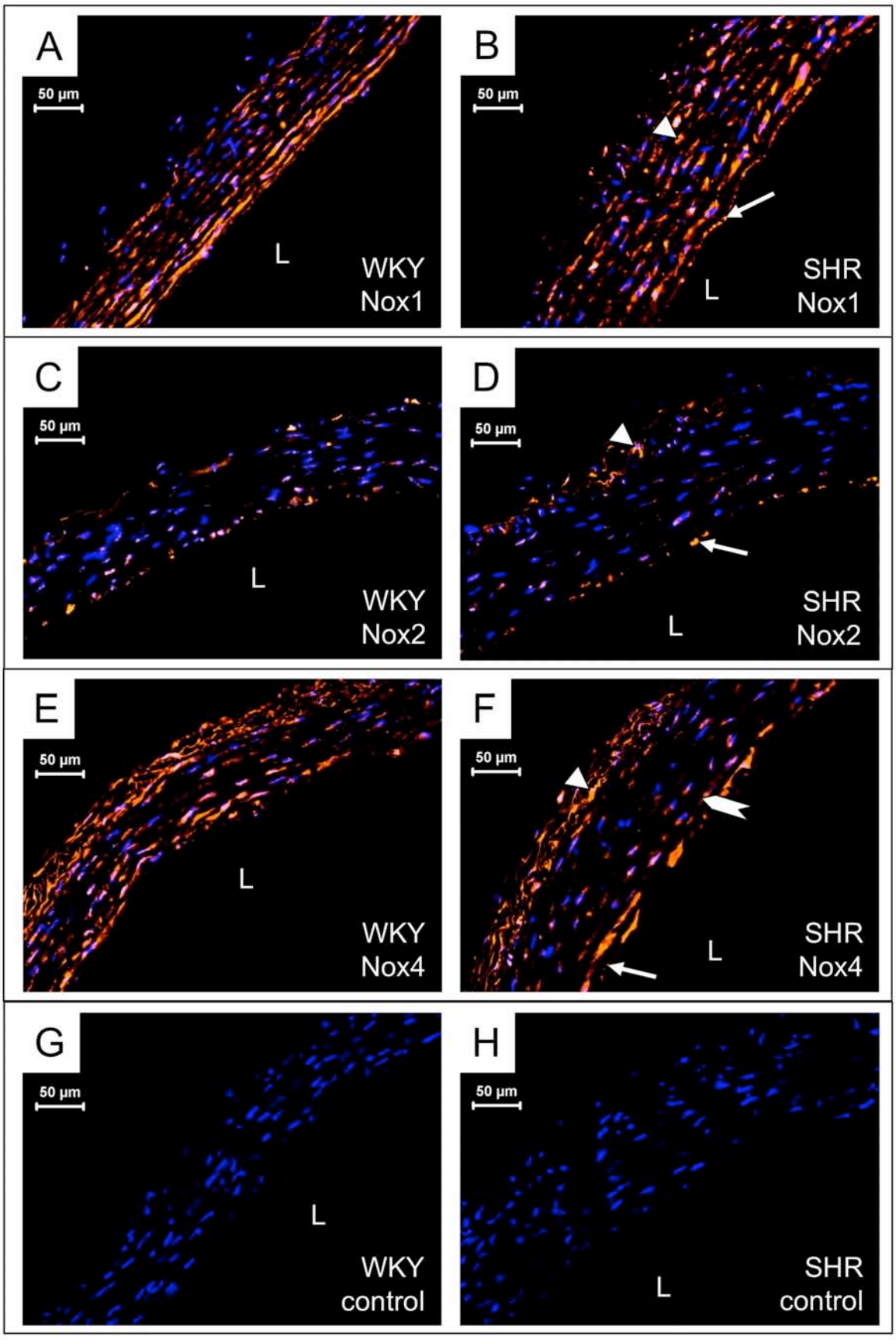
A
50 µm
L
WKY
Nox1
B
50 µm
L
SHR
Nox1
C
50 µm
L
WKY
Nox2
D
50 µm
L
SHR
Nox2
E
50 µm
L
WKY
Nox4
F
50 µm
L
SHR
Nox4
G
50 µm
L
WKY
control
H
50 µm
L
SHR
control

Figure 5.6: Distribution of Nox isoforms in SHR and WKY aortae. Nox1 immunofluorescence was detected in the media and weakly in the intima of WKY aortae (**A**). In contrast, Nox1 immunosignals in SHR aortae (**B**) were found in the media (arrowhead) and were increased in the intima (arrow). Nox2 protein was detected in the adventita and the intima of WKY aortae (**C**). The same expression pattern for Nox2 was found in SHR (**D**), where signals in the adventita (arrowhead) and the intima (arrow) are labeled. As shown for WKY (**E**) and SHR (**F**), Nox4 protein was found in all layers of the aortic wall with a strong signal in the adventitia (arrowhead) and the inner layers of the media (chevron). Signals in the intima (arrow) appeared to be comparatively less pronounced. Control experiments, where the primary antibody was omitted, are shown for WKY (**G**) and SHR (**H**). Antigen-antibody-complexes were visualized with a Cy3-coupled secondary antibody leading to a red fluorescence and nuclei were counterstained with Hoechst 33342 (blue). L: lumen. Images are representative for n = 6 animals per group.

Nox2 was detected in the adventitia and the intima of aortic sections, while the media appeared to be devoid of Nox2 protein. Both rat strains displayed the same distribution of this Nox isoform, which is in line with the expression of Nox2 in fibroblasts and EC, but not in VSMC of conduit arteries.

Finally, Nox4 protein was found in all the three layers of the aortic wall with an apparently stronger staining in the adventitia. Interestingly, similar to the Nox1 protein pattern, the luminal side of the media also exhibited an increased Nox4 positive immunoreactivity.

5.6 Quantitative Western blot analysis of aortic homogenates

5.6.1 Nox1, Nox2 and Nox4 protein expression in SHR and WKY aortae

Protein expression of the vascular Nox isoforms Nox1, Nox2 and Nox4 was assessed in the aortic homogenates of aged SHR and WKY rats to determine which of the catalytic NADPH oxidase subunits are involved in the increased oxidative stress observed in SHR.

Figure 5.7 shows representative Western blots with the Nox1 antibody in aortic homogenates of SHR and WKY rats. The antibody detected a 60 kD band which is close to the predicted Nox1 protein size of 65 kD. Densitometric analysis of this band and normalization to the respective actin levels demonstrated a 3.4 ± 0.6 times higher expression of Nox1 in SHR compared to WKY aortae. However, the antibody detected two additional bands at 126 kD and 138 kD and also a faint band at 50 kD (relative to the molecular weight standard). To test if these immunoreactive bands are specific, antibody binding was blocked by preincubation with the peptide used for immunization. As shown in panel B of **Figure 5.7**, the high molecular weight bands as well as the 60 kD band were no longer detectable after peptide blocking, which suggests that they were specific for the Nox1 antibody. In contrast, the faint 50 kD band was not peptide-blockable pointing to a non-specific binding. To investigate whether the detected proteins were glycosylated, PNGase digestion was performed with aortic homogenates of SHR. This experiment indicated a slight glycosylation of the 60 kD band; there was no effect on the band size of the larger two bands.

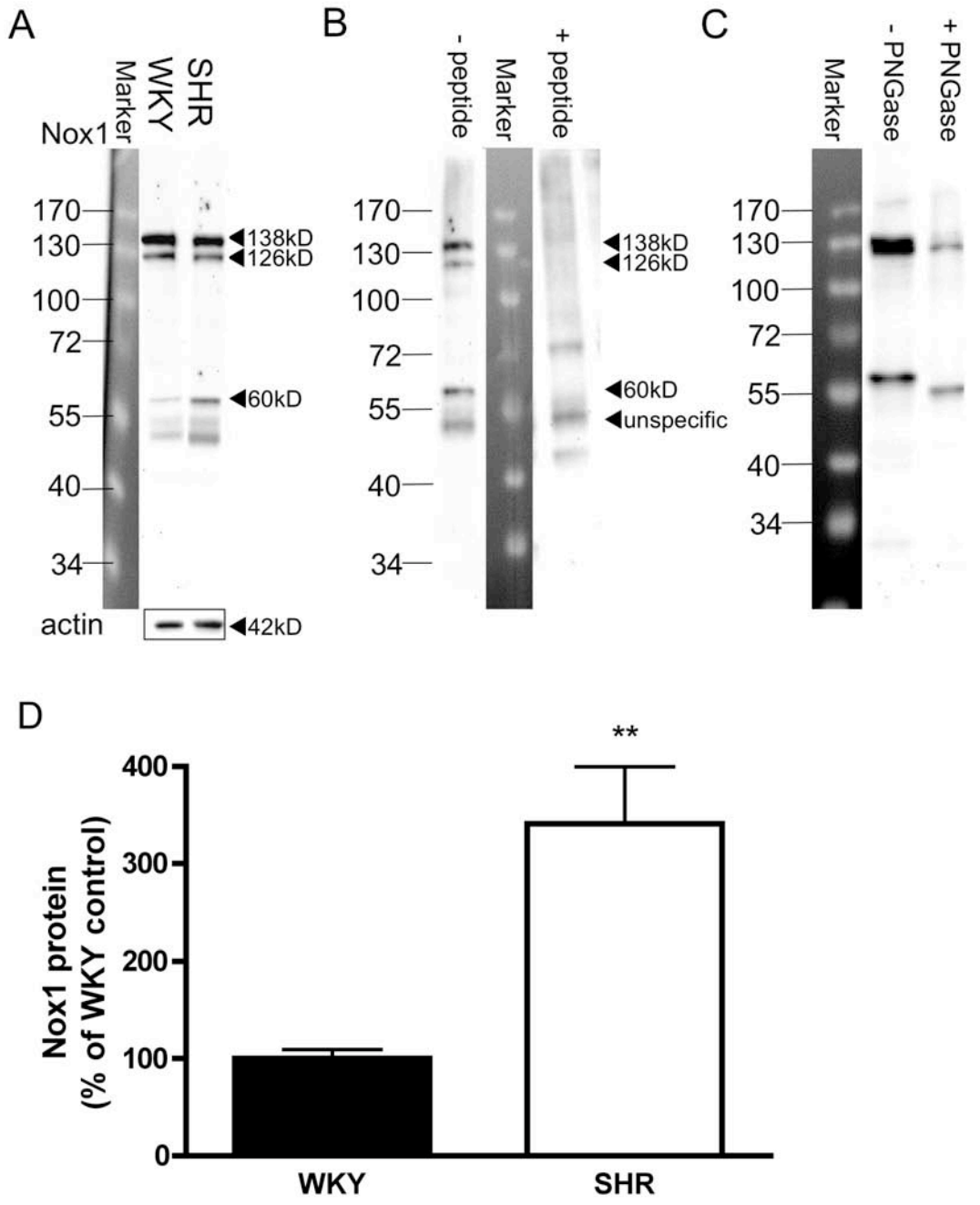

Figure 5.7: **Nox1 protein expression in aortic homogenates of SHR and WKY rats.** Representative Western blot showing Nox1 and related actin expression (**A**). Peptide block identifying three Nox1 positive protein bands at 60 kD, 126 kD and 138 kD in SHR aortic homogenates (**B**). PNGase digestion of SHR aortic homogenate revealed a glycosylation of the 60 kD band (**C**). Densitometric analysis of the 60 kD band demonstrated that Nox1 protein is significantly upregulated in SHR compared to the WKY aortic homogenate (**D**). Signals of the Nox1 band were normalized to actin and shown as percent of the level seen in WKY. Values represent means ± SEM of n = 6 animals (**p<0.01).

Figure 5.8 shows Nox2 protein expression and respective β-actin levels in SHR and WKY aortic homogenates. A single band was detected at 75 kD, which was described as a glycosylated form of Nox2. Densitometric analysis and normalization to the actin standard revealed an upregulation of Nox2 protein in SHR aortae (1.6 x ± 0.1, $p<0.01$) in comparison to the age matched WKY control rats.

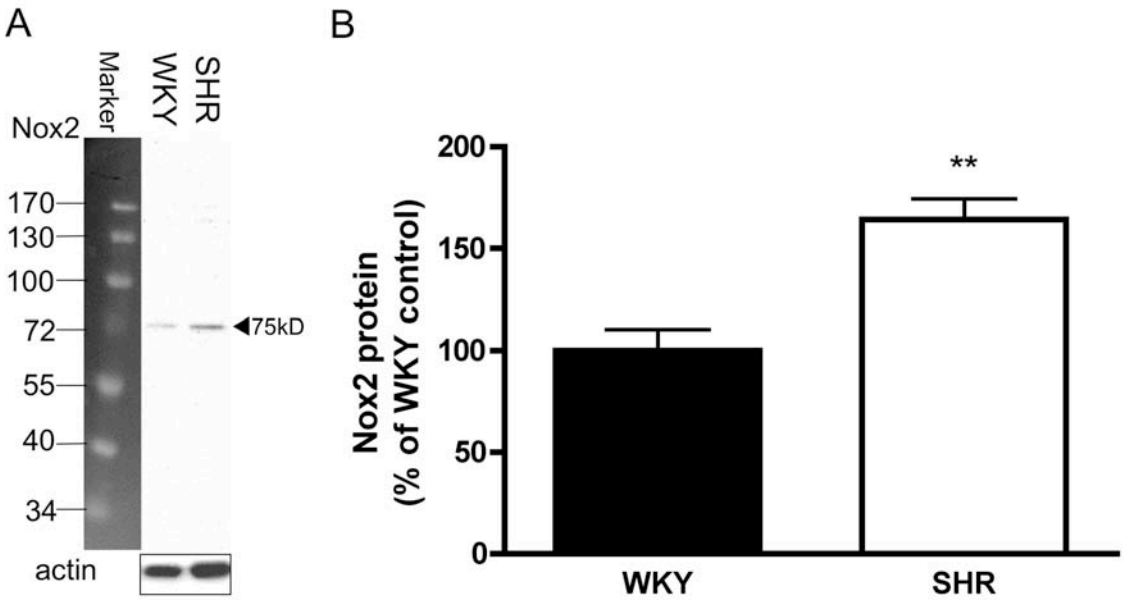

Figure 5.8: Nox2 protein expression in aortic homogenates of SHR and WKY rats. Representative Western blot showing Nox2 and related actin expression (**A**). Densitometric analysis of Nox2 immunoblots (**B**). Signals were normalized to actin and expressed as percent of the level in WKY. Nox2 protein shows a significantly higher expression in SHR than in WKY aortic homogenates. Values represent means ± SEM of n = 6 animals. (**p<0.01)

Finally, Nox4 protein expression was determined in the aortic homogenates of SHR and WKY rats. As shown in **Figure 5.9** a single band was detected at 58 kD with the polyclonal Nox4 antibody. Densitometric analysis of the blots and normalization to actin revealed no significant difference in Nox4 expression between the two rat strains (WKY: 100.0 ± 30.5%, SHR: 168.9 ± 22.3%, p=0.10).

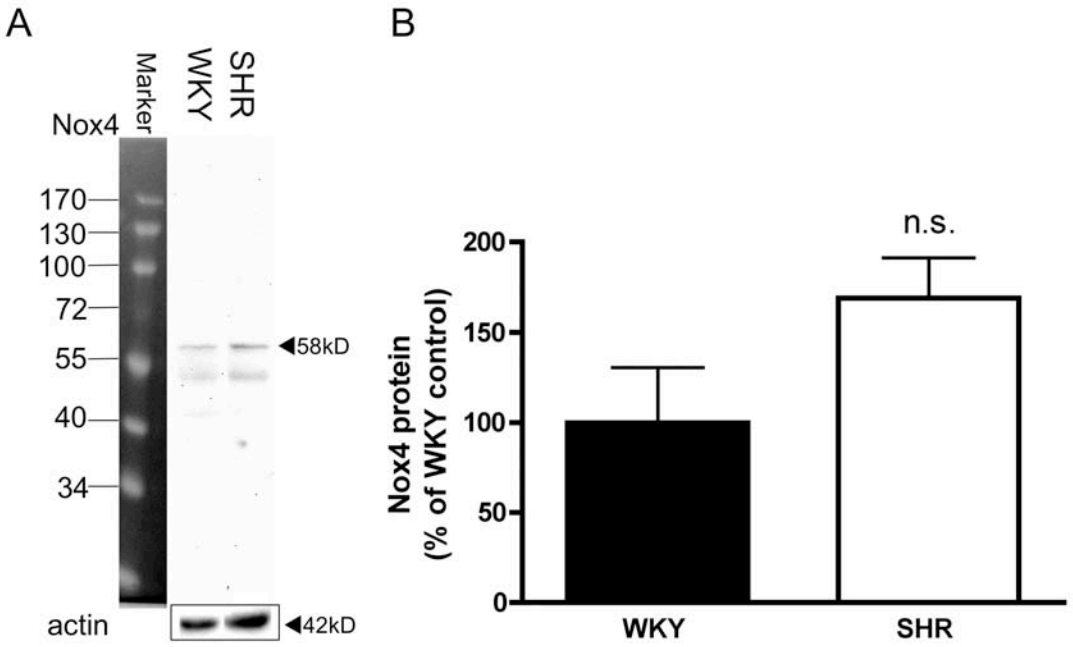

Figure 5.9 Nox4 protein expression in aortic homogenates of SHR and WKY rats. Representative Western blots showing Nox4 and related actin expression (**A**). Densitometric analysis of Nox4 immunoblots (**B**). Signals were normalized to actin and expressed as percent of the level seen in WKY. Nox4 protein levels were not statistically different in SHR compared to WKY aortic homogenates. Values represent means ± SEM of n = 6 (SHR) and n = 5 (WKY) animals.

5.6.2 Expression of eNOS protein in SHR and WKY aortae

Since eNOS is crucial in regulating vascular tone and endothelial function, we next compared the protein expression of this enzyme. Thus, Western blots with aortic homogenates of SHR and WKY were performed using a monoclonal antibody against eNOS. As shown in **Figure 5.10**, eNOS protein bands were detected at a molecular weight of 140 kD which is the expected molecular weight. Densitometric analysis and normalization to the respective actin levels revealed no statistical difference of eNOS expression between SHR and WKY aortae (WKY: 100.0 ± 10.0%, SHR: 147.7 ± 35.9%, p=0.23).

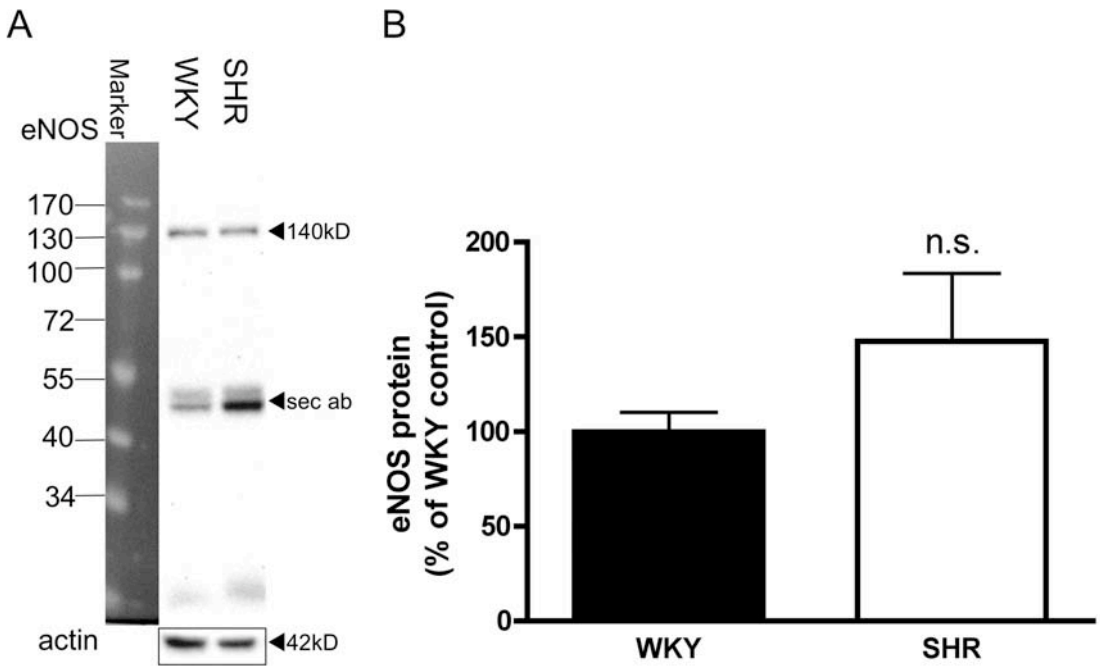

Figure 5.10: eNOS protein expression in aortic homogenates of SHR and WKY rats. Representative Western blot showing eNOS and related actin expression (**A**). The eNOS specific band was detected at 140 kD. The doubleband at 50 kD was not specific for the primary antibody, but was derived from the secondary antibody. Densitometric analysis of eNOS immunoblots (**B**). Signals were normalized to actin and shown as percent of the level in WKY. eNOS protein levels were not statistically different in SHR in comparison to WKY aortic homogenates. Values represent means ± SEM of n = 6 animals.

5.7 Colocalization of Nox1 with α-SM-actin, RECA-1 and ROS formation

While the localization of Nox2 protein in the aortic wall is well elucidated and could be confirmed in the present study, the protein expression patterns of the novel isoforms Nox1 and Nox4 are less explored in rat aortae. Thus, Nox1 and Nox4 distribution was investigated in more detail by immunohistochemical colocalization with α-SM-actin, a marker for VSMC. As shown in **Figure 5.11**, Nox1 detection matches with the α-SM-actin localization in medial VSMC. However, in addition to the colocalization with α-SM-actin, SHR aortae exhibited a strong Nox1 immunosignal in α-SM-actin negative intimal cells and even a diffuse immunofluorescence in the adventitia. In contrast, WKY

aortae mainly expressed Nox1 in cells, which also expressed α-SM-actin, but not or very weak in intima and adventitia.
Moreover, Nox4 immunosignals matched with the α-SM-actin immunostaining in SHR and WKY aortae demonstrating its expression in VSMC. Both strains displayed a strong Nox4 signal in α-SM-actin negative cells of the adventitia and to a smaller extend in the intima. Noticeable is that the enhanced Nox1 and Nox4 immunofluorescence in the luminal situated layers of the media matched perfectly with α-SM-actin verifying that VSMC are the major side of Nox1 and Nox4 expression in SHR as well as WKY aortae.

For further cytological characterization of the Nox1 immunofluorescence in SHR aortae, additional colocalization experiments were performed. **Figure 5.12** shows the colocalization with α-SM-actin as a marker for VSMC, with RECA-1 as a marker for endothelial cells and with oxidized DHE as a marker for ROS production. As already shown in **Figure 5.11**, Nox1 was detected in VSMC, but was also found in the α-SM-actin negative intimal layer of SHR aortae. The Nox1 immunosignal in the intimal layer matched well with the RECA-1 immunofluorescence verifying the Nox1 detection in EC. Furthermore, combination of immunofluorescence with DHE-mediated *in situ* ROS detection revealed the presence of Nox1 protein in ROS generating cells in the media as well as in the intima of SHR aortae. However, the DHE signals in the adventitia and partly in the intima did not match with Nox1 detection indicating other sources of ROS within these parts of the vessel.

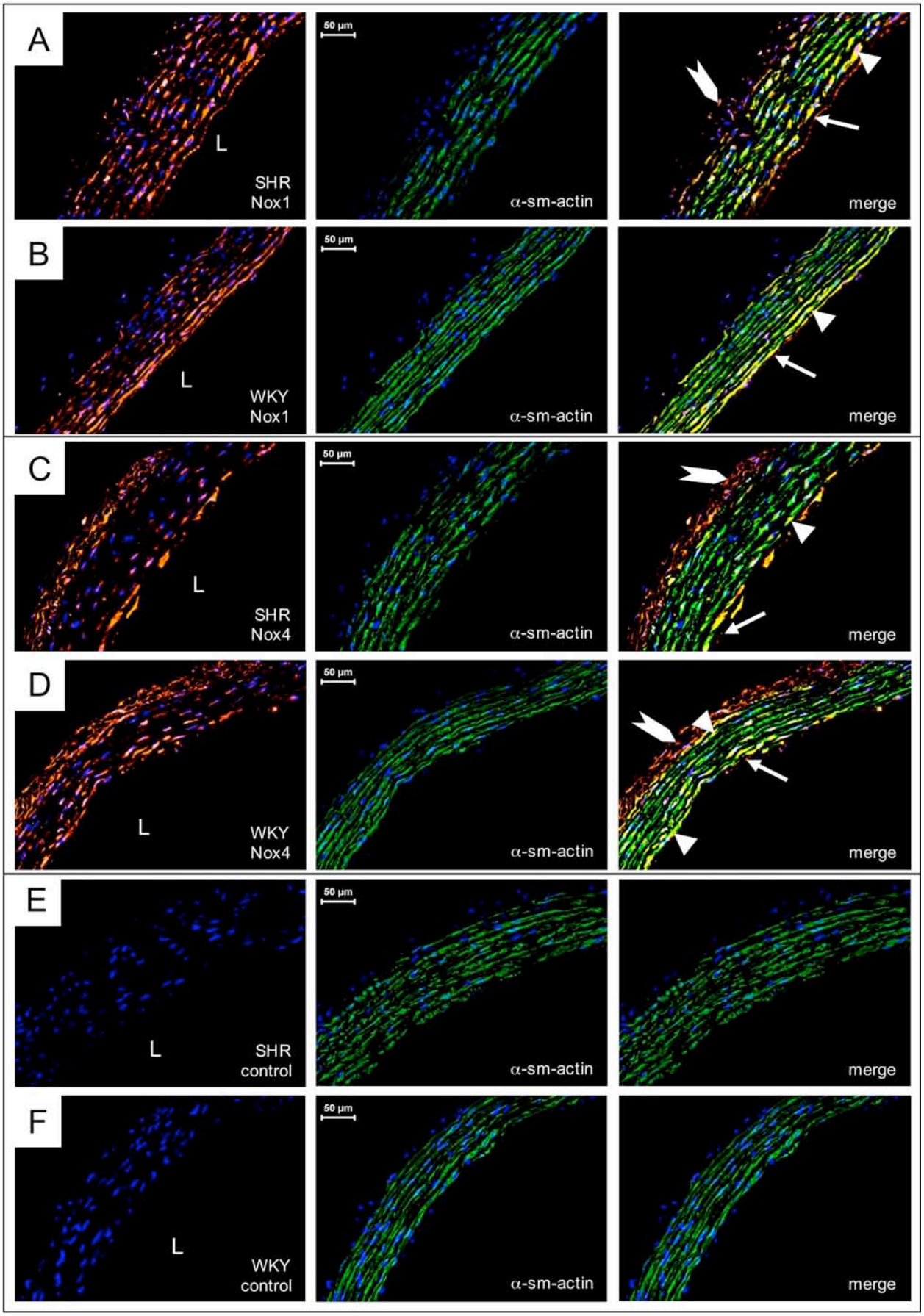
A
L
SHR
Nox1
50 µm
α-sm-actin
merge
B
L
WKY
Nox1
50 µm
α-sm-actin
merge
C
L
SHR
Nox4
50 µm
α-sm-actin
merge
D
L
WKY
Nox4
50 µm
α-sm-actin
merge
E
L
SHR
control
50 µm
α-sm-actin
merge
F
L
WKY
control
50 µm
α-sm-actin
merge

Figure 5.11: Colocalization of Nox1 and Nox4 protein with α-SM-actin in SHR and WKY aortae. Images on the left show the detection of the Nox isoforms (red-orange fluorescence of the Cy3-coupled secondary antibody), images in the middle represent the α-SM-actin immunosignals (green fluorescence of the FITC-coupled secondary antibody), and images on the right show the merge of the stainings. Nox1 and α-SM-actin colocalization in SHR aorta (**A**). The merge of the two images revealed the expression of Nox1 in α-SM-actin positive cells of the media (yellow signal, arrowhead), but also in the α-SM-actin negative intimal (arrow) and adventitial layer (chevron). Nox1 immunofluorescence in the media of WKY aorta colocalizes with α-SM-actin (arrowhead), but there was none or at least a very weak signal in the intimal (arrow) and adventitial layer (**B**). Nox4 distribution was similar in the aortic wall of SHR (**C**) and WKY (**D**). Nox4 colocalizes with α-SMC-actin (arrowheads), but preferably in the luminal situated cell layers of the media. In addition, there is a strong positive Nox4 signal in the adventitia (chevrons) and in the intima (arrows), which do not merge with α-SM-actin. Control experiments where the primary antibodies were omitted are shown for SHR (**E**) and WKY (**F**) aortae. L = lumen. Images are representative for n = 6 animals per group.

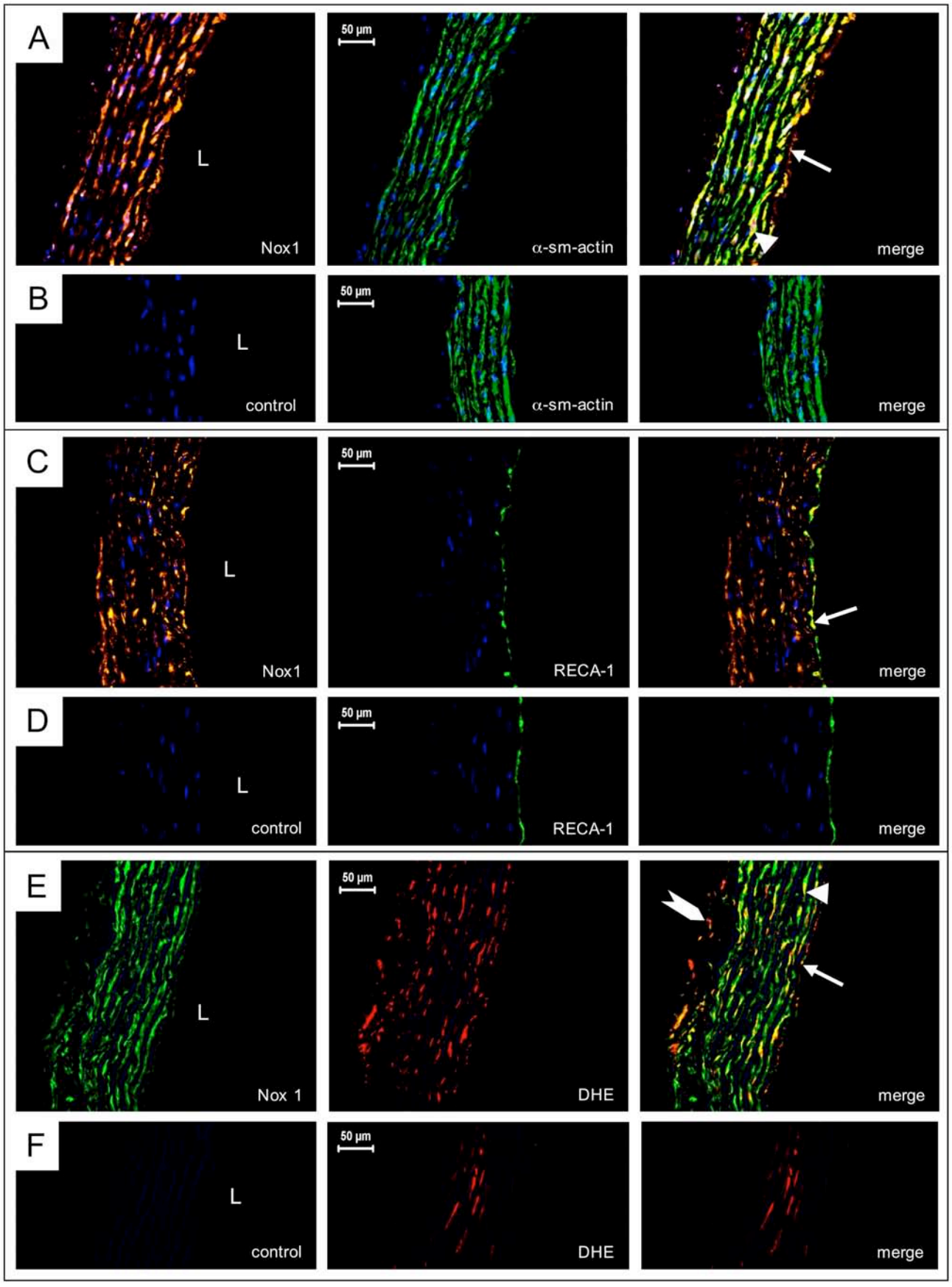
A
L
Nox1
50 µm
α-sm-actin
merge
B
L
control
50 µm
α-sm-actin
merge
C
L
Nox1
50 µm
RECA-1
merge
D
L
control
50 µm
RECA-1
merge
E
L
Nox 1
50 µm
DHE
merge
F
L
control
50 µm
DHE
merge

Figure 5.12: Colocalization of Nox1 protein with α-SM-actin, RECA-1 and oxidized DHE in SHR aortae. Images on the left show the detection of Nox1 (red-orange fluorescence of the Cy3-coupled secondary antibody and green fluorescence of the FITC-coupled secondary antibody, respectively), images in the middle represent the α-SM-actin or RECA-1 labeling (green fluorescence of the FITC-coupled secondary antibody) or the red fluorescence of oxidized DHE. Images on the right show the merge of the stainings. Nox1 and α-SM-actin colocalization in SHR aortae (**A**). Nox1 signals matched with α-SM-actin in the medial layer of SHR aorta (arrowhead), whereas the Nox1 fluorescence in the intima did not match (arrow). Control experiments, where the Nox1 antibody was omitted, indicated the specificity of the immunosignals (**B**). The intimal Nox1 signal matched with RECA-1 labeled EC (arrow, **C**). Control experiments, where the Nox1 antibody was omitted, indicated the specificity of the immunosignals (**D**). Nox1 was localized in ROS producing cells as demonstrated by DHE oxidation (**E**). Immunofluorescence and DHE signals matched in the media (arrowhead) and partly in the intima (arrow) of SHR aortae. However, there were also ROS generating cells showing no Nox1 immunofluorescence, mainly in the adventitia (chevron) and to some extend in the intima of SHR aortae. Control experiments with the secondary FITC-coupled antibody revealed the specifity of the Nox1 signals (**F**). L = lumen. Images are representative for n = 6 animals per group.

5.8 Endothelial function in SHR and WKY aortae

To test the hypothesis that NADPH oxidase-dependent oxidative stress is involved in aortic endothelial dysfunction of SHR, acetylcholine (ACh)-induced endothelium-dependent relaxation was investigated in aortic rings of SHR and WKY. As shown in **Figure 5.13**, the maximal relaxation response to ACh was indeed reduced in SHR aortae (SHR: 56.2 ± 1.1% *versus* WKY: 67.9 ± 2.7% of PE-induced contraction). The NADPH oxidase inhibitors apocynin (100 µM) as well as the novel compound VAS2870 (10 µM) significantly improved the endothelium-dependent relaxation in SHR aortae (77.8 ± 4.9% and 80.8 ± 3.6% of PE-induced contraction, respectively). Remarkably, the maximal relaxation effect to ACh in WKY rats was significantly increased in the presence of apocynin or VAS2870 (79.4 ± 2.2% and 80.2 ± 2.6% of PE-induced contraction, respectively) suggesting that also in this rat strain NADPH oxidases are involved in a reduction of NO bioavailability. However, NADPH oxidase inhibition leads to an increased endothelium-dependent relaxation of about 80% in both strains, which demonstrates that the improvement of relaxation is more pronounced in SHR. In addition, this indicates that indeed NADPH oxidases are involved in the impairment of the relaxation response to ACh in aortae of SHR.

Moreover, VAS2870 and apocynin themselves displayed a strong direct relaxation activity (**Figure 5.14**) in aortic rings. This suggests that NADPH oxidase-derived ROS impede relaxation mechanisms also in the absence of stimuli of NO production. This effect seems to be more pronounced in SHR than in WKY aortae and is in line with a higher basal NADPH oxidase activity in this model. However, the higher relaxation activity in SHR reached significance only for apocynin, probably due to a higher variance that was observed when using VAS2870.

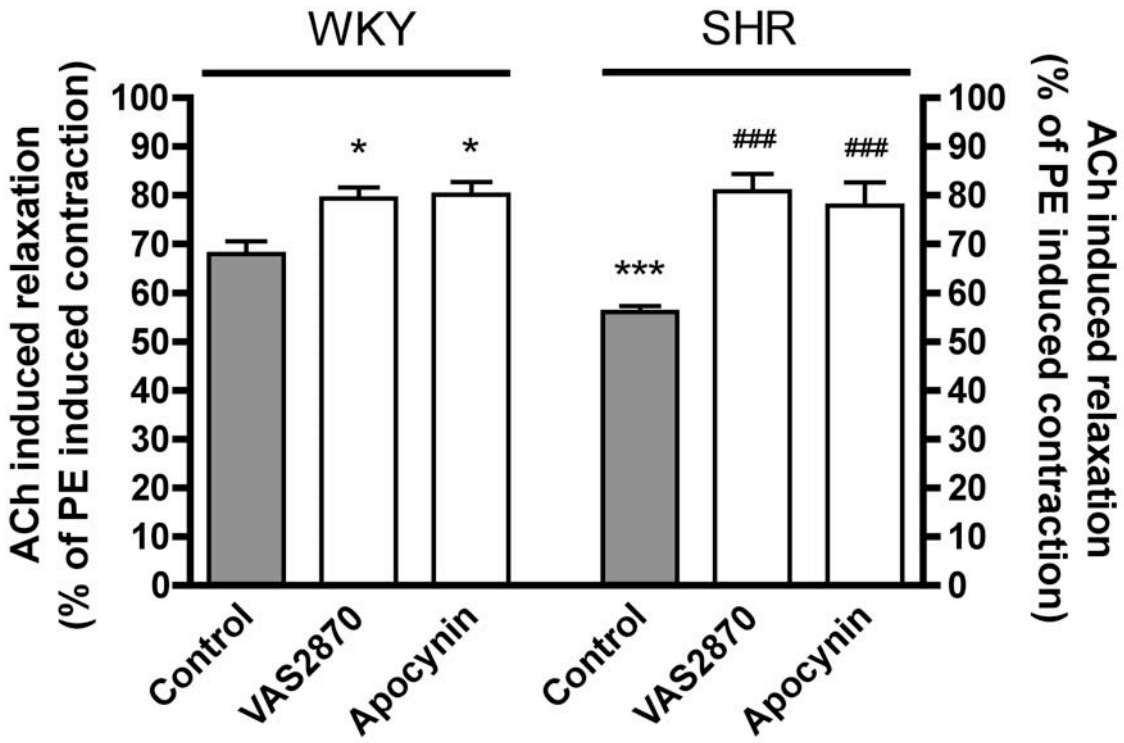

Figure 5.13: VAS2870 and apocynin improved the impaired endothelium-dependent relaxation in SHR aortae. Acetylcholine (ACh)-induced relaxation was significantly impaired in aortic rings of SHR in comparison to WKY (as depicted in the control columns, which represent relaxation in the absence of any compound). The NADPH oxidase inhibitors VAS2870 (10 µM) and apocynin (100 µM) compensated the impaired relaxation response to ACh in SHR, but also led to an enhanced maximal relaxation in WKY aortic rings (values are means ± SEM, $n \geq 5$, *$p<0.05$, ***$p<0.001$ in comparison to WKY control, $^{###}P<0.001$ in comparison to SHR control).

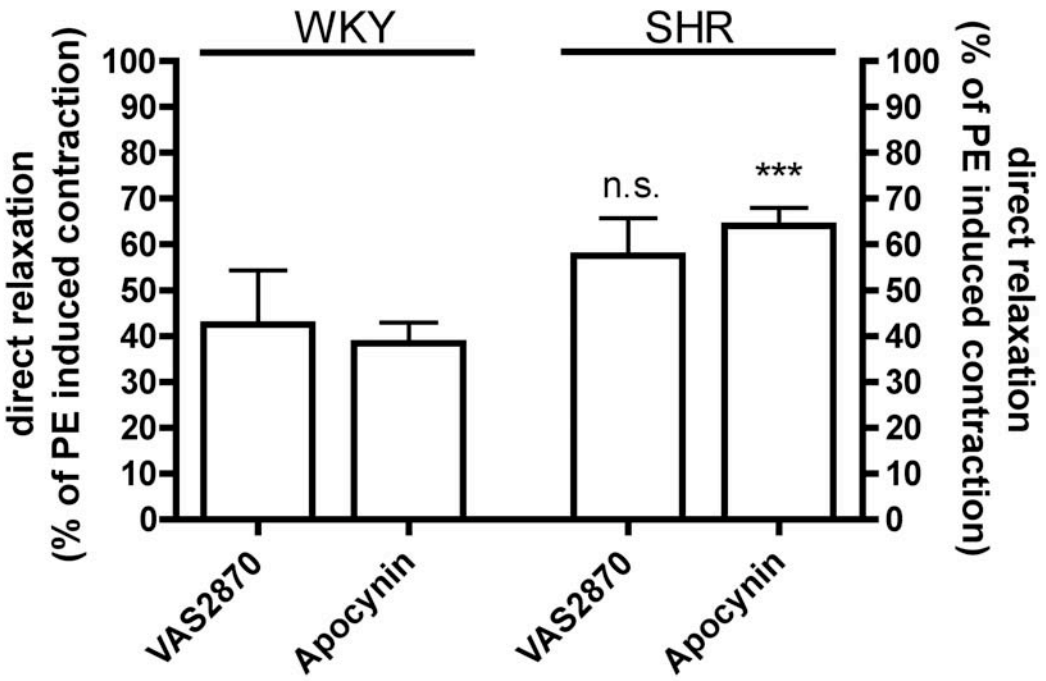

Figure 5.14: Increased direct relaxation induced by NADPH oxidase inhibitors in SHR aortic rings. VAS2870 (10 µM) and apocynin (100 µM) directly dilated aortic rings (42.6 ± 11.8 % and 38.4 ± 4.5% of PE-induced contraction, respectively), an effect that appeared to be more pronounced in SHR rings (57.5 ± 8.2% and 64.0 ± 3.9%, respectively). This increase in relaxation activity was significant for apocynin only (values are presented as means ± SEM, $n \geq 5$, ***$p<0.001$ in comparison to apocynin (WKY))

6 DISCUSSION

6.1 Contribution of NADPH oxidases to oxidative stress in aortae of SHR

Hypertension is accompanied by oxidative stress in the vessel wall whereby NADPH oxidases, uncoupled eNOS and XOD are discussed as relevant sources of ROS generation (Cai & Harrison, 2000). The exact contribution of these individual enzymes is still a matter of debate. Thus, the involvement of these enzymes in aortic ROS production was investigated in aged SHR - an established model of chronic hypertension.

In situ ROS production in rat aortae was detected using dihydroethidium (DHE). Oxidation of DHE results in the formation of ethidium, which binds to DNA and leads to a bright red fluorescence (Rothe & Valet, 1990; Miller et al., 1998; Sorescu et al., 2002). This DHE signal was ~6 times higher in SHR than in WKY indicating increased ROS production in the aorta of these hypertensive animals. This is in line with several studies showing increased aortic superoxide formation measured with lucigenin chemiluminescence in SHR (Zalba et al., 2001; Ulker et al., 2003) as well as SHR-stroke-prone (SHR-SP) rats (Hamilton et al., 2001). Scavenging of superoxide by Tiron and and its dismutation by PEG-SOD reduced the ROS formation in SHR to the levels of WKY suggesting that indeed superoxide is the predominant species responsible for the signal. The NOS inhibitor L-NAME had no effect on DHE fluorescence indicating that uncoupled eNOS does not contribute to aortic ROS production in aged SHR. Oxypurinol which inhibits XOD seemed to slightly suppress the DHE signal, but this effect did not reach statistical significance probably due to the high variance observed in this semi-quantitative assay. However, these data give evidence that XOD plays no or at least only a minor role in aortic ROS production.

In contrast, NADPH oxidase was identified as the main source of ROS generation in the SHR model. On the one hand, the enhanced ROS formation in SHR was reduced to the levels of WKY in presence of DPI, apocynin and VAS2870. On the other hand, NADPH oxidase activity as measured by

NADPH-induced lucigenin chemiluminescence was significantly enhanced in SHR aortae. In this context, it should be mentioned that DPI and VAS2870 appeared to be more potent and more effective than apocynin in suppressing NADPH oxidase-mediated ROS formation in the DHE assay. A reason for this observation may be that a part of the NADPH oxidase activity measured is independent on $p47^{phox}$ translocation, which is suggested to be the targeted event of apocynin (Stolk et al., 1994; Meyer et al., 1999) and thus not inhibitable by apocynin. Furthermore, conversion of apocynin to its active metabolite could be insufficient depending on the conditions used in the assay (Stolk et al., 1994; Cifuentes & Pagano, 2006). However, the difference in efficacy between apocynin and VAS2870 was not significant in the DHE assay and could not be detected in the NADPH oxidase activity assay using lucigenin.

The lucigenin assay revealed a twofold increase of NADPH oxidase activity in SHR aortic homogenates in comparison to WKY, a magnitude of activity that was also found by other groups (Zalba et al., 2000; Ulker et al., 2003). In contrast, the DHE assay revealed a nearly 6-fold increase in ROS production that was mainly caused by NADPH oxidase-derived superoxide. The reason for this discrepancy may be the different detection methods used. The DHE assay is based on the oxidation of DHE to ethidium which binds to DNA and gives a bright red fluorescence (excitation: 500-530 nm; emission: 590-620 nm) (Sorescu et al., 2002). A recent publication showed that superoxide itself reacts with DHE to oxyethidium which represents a different fluorescent product (excitation: 480 nm; emission: 567 nm) and is overlayed by the ethidium fluorescence (Zhao et al., 2003). Since the superoxide scavengers, tiron and PEG-SOD, strongly inhibit the ethidium signal, the formation of ethidum appears to be caused by the reaction with other ROS (Fridovich, 2003), in which superoxide is the progenitor. This *in situ* assay therefore reflects an indirect measure of superoxide. In contrast, lucigenin is suggested to react directly and specifically with superoxide (Munzel et al., 2002). Taken together, these results indicate that the reactive products originating from superoxide are quantitatively more relevant than superoxide itself. Another reason for the observed differences could be that the DHE assay is an *in situ*

detection method whereas the lucigenin assay was performed with homogenates and after addition of high amounts of the substrate, NADPH. Finally, both assays have their limitations. The DHE assay is semi-quantitative and the lucigenin assay, which was performed in a 96-wellplate-reader, is probably not as sensitive as other chemiluminescence-based methods. This could also be the explanation for the relative inefficiency of the superoxide scavengers and NADPH oxidase inhibitors to significantly suppress the basal ROS production in WKY aortae. However, the low signals detected suggest that there is no significant oxidative stress in aortae of these normotensive animals.

In summary, these data suggest that NADPH oxidases are the major source of oxidative stress in the aortae of 12-14 month old SHR rats. The overactivity of this enzyme system in genetic hypertension was also shown in other organs such as mesenteric arteries and the kidney where increased ROS production was accompanied by upregulation of $p47^{phox}$ in the renal vasculature, macula densa and distal nephron (Touyz, 2004). Therefore, NADPH oxidases appear to be involved in ROS-mediated alterations of the cardiovascular system during hypertension and thus represent a promising target for retarding or even reversing these processes.

6.2 Effect of NADPH oxidase inhibition on endothelial function

Endothelial function was assessed by ACh-induced vasorelaxation of phenylephrine precontracted aortic rings. The relaxation response in SHR was significantly impaired in comparison to their normotensive controls indicating that the vascular NO bioavailability is decreased in these animals. Ulker et al. (2003) observed the same in aortae of 22 week old SHR and WKY and could show that preincubation of aortic rings with the antioxidants vitamin C and E prevents the impaired relaxation observed in SHR suggesting the involvement of ROS. Another study described that *in vivo* administration of the antioxidants, vitamins C and E or tempol, reversed the age-related reduction of endothelium-dependent relaxation in 16 month old SHR to the levels

measured in 3 month old SHR. Furthermore, this enhancement of relaxation was eliminated by pre-treatment of the vessels with the eNOS inhibitor L-NAME or an inhibitor of soluble guanylyl cyclase, ODQ (Payne et al., 2003). In summary, the data indicates that oxidative stress-mediated impairment of the NO-cGMP pathway leads to the diminished endothelium-dependent relaxation.

To support the concept of oxidative stress-derived endothelial dysfunction seen in the aorta of SHR, vessels were treated with the NADPH oxidase inhibitors, apocynin and VAS2870, which resulted in a significantly improved vasorelaxation response to ACh. This suggests that NADPH oxidase-derived ROS decrease the endothelium-dependent relaxation by scavenging NO and thereby reducing its bioavailability. In another study similar experiments were performed with other NADPH oxidase inhibitors, namely DPI, PAO and AEBSF (Ulker et al., 2003). As expected, application of DPI impaired the ACh-induced relaxation attributed to the fact that DPI also targets the flavoenzyme eNOS. The observed inefficiency of AEBSF and PAO can be explained by their non-specific actions, since PAO conjugates to vicinal sulfhydryl groups (Vignais, 2002) of many enzymes and AEBSF is a serine protease inhibitor (Diatchuk et al., 1997). In agreement with these results, Hamilton et al. (2002) showed that PAO and AEBSF were not able to increase NO bioavailability in carotid arteries of 9-12 month old WKY and SHR-SP. In contrast, PEG-SOD as well as apocynin were able to significantly improve NO bioavailability in the same study. The present work confirmed these findings for apocynin and, moreover, brings forth the new compound VAS2870 as an effective NADPH oxidase inhibitor that improves the endothelium-dependent aortic relaxation in SHR even in lower concentrations (10 µM) than apocynin (100 µM).

Interestingly, the ACh-induced relaxation in WKY aortae was improved by apocynin and VAS2870, too. An explanation for this observation could be a NADPH oxidase-mediated and age-related development of endothelial dysfunction in these normotensive animals, although less pronounced than in SHR. Importantly, the 12-14 month old WKY rats showed a pronounced obesity (in average 170 g heavier than age-matched SHR), an observation that was also described by other groups (Intengan & Schiffrin, 2000). This

raises the question whether WKY rats can be considered as an appropriate control in studies investigating endothelial dysfunction of SHR; however, it provides an explanation for an impaired relaxation, since it was also shown that obesity is accompanied with ROS-mediated endothelial dysfunction (Viswanad et al., 2006). Another likely possibility could be that NADPH oxidases contribute to the maintainance of vascular tension via counterbalancing the NO production under physiological conditions. Cai and Harrison (2000) hypothesized that there is always some superoxide reacting with NO even under basal conditions. Therefore, inhibition of the enzymatic source of superoxide would lead to an enhanced NO bioavailability and increased NO-mediated vasorelaxation. However, these interpretations remain speculative, since in the present study no significant suppression of ROS generation in WKY aortae could be detected using apocynin as well as VAS2870. The findings of Hamilton and colleagues would favour the second hypothesis for a physiological role of ROS in maintaining vascular tension, because they showed that apocynin improved NO bioavailability in young as well as aged WKY aortae (Hamilton et al., 2002).

Apocynin as well as VAS2870 directly relaxed precontracted aortic rings of WKY and SHR. However, the relaxation response in SHR was more pronounced suggesting that the aortae of these rats exhibits a basal eNOS activity as well as an increased NADPH oxidase activity. This observation is in line with the hypothesis that NO is constantly scavenged by ROS generated by NADPH oxidases. Interestingly, Hamilton et al. (2002) could observe this direct relaxation effect in vessels of patients that underwent coronary artery revascularization and found that the apocynin-induced relaxation is more pronounced in veins than in arteries. However, whether this strong relaxation effect is solely due to prevention of NO scavenging remains to be determined.

6.3 Expression of vascular Nox isoforms in aortae of SHR

The phagocytic NADPH oxidase is a multimeric complex composed of two membrane integrated subunits, the catalytic subunit Nox2 and $p22^{phox}$, and at least three cytosolic proteins, $p47^{phox}$, $p67^{phox}$ and rac1/2 which translocate to the membrane upon activation (Babior, 1999). Vascular NADPH oxidases are structurally different. They contain one of the catalytic Nox homologues Nox1, Nox2 or Nox4 (Lassegue & Clempus, 2003) which all require $p22^{phox}$ for functional activity (Ambasta et al., 2004). The role of the cytosolic NADPH oxidase subunits for the individual Nox1, Nox2 or Nox4-comprising enzyme complexes is not clarified yet. Studies in $p47^{phox}$ knockout-mice gave evidence that this subunit could be involved in pathological ROS production such as found in angiotensin II-mediated hypertension (Landmesser et al., 2002). In aged SHR, expression of the membrane subunit $p22^{phox}$ was found to be upregulated on the mRNA (Zalba et al., 2000) as well as on the protein level (Hamilton et al., 2001) compared to their age-matched WKY controls. However, the role of the individual Nox isoforms in these animals has not been clarified yet and therefore Western blot analysis was performed using antibodies raised against Nox1, Nox2 or Nox4 in the present study. The Nox1 as well as Nox2 protein was significantly upregulated in aortae of SHR, whereas there was no significant change in the level of Nox4 protein. This is the first study which shows that the increased NADPH oxidase activity in SHR is accompanied by increased protein expression of Nox1 and Nox2. Hamilton and colleagues investigated the mRNA expression of Nox1 and Nox2 in young and aged SHR and WKY, but they could not find any statistical differences. This might be due to the low n-number used in their study and the very low expression levels of Nox1 observed (Hamilton et al., 2002). In addition, it becomes apparent that the Nox expression levels differ rather at the protein than at the mRNA level. Furthermore, several studies are in agreement with an increased Nox1 and Nox2 expression in animal models of endothelial dysfunction. For example, angiotensin II infusion in C57B1/6 mice caused a marked upregulation of $p67^{phox}$ and Nox2 protein in the thoracic aorta (Cifuentes et al., 2000). Wistar rats infused for 7 days with angiotensin II

showed an increased Nox1 (6 to 7-fold), Nox2 (3-fold) and $p22^{phox}$ (3-fold) mRNA expression, whereas Nox4 mRNA was only marginally increased (1.5-fold) compared to sham-treated rats (Mollnau et al., 2002). Moreover, aortae of diabetic rats, which exhibit endothelial dysfunction and increased oxidative stress, showed higher Nox1 protein and Nox2 mRNA levels, while Nox4 protein levels remained unchanged in comparison to their respective controls (Hink et al., 2001; Wendt et al., 2005). Finally, a very recent study demonstrated that the endothelial dysfunction that was observed in mice deficient in BKβ1 (a subunit of a large conductance Ca^{2+}-activated K^+-channel) was accompanied by oxidative stress, increased $p67^{phox}$ and Nox1 protein expression and could be normalized by apocynin (Oelze et al., 2006).

Studies in Nox2-deficient mice conducted so far could not clarify the role of this catalytic subunit in hypertension. For example, the published results describing the effect of Nox2 on the basal blood pressure are contradictory (Wang et al., 2001; Touyz et al., 2005). In addition, a role for Nox2 in mediating angiotensin II-induced hypertension could not be demonstrated under acute as well as chronic conditions. Deletion of Nox2 prevented vascular hypertrophy after acutely elevated angiotensin II levels (6 days infusion) (Wang et al., 2001), but not under chronic settings of angiotensin II upregulation (TTRhRen transgenic/Nox2 deficient mice) (Touyz et al., 2005).

The role of Nox1 in angiotensin II-mediated hypertension is highlighted in three recent publications. Dikalova and colleagues showed that in transgenic mice, which overexpress Nox1 in smooth muscle cells, oxidative, pressor and hypertrophic responses to angiotensin II were increased (Dikalova et al., 2005). Matsuno et al. (2005) reported decreased pressor responses to angiotensin II infusion in Nox1-deficient mice due to increased NO bioavailability. In line with this, the endothelium-dependent relaxation was preserved in aortae of knockout mice infused with angiotensin II (Matsuno et al., 2005). Furthermore, there was no change in the basal blood pressure. In contrast to that, Gavazzi and colleagues found that the basal blood pressure was moderately decreased in a different line of Nox1-deficient mice (Gavazzi et al., 2006). Gavazzi et al. (2006) reported further, that the sustained blood pressure response to angiotensin II infusion was lost in the knockout animals

and that aortic media hypertrophy was significantly reduced due to a decrease in extracellular matrix accumulation in comparison to sham treated wild-type mice. In contrast, Matsuno and colleagues did not find any differences in aortic hypertrophy in knockout and wildtype mice that were infused with angiotensin II. The discrepancy between the two studies was explained by the use of animals of different ages and different angiotensin II doses (3 mg/kg/day Gavazzi et al., 0.7 mg/kg/day Matsuno et al.). However, all these studies point to the involvement of Nox1 in endothelial dysfunction and hypertension and are in agreement with a pathological role of increased Nox1 expression in aged SHR observed in the present study. Based on this, it can be proposed that Nox1-derived superoxide scavenges NO and leads to endothelial dysfunction in this model of genetic hypertension. Taking into account the findings of Gavazzi et al. (2006), it can be further assumed that Nox1 is involved in the increased ECM accumulation observed in SHR aortae. In this context, it should be mentioned that ROS have more pathogenic effects than only scavenging NO, e.g. direct regulation of matrix metalloproteinases (Rajagopalan et al., 1996) and VSMC proliferation, processes that are involved in the remodeling of vessels (Taniyama & Griendling, 2003). Nevertheless, the correlation between Nox1 overexpression and ECM accumulation in SHR remains hypothetically and the observed vascular remodeling should rather be considered a multifactorial consequence of the chronic hypertension in these animals.

In contrast to Nox1 and Nox2 protein levels, Nox4 levels were not significantly changed in SHR. Thus, it is tempting to suggest a physiological role for Nox4 in maintaining steady-state levels of ROS. Such a basic function of Nox4 is also supported by the fact that this isoform is highly expressed in endothelial cells (Ago et al., 2004) and VSMC (Wingler et al., 2001). Its activation seems to be independent of cytosolic subunits, in particular $p47^{phox}$ (Martyn et al., 2006), and may therefore not be inhibitable by apocynin. Unlike Nox4, Nox1 and Nox2 preferably mediate stress responses under pathophysiological conditions and therefore represent promising targets for the treatment of vascular diseases. Indeed, a putative therapeutic relevance of targeting Nox1 in vascular diseases was indicated in a recent publication linking the

antioxidative effect of atorvastatin to decreased mRNA expression levels of Nox1 and $p22^{phox}$ in SHR treated with this compound (Wassmann et al., 2002). In contrast to the clearer role of Nox1, the function of increased Nox2 expression remains to be elucidated.

Interestingly, in addition to the expected Nox1 protein band of approximately 60 kD another two bands at the size of 126 kD and 138 kD were observed. These were not detectable when the Nox1 antibody was preincubated with the immunizing peptide suggesting their specificity for Nox1. Since Nox2 was shown to be highly glycosylated, it was tested whether these high molecular weight bands result from a glycosylation of Nox1, but deglycosylation experiments with PNGase F have failed. Another hypothesis could be that the high molecular weight bands resulted from complexes of Nox1, either with itself (homodimers) or possibly with other proteins. Assuming that these high molecular weight bands are really complexes of Nox1, the bonds have to be very strong since neither mercaptoethanol, SDS nor heating were able to cleave them. Such Nox1 derivatives could be storage forms that could also explain why changes in Nox1 expression were observed on a protein but not on a mRNA level. However, further studies have to be carried out to reveal the exact identity and function of these Nox1 positive bands. Current investigations employ low-temperature SDS-PAGE to test whether the stability/formation of the high molecular Nox1 variants is temperature-dependent and MALDI-TOF analysis to reveal the exact composition of these protein bands.

6.4 Localization of Nox isoforms in the aortic wall

NADPH oxidase activity has been detected in all layers of the vasculature. Concomitant, $p22^{phox}$, which has been described to colocalize with Nox1, Nox2 and Nox4, was found in all vascular cells (Brandes & Kreuzer, 2005). However, the distribution of the Nox isoforms is poorly investigated at the protein level in rats. Therefore, immunohistochemical studies were performed

in SHR and WKY aortae using Nox1, Nox2 and Nox4 antibodies. The distribution of Nox isoforms in SHR and WKY was compared and the colocalization of the relevant isoform, Nox1, with specific EC and VSMC markers as well as the signal arising from ROS-mediated DHE fluorescence was studied.

Nox1 was mainly expressed in the media of the aortic wall where it colocalized with α-SM-actin verifying that it is expressed in VSMC. This is in line with several studies showing Nox1 mRNA and protein in isolated rat as well as human VSMC (Lassegue & Clempus, 2003; Hanna et al., 2004). In a recent immunohistochemical study, Nox1 was detected in the aortic media of 5 week old Sprague-Dawley rats confirming this observation (Ago et al., 2005). In a previous publication, Ago et al. (2004) were not able to detect Nox1 in aortic endothelial cells of Sprague Dawley rats. Interestingly, while no or at least very little Nox1 protein was detected in the intima of normotensive WKY in the present study, the Nox1 signal was very strong in the intima of SHR aortae. Colocalization of the Nox1 signal with the endothelial cell marker, RECA-1, demonstrated a SHR-specific expression in EC. Nox1 immunoreactivity was also found in the adventitia of SHR aortae, while it appeared to be absent in the adventitial layer of WKY. However, these adventitial Nox1 fluorescence signal was rather weak and merged with the nuclear staining; therefore the results require cautious interpretation. Altogether it seems that chronic hypertension, as observed in aged SHR, is accompanied by an enhanced Nox1 expression in the media and especially in the intima, while the normotensive WKY controls mainly express Nox1 in the aortic media.

The link between enhanced Nox1 immunofluorescence and increased ROS production was investigated by combining immunohistochemistry of Nox1 with *in situ* detection of ROS using DHE. Nox1 signals matched well with the ROS formation in the media and in the intima of SHR aortae pointing to a significant role of this Nox isoform in oxidative stress and endothelial dysfunction in these animals.

Nox2 was detected in the adventitia and the intima and seemed to be absent in the media. This distribution is in agreement with the localization of Nox2 in

EC (Gorlach et al., 2000) and fibroblasts (Rey & Pagano, 2002), but not in VSMC of conduit vessels (Lassegue & Clempus, 2003). In the present study, only a slight difference in Nox2 expression between SHR and WKY aortae was detected immunohistochemically. In this context it should be mentioned that results of DHE measurements combined with Nox1 immunofluorescence showed areas in the intima and the adventitia of SHR that did not match, while the NADPH oxidase inhibitor VAS2870 suppressed the ROS formation in all layers of the aortic wall. Therefore it can be suggested that the remaining ROS formation that did not colocalize with Nox1 was produced from Nox2-containing NADPH oxidases. This is supported by the upregulation of Nox2 protein in aortic homogenates of SHR in comparison to their WKY controls.

Nox4 protein was found throughout the vessel wall, with a strong signal in the adventitia and in the media, but also some expression in the intima of SHR and WKY aortae. In line with these findings, Nox4 was described to be abundantly expressed in all vascular cells (Brandes & Kreuzer, 2005). Nox4 colocalized with α-SM-actin indicating its expression in VSMC. In mice aortic smooth muscle cells, it was shown that the NADPH oxidase activity largely depended on Nox4 under resting conditions, and proatherogenic stimuli such as IL-β, thrombin and PDGF decreased activity and expression of Nox4 (Ellmark et al., 2005). In rat and human EC, Nox4 was considered to be the major catalytic NADPH oxidase component (Ago et al., 2004). In the present study, the most intensive signals of Nox4 were found in the adventitia of SHR and WKY aortae, while the expression in the EC layer appeared to be comparatively weak. However, quantitative statements concluded from immunohistochemistry have to be cautiously interpreted and should be confirmed by Western blot analysis in future studies. In summary, the abundant expression, which was found in SHR as well as WKY rats, together with the constitutive, stimuli- and subunit-independent activity of Nox4-based NADPH oxidases is suggestive of a physiological role of Nox4 in homeostasis and signaling in vascular cells rather than a pathophysiological role.

6.5 Role of eNOS in aortic endothelial dysfunction of aged SHR

Decreased NO bioavailability is the hallmark of endothelial dysfunction (Cai & Harrison, 2000). It can be a result of either increased scavenging or decreased production of NO (Forstermann, 2006). This study could demonstrate that increased scavenging via NADPH oxidase-derived ROS is a principal cause for endothelial dysfunction in SHR aortae. Furthermore, to investigate whether the expression of eNOS, the NO producing enzyme, is altered, protein expression analysis was perfomed in SHR and WKY aortae. However, no significant differences in protein expression were observed between SHR and normotensive WKY rats; quite to the contrary, eNOS protein expression appeared to be increased. Thus the hypothesis that a decrease in the expression of eNOS contributes to endothelial dysfunction could not be confirmed. This is in line with several other investigations which showed that cardiovascular diseases are associated with an increase in eNOS expression (Vaziri et al., 1998; Hink et al., 2001; Guzik et al., 2002). Likewise in young (Vaziri et al., 1998) and 7 month old SHR rats (Ulker et al., 2003), eNOS expression was found to be significantly upregulated. The increased eNOS expression could serve as an initial compensatory response to hypertension. Since the observed differences in the expression level were only marginal between aged SHR and WKY rats this compensatory effect may be eliminated with age. However, the protein levels of eNOS may also not reflect the activity of the enzyme. Thus eNOS activity in the aortae should be measured in follow up studies.

Another mechanism contributing to endothelial dysfunction is the “uncoupling” of the eNOS enzyme. “Uncoupled” eNOS produces superoxide instead of NO due to a deficiency of its substrate L-arginine, its co-factor BH_4 and/or oxidation of the zinc thiolate cluster of the enzyme (Forstermann, 2006). Since L-NAME did not have any effect on the ROS levels detected with the DHE assay, eNOS “uncoupling” does not seem to be involved in oxidative stress and endothelial dysfunction found in SHR aortae. Some studies have shown that oxidative stress and endothelial dysfunction can be reversed by supplementation with BH_4 in SHR (Hong et al., 2001) and other disease

models (Pieper, 1997; Shinozaki et al., 2000). However, it is difficult to confirm the role of eNOS uncoupling from these studies. On the one hand, BH_4 is a strong antioxidant (Forstermann, 2006) and can therefore combat oxidative stress and improve the endothelial function due to unspecific ROS scavenging effects. On the other hand, if BH_4 specifically targets eNOS, this would result in an increased NO production, which then is in competition with all ROS irrespective of their source of production.

In summary, the data obtained in this study suggest that eNOS does not play a significant role in the oxidative stress and endothelial dysfunction observed in SHR aortae.

6.6 VAS2870, a novel compound in the pharmacology of NADPH oxidases

Although it is generally agreed that NADPH oxidases are an important component responsible for the generation of oxidative stress in numerous diseases, the pharmacology of NADPH oxidases is poorly developed. The compounds used so far to target this enzyme complex are either non-specific and/or mechanistically not well understood. For example, the frequently used substance, DPI, is an inhibitor of all flavoenzymes and thereby potentially inhibits other ROS sources like xanthine oxidase or uncoupled eNOS. Therefore, the application of DPI is limited to *in vitro* assays, where the DPI-inhibitable ROS generation can be specified by the additional use of specific inhibitors of the other flavoenzymes like oxypurinol and L-NAME, respectively. Apocynin, which has also been used in this study, is most frequently applied as a specific inhibitor of NADPH oxidases. The proposed mechanism of action of this vanilloid substance is the prevention of $p47^{phox}$ translocation to the membranic NADPH oxidase subunits. Apocynin is not toxic and possesses a good oral bioavailability and was therefore described as a promising candidate for *in vivo* research and therapeutic applications. However, the use of this compound in the pharmacological research of NADPH oxidases is questionable due to several reasons. For example, two studies have shown

that apocynin increases ROS production in fibroblasts and neuronal cells instead of decreasing it (Riganti et al., 2005; Vejrazka et al., 2005). According to its proposed mechanism of action, apocynin targets the $p47^{phox}$-based NADPH oxidases only and therefore should not interfere with NADPH oxidases that are independent of $p47^{phox}$ like Nox4. However, this could also be a positive aspect, if solely $p47^{phox}$-based NADPH oxidases are involved in the pathology. Moreover, apocynin has to be activated by peroxidases, which probably does not occur in all types of tissues. Furthermore, studies in our lab showed that apocynin interferes with several ROS detection dyes and/or possesses unspecific antioxidant properties. Although this substance was effective in the present study and even in several *in vivo* studies, results obtained with apocynin should always be interpretated with caution due to the reasons described above.

In the present study, the novel NADPH oxidase inhibitor VAS2870 (Tegtmeier F et al., 2005) was investigated and characterized. The compound was effective in suppressing oxidative stress and improving endothelial dysfunction of aged SHR rats. This is the first study showing that VAS2870 is effective in diseased tissue. Very recently Ten Freyhaus et al. (2006) reported that VAS2870 inhibited PDGF-induced NADPH oxidase activity, ROS formation and migration of VSMC that were isolated from the aorta of 6-10 week old WKY rats. In another study, VAS2870 was effective in preventing the oxidized low-density lipoprotein (oxLDL)-mediated ROS formation in primary human umbilical vein EC (HUVEC) (Stielow et al., 2006). Both studies showed the efficiency of VAS2870 in suppressing NADPH oxidase activity in vascular cells while not being toxic at least in the concentrations investigated. While the PDGF-mediated ROS formation in VSMC appears to depend mainly on Nox1 expression (Lassegue et al., 2001; Pleskova et al., 2006), Nox4 is the major isoform in HUVEC (Ago et al., 2004) and was therefore related to the oxLDL-mediated ROS formation (Stielow et al., 2006). Since VAS2870 also inhibited the Nox2-mediated oxidative burst in HL60 cells (Tegtmeier F et al., 2005) and in a cell-free system of human neutrophils (Ten Freyhaus et al., 2006), it is concluded that VAS2870 is not selective for any Nox isoforms. This conclusion can also be drawn from the present study, in which VAS2870

suppressed ROS formation throughout the whole vessel wall of SHR. While Nox1 was shown to colocalize with the ROS formation in the media and partly the intima of SHR aorta, distinct VAS2870 inhibitable ROS formation was found in the adventitia and intima indicating that its sources are Nox2 and/or Nox4.

Own investigations in which the NADPH oxidase inhibitors apocynin, AEBSF and DPI were compared with VAS3947 (3-benzyl-7-(2-oxazolyl)thio-1,2,3-triazolo[4,5-*d*]pyrimidine), a derivative of VAS2870, are in line with such a hypothesis. In this study, VAS3947 suppressed NADPH oxidase activity in different cell lines that predominantly express either Nox1, Nox2 or Nox4 with IC_{50} values in the low µM range. Furthermore, it was shown that VAS3947 has no antioxidative potential and is not a flavoenzyme inhibitor like DPI. The high potency of the VAS compounds is also confirmed in the present study where a concentration of 10 µM VAS2870 was equally effective as 100 µM and 1 mM apocynin, respectively. These high concentrations of apocynin, which are needed to successfully suppress NADPH oxidases, are a further disadvantage of this compound, because the likelihood of unspecific actions increases with concentration. The high potency and apparently high specificity of VAS2870 for NADPH oxidases makes this inhibitor to a very powerful tool in experimental pharmacology. With regard to the therapeutic potential of VAS2870 the unselectivity for the Nox isoforms could be a disadvantage in the treatment of oxidative stress, since inhibition of Nox2 should result in impaired immune function and inhibition of Nox4 which is proposed in cell signaling could potentially lead to the interruption of important physiological pathways. However, the unselectivity could be also an advantage, since several Nox isoforms seem to be involved in vascular pathology including Nox2. Therefore, a modulation rather then a full inhibition of these enzymes and/or a local delivery (e.g. via stents) of the inhibitors should circumvent possible immune-suppressing effects. Moreover, statins which should also inhibit Nox2-based NADPH oxidases were not found to possess side effects like suppression of the immune response.

Future studies should elucidate the mechanism of action of VAS2870, which appears to be different from most of the other NADPH oxidase inhibitors. While substances like apocynin, AEBSF or gp91^{phox} were shown to target the assembly of NADPH oxidase subunits (Stolk et al., 1994; Diatchuk et al., 1997; Rey et al., 2001), it was shown that VAS2870 does not affect PMA stimulated p47^{phox} translocation in human PMNs (Ten Freyhaus et al., 2006). In line with this is the observation that VAS2870 and VAS3947 inhibit NADPH oxidase activity in cells that predominantly express Nox4, since Nox4 was shown to be active independently of p47^{phox} and p67^{phox} (Shiose et al., 2001; Ago et al., 2004). Therefore, it seems likely that VAS2870 directly interacts with the catalytic Nox proteins. As a 1,2,3-triazolo[4,5-*d*]pyrimidine, VAS2870 appears to be structurally related to purines such as guanosine and even more closely to adenosine. Considering this analogy, the NADPH or the FAD binding sides of the Nox proteins appear to be reasonable target points for VAS2870. However, due to the analogy to purines one has to consider that this compound potentially modulates other targets in addition to NADPH oxidases implying supplementary effects in a physiological system. Indeed, 7-amino-derivatives of 1,2,3-triazolo[4,5-d]pyrimidines were already described to possess affinity to A_1 and A_{2A} adenosine receptors (Betti et al., 1998). Additionally, purinoreceptors such as P2X appear to be a potential target, since they are also involved in vascular tone (Judkins et al., 2006) and inhibitors of these receptors were found to inhibit vascular NADPH oxidases (Drummond 2006, unpublished observations). Hence, an interaction of VAS2870 with adenosine and purine receptors should be investigated in future studies.

6.7 Targeting ROS as a treatment of cardiovascular diseases

Many experimental studies suggest that oxidative stress is involved in the pathophysiology of cardiovascular diseases. Animal studies, for the most part, support the fundamental role of ROS in diseases such as atherosclerosis, hypertension, diabetes and restenosis. In line with this, humans with

hypercholesterolemia, hyperhomocysteinemia, diabetes mellitus or renovascular hypertension exhibit increased ROS generation as suggested amongst others by elevated F_2 isoprostane levels (for a review see Griendling & FitzGerald (2003)). Therefore, recent therapeutic approaches have been aimed at combating oxidative stress with antioxidants such as Vitamin E and C. On the whole, clinical trials with antioxidants have been disappointing. For example, the Heart Outcomes Prevention Evaluation (HOPE) study, the Medical Research Council/ British Heart Foundation (MRC/BHF) heart protection study and several other clinical trials failed to demonstrate significant benefits of vitamin E or C supplementation on cardiovascular endpoints. However, from the twelve prospective antioxidant clinical trials published so far, five studies such as the Antioxidant Supplementation in Atherosclerosis Prevention (ASAP) study could demonstrate a positive effect of antioxidant supplementation (for a review, see Jialal and Devaraj (2003) and Singh & Jialal (2006)). Still, overall results of clinical trials are rather sobering in consideration of the promising experimental data. Potential reasons for the failure of these studies have been frequently discussed and centered around inappropriate study designs and investigated patient populations as well as the antioxidants used (Jialal & Devaraj, 2003; Touyz, 2004). Indeed, the most widely examined antioxidants in trials, vitamins E and C, may also have prooxidant properties (Podmore et al., 1998; Abudu et al., 2004). Furthermore, these vitamins mainly react with superoxide by abstracting an electron and converting it into H_2O_2, thereby leaving HOCl unaffected and even increasing H_2O_2 production (Touyz, 2004). It cannot be ruled out that these ROS are more important in mediating vascular damage than superoxide itself. For these reasons, direct inhibition of the ROS sources should be more efficacious in ameliorating oxidative stress than scavenging ROS when they are already present. NADPH oxidases have been identified as the main source of oxidative stress in the present as well as in other studies. Thus, modulating these enzymes with inhibitors such as the novel compound, VAS2870, promises to be more successful in treating diseases mediated by oxidative stress than a treatment with antioxidants like vitamins E and C.

6.8 Future perspectives

The present study provides strong evidence that NADPH oxidases are the major source of oxidative stress and associated endothelial dysfunction in a rat model of progressed genetic hypertension. The catalytic subunit Nox1 appears to possess a predominant role in the NADPH oxidase-mediated oxidative stress. However, an upregulation of Nox1 was only found on the protein level and – in addition to the expected protein band – two high molecular weight variants were detected in the Western blots. Future studies are necessary to elucidate the constitution, formation and relevance of these Nox1 immunoreactive bands. Immunoprecipitation followed by MALDI-TOF analysis as well as low temperature SDS-PAGE should contribute to a more detailed understanding towards the significance of these bands.

VAS2870 was shown to effectively inhibit NADPH oxidase-mediated oxidative stress and thereby to significantly improve endothelial dysfunction in SHR aortae. Considering the need of specific inhibitors of NADPH oxidases and the role of the enzymes in far more diseases than hypertension, VAS2870 may be an interesting model compound for the treatment of diseases associated with oxidative stress and deserves further investigations. Future studies should investigate the mechanism of action, its specifity for NADPH oxidases and whether any possible selectivity for one of the Nox isoforms exists. Activity studies in Nox isoform-overexpressing cells could address such demands. Furthermore, future investigations have to determine the *in vivo* efficacy, the toxicity profile and the pharmacokinetics of VAS2870.

7 SUMMARY

Vascular oxidative stress is associated with a dysfunction of endothelium-dependent relaxation. Inactivation of nitric oxide by superoxide and other reactive oxygen species (ROS) appears to occur under conditions such as diabetes mellitus, hypercholesterolemia or arterial hypertension. NADPH oxidases have been identified as major source of ROS in blood vessels. The present study investigates the role of NADPH oxidases in aortae of 12-14 month old spontaneously hypertensive rats (SHR) in comparison to age-matched Wistar Kyoto rats (WKY).

ROS production was largely increased in aortae of SHR as measured by *in situ* detection of DHE fluorescence. Suppression of ROS formation by the NADPH oxidase inhibitors, apocynin and the novel compound VAS2870, but not by the eNOS inhibitor L-NAME or the xanthine oxidase inhibitor oxypurinol, suggested NADPH oxidases as a major source of oxidative stress. In line with these findings, NADPH oxidase activity in aortic homogenates of SHR was significantly elevated.

NADPH oxidases are multimeric complexes consisting of several cytosolic and two membranic subunits, namely $p22^{phox}$ and a catalytic Nox isoform. In rat aortae, the isoforms Nox1, Nox2 and Nox4 are expressed, which was confirmed by RT-PCR in aortic homogenates of SHR and WKY. Immunohistochemical analysis of the vessels demonstrated a predominant location of Nox1 in the aortic media. Nox2 was localized in the adventitia as well as the intima and Nox4 was located throughout the aortic wall. Quantitative Western blot analysis revealed increased levels of Nox1 and Nox2 protein in SHR aortic homogenates, while Nox4 expression was not significantly changed. Furthermore, Nox1 protein appeared to be upregulated especially in the intima of SHR aortae as indicated by colocalization of Nox1 immunofluorescence with the VSMC marker α-SM-actin and the endothelial cell marker RECA-1. These data suggest that Nox1 and Nox2-based NADPH oxidases are mainly responsible for oxidative stress in the aortic wall of aged SHR.

Acetylcholine-induced endothelial-dependent relaxation was determined to investigate whether the NADPH oxidase-produced oxidative stress is linked to endothelial dysfunction. Vasorelaxation was impaired in aortic rings of SHR in comparison to the WKY controls. However, it was significantly improved in the presence of apocynin and VAS2870 in SHR and to a smaller extent in WKY, indicating the functional relevance of the enhanced NADPH oxidase activity.

In conclusion, Nox1 and Nox2 comprising NADPH oxidases were identified as major sources of oxidative stress in SHR aortae and thus contributed significantly to endothelial dysfunction. Targeting these enzymes therefore promises to be of immense therapeutic relevance. The novel NADPH oxidase inhibitor VAS2870 was shown to effectively suppress the oxidative stress and to improve the endothelial function in SHR. In consequence, the present study highlights VAS2870 as an experimental tool in the pharmacology of NADPH oxidases and – furthermore - as an interesting model compound for the treatment of cardiovascular and other diseases associated with oxidative stress.

8 ZUSAMMENFASSUNG

Vaskulärer oxidativer Stress führt zu einer Beeinträchtigung der endothelabhängigen Gefäßrelaxation. Stickstoffmonoxid scheint unter Bedingungen, wie sie bei Diabetes mellitus, Hypercholesterolämie oder arteriellem Bluthochdruck vorliegen, von Superoxid und anderen reaktiven Sauerstoffspezies (ROS) inaktiviert zu werden. Als Hauptquellen für ROS in Blutgefässen sind NADPH Oxidasen identifiziert worden. Die vorliegende Arbeit untersucht die Rolle von NADPH Oxidasen in Aorten von 12 bis 14 Monate alten spontan-hypertensiven Ratten (SHR) im Vergleich zu gleichaltrigen Wistar Kyoto Ratten (WKY).

Die *in-situ* Detektion von ROS mittels DHE Fluoreszenz zeigte, dass die ROS Produktion in Aorten von SHR stark erhöht ist. Die NADPH Oxidase-Inhibitoren Apocynin und die neue Substanz VAS2870, nicht aber der eNOS-Hemmstoff L-NAME oder der Xanthinoxidase-Inhibitor Oxypurinol unterdrücken diese ROS Bildung, was auf NADPH Oxidasen als Hauptquelle für oxidativen Stress hinweist. Mit diesem Befund einhergehend zeigten SHR Aorten eine erhöhte NADPH Oxidase Aktivität.

NADPH Oxidasen sind Multimer-Komplexe, die aus verschiedenen zytosolischen und zwei membranständigen Untereinheiten, $p22^{phox}$ und einer katalytischen Nox Isoform, bestehen. In Rattenaorten sind die Isoformen Nox1, Nox2 und Nox4 exprimiert, wie mittels RT-PCR in Aortenhomogenaten von SHR und WKY bestätigt wurde. Die immunhistochemische Analyse der Gefässe deutete eine primäre Lokalisation von Nox1 in der Media an, während Nox2 in Adventitia und Intima und Nox4 in der gesamten Aortenwand gefunden wurden. Im Vergleich zu WKY, konnten erhöhte Nox1 und Nox2 Proteinspiegel im SHR-Aortenhomogenat mittels quantitativer Western Blot Analyse nachgewiesen werden, während die Nox4 Expression nicht signifikant verändert war. Weiterhin war die Nox1 Expression im Endothel der SHR Aorten hochreguliert, wie Kolokalisierungsexperimente von Nox1 mit dem glatten Muskelzell-Marker α-SM-actin und dem Endothelzell-spezifischen Marker RECA-1 zeigten. Zusammenfassend weisen diese Daten

darauf hin, dass Nox1 und Nox2-basierte NADPH Oxidasen den oxidativen Stress in der Aortenwand gealteter SHR verursachen.

Um zu untersuchen, ob der durch NADPH Oxidasen hervorgerufene oxidative Stress mit einer endothelialen Dysfunktion der Aorten zusammenhängt, wurde die Azetylcholin-induzierte, endothelabhängige Gefässdilatation bestimmt. In SHR-Aorten war die Relaxation im Vergleich zur WKY Kontrolle beeinträchtigt, konnte aber in Anwesenheit von Apocynin und VAS2870 signifikant verbessert werden. Diese, durch die Inhibitoren bewirkte Verbesserung der Relaxation war in WKY Aorten weniger ausgeprägt, was auf die funktionelle Relevanz der erhöhten NADPH Oxidase Aktivität hindeutet.

Daraus lassen sich folgende Schlussfolgerungen ableiten: Nox1 und Nox2-basierte NADPH Oxidasen wurden als Hauptquellen für oxidativen Stress in SHR Aorten identifiziert und tragen damit signifikant zur endothelialen Dysfunktion bei. Deshalb stellt die Hemmung dieser Enzyme einen vielversprechenden, therapeutischem Ansatz dar. Der neuartige NADPH Oxidase Hemmstoff VAS2870 konnte den oxidativen Stress in SHR Aorten wirksam reduzieren und damit deren endotheliale Funktion verbessern. Somit verdeutlicht die vorliegende Arbeit das Potential von VAS2870 als experimentelles „Tool“ in der Pharmakologie von NADPH Oxidasen. Darüberhinaus stellt VAS2870 auch eine interessante Modellsubstanz für die Behandlung kardiovaskulärer und anderer mit oxidativem Stress assoziierten Erkrankungen dar.

9 REFERENCES

1. Abudu N, Miller JJ, Attaelmannan M and Levinson SS (2004). "Vitamins in human arteriosclerosis with emphasis on vitamin C and vitamin E." Clin Chim Acta 339(1-2): 11-25.

2. Ago T, Kitazono T, Kuroda J, Kumai Y, Kamouchi M, Ooboshi H, Wakisaka M, Kawahara T, Rokutan K, Ibayashi S and Iida M (2005). "NAD(P)H oxidases in rat basilar arterial endothelial cells." Stroke 36(5): 1040-6.

3. Ago T, Kitazono T, Ooboshi H, Iyama T, Han YH, Takada J, Wakisaka M, Ibayashi S, Utsumi H and Iida M (2004). "Nox4 as the major catalytic component of an endothelial NAD(P)H oxidase." Circulation 109(2): 227-33.

4. Ago T, Kuribayashi F, Hiroaki H, Takeya R, Ito T, Kohda D and Sumimoto H (2003). "Phosphorylation of p47phox directs phox homology domain from SH3 domain toward phosphoinositides, leading to phagocyte NADPH oxidase activation." Proc Natl Acad Sci U S A 100(8): 4474-9.

5. Al-Mehdi AB, Zhao G, Dodia C, Tozawa K, Costa K, Muzykantov V, Ross C, Blecha F, Dinauer M and Fisher AB (1998). "Endothelial NADPH oxidase as the source of oxidants in lungs exposed to ischemia or high K+." Circ Res 83(7): 730-7.

6. Alderton WK, Cooper CE and Knowles RG (2001). "Nitric oxide synthases: structure, function and inhibition." Biochem J 357(Pt 3): 593-615.

7. Ambasta RK, Kumar P, Griendling KK, Schmidt HH, Busse R and Brandes RP (2004). "Direct interaction of the novel Nox proteins with p22phox is required for the formation of a functionally active NADPH oxidase." J Biol Chem 279(44): 45935-41.

8. Ambasta RK, Schreiber JG, Janiszewski M, Busse R and Brandes RP (2006). "Noxa1 is a central component of the smooth muscle NADPH oxidase in mice." Free Radic Biol Med 41(2): 193-201.

9. Babior BM (1999). "NADPH oxidase: an update." Blood 93(5): 1464-76.

10. Banfi B, Clark RA, Steger K and Krause KH (2003). "Two novel proteins activate superoxide generation by the NADPH oxidase NOX1." J Biol Chem 278(6): 3510-3.

11. Banfi B, Molnar G, Maturana A, Steger K, Hegedus B, Demaurex N and Krause KH (2001). "A Ca(2+)-activated NADPH oxidase in testis, spleen, and lymph nodes." J Biol Chem 276(40): 37594-601.

12. Barry-Lane PA, Patterson C, van der Merwe M, Hu Z, Holland SM, Yeh ET and Runge MS (2001). "p47phox is required for atherosclerotic lesion progression in ApoE(-/-) mice." J Clin Invest 108(10): 1513-22.

13. Basu K, Dasgupta B, Bhattacharya SK and Debnath PK (1971). "Chemistry and pharmacology of apocynin, isolated from Picrorhiza kurroa Royle ex Benth." Curr. Sci. 22(40): 603-4.

14. Beswick RA, Dorrance AM, Leite R and Webb RC (2001). "NADH/NADPH oxidase and enhanced superoxide production in the mineralocorticoid hypertensive rat." Hypertension 38(5): 1107-11.

15. Betti L, Biagi G, Giannaccini G, Giorgi I, Livi O, Lucacchini A, Manera C and Scartoni V (1998). "Novel 3-aralkyl-7-(amino-substituted)-1,2,3-triazolo[4,5-d]pyrimidines with high affinity toward A1 adenosine receptors." J Med Chem 41(5): 668-73.

16. Brandes RP (2003). "A radical adventure: the quest for specific functions and inhibitors of vascular NAPDH oxidases." Circ Res 92(6): 583-5.

17. Brandes RP and Kreuzer J (2005). "Vascular NADPH oxidases: molecular mechanisms of activation." Cardiovasc Res 65(1): 16-27.

18. Bruckdorfer R (2005). "The basics about nitric oxide." Mol Aspects Med 26(1-2): 3-31.

19. Cai H, Griendling KK and Harrison DG (2003). "The vascular NAD(P)H oxidases as therapeutic targets in cardiovascular diseases." Trends Pharmacol Sci 24(9): 471-8.

20. Cai H and Harrison DG (2000). "Endothelial dysfunction in cardiovascular diseases: the role of oxidant stress." Circ Res 87(10): 840-4.

21. Cardillo C, Kilcoyne CM, Cannon RO, 3rd, Quyyumi AA and Panza JA (1997). "Xanthine oxidase inhibition with oxypurinol improves endothelial vasodilator function in hypercholesterolemic but not in hypertensive patients." Hypertension 30(1 Pt 1): 57-63.

22. Cayatte AJ, Rupin A, Oliver-Krasinski J, Maitland K, Sansilvestri-Morel P, Boussard MF, Wierzbicki M, Verbeuren TJ and Cohen RA (2001). "S17834, a new inhibitor of cell adhesion and atherosclerosis that targets nadph oxidase." Arterioscler Thromb Vasc Biol 21(10): 1577-84.

23. Chan YR, Zanetti M, Gennaro R and Gallo RL (2001). "Anti-microbial activity and cell binding are controlled by sequence determinants in the anti-microbial peptide PR-39." J Invest Dermatol 116(2): 230-5.

24. Cheng G and Lambeth JD (2004). "NOXO1, regulation of lipid binding, localization, and activation of Nox1 by the Phox homology (PX) domain." J Biol Chem 279(6): 4737-42.

25. Cheng G, Ritsick D and Lambeth JD (2004). "Nox3 regulation by NOXO1, p47phox, and p67phox." J Biol Chem 279(33): 34250-5.

26. Cifuentes ME and Pagano PJ (2006). "Targeting reactive oxygen species in hypertension." Curr Opin Nephrol Hypertens 15(2): 179-86.

27. Cifuentes ME, Rey FE, Carretero OA and Pagano PJ (2000). "Upregulation of p67(phox) and gp91(phox) in aortas from angiotensin II-infused mice." Am J Physiol Heart Circ Physiol 279(5): H2234-40.

28. Cosentino F and Luscher TF (1998). "Tetrahydrobiopterin and endothelial function." Eur Heart J 19 Suppl G: G3-8.

29. Dana R, Leto TL, Malech HL and Levy R (1998). "Essential requirement of cytosolic phospholipase A2 for activation of the phagocyte NADPH oxidase." J Biol Chem 273(1): 441-5.

30. De Deken X, Wang D, Many MC, Costagliola S, Libert F, Vassart G, Dumont JE and Miot F (2000). "Cloning of two human thyroid cDNAs encoding new members of the NADPH oxidase family." J Biol Chem 275(30): 23227-33.

31. DeLeo FR, Yu L, Burritt JB, Loetterle LR, Bond CW, Jesaitis AJ and Quinn MT (1995). "Mapping sites of interaction of p47-phox and flavocytochrome b with random-sequence peptide phage display libraries." Proc Natl Acad Sci U S A 92(15): 7110-4.

32. Diatchuk V, Lotan O, Koshkin V, Wikstroem P and Pick E (1997). "Inhibition of NADPH oxidase activation by 4-(2-aminoethyl)-benzenesulfonyl fluoride and related compounds." J Biol Chem 272(20): 13292-301.

33. Dikalova A, Clempus R, Lassegue B, Cheng G, McCoy J, Dikalov S, San Martin A, Lyle A, Weber DS, Weiss D, Taylor WR, Schmidt HH, Owens GK, Lambeth JD and Griendling KK (2005). "Nox1 overexpression potentiates angiotensin II-induced hypertension and vascular smooth muscle hypertrophy in transgenic mice." Circulation 112(17): 2668-76.

34. Ding Y, Chen ZJ, Liu S, Che D, Vetter M and Chang CH (2005). "Inhibition of Nox-4 activity by plumbagin, a plant-derived bioactive naphthoquinone." J Pharm Pharmacol 57(1): 111-6.

35. Droge W (2002). "Free radicals in the physiological control of cell function." Physiol Rev 82(1): 47-95.

36. Ellmark SH, Dusting GJ, Fui MN, Guzzo-Pernell N and Drummond GR (2005). "The contribution of Nox4 to NADPH oxidase activity in mouse vascular smooth muscle." Cardiovasc Res 65(2): 495-504.

37. Fawell S, Seery J, Daikh Y, Moore C, Chen LL, Pepinsky B and Barsoum J (1994). "Tat-mediated delivery of heterologous proteins into cells." Proc Natl Acad Sci U S A 91(2): 664-8.

38. Forstermann U (2006). "Endothelial NO synthase as a source of NO and superoxide." Eur J Clin Pharmacol 62 Suppl 13: 5-12.

39. Fortepiani LA and Reckelhoff JF (2005). "Treatment with tetrahydrobiopterin reduces blood pressure in male SHR by reducing testosterone synthesis." Am J Physiol Regul Integr Comp Physiol 288(3): R733-6.

40. Frederiks WM and Bosch KS (1996). "The proportion of xanthine oxidase activity of total xanthine oxidoreductase activity in situ remains constant in rat liver under various (patho)physiological conditions." Hepatology 24(5): 1179-84.

41. Frey RS, Rahman A, Kefer JC, Minshall RD and Malik AB (2002). "PKCzeta regulates TNF-alpha-induced activation of NADPH oxidase in endothelial cells." Circ Res 90(9): 1012-9.

42. Fridovich I (1998). "Oxygen toxicity: a radical explanation." J Exp Biol 201(Pt 8): 1203-9.

43. Fridovich I (2003). "Editorial commentary on "Superoxide reacts with hydroethidine but forms a fluorescent product that is distinctly different from ethidium: potential implications in intracellular fluorescence detection of superoxide" by H. Zhao et al." Free Radic Biol Med 34(11): 1357-8.

44. Fukui T, Ishizaka N, Rajagopalan S, Laursen JB, Capers Qt, Taylor WR, Harrison DG, de Leon H, Wilcox JN and Griendling KK (1997). "p22phox mRNA expression and NADPH oxidase activity are increased in aortas from hypertensive rats." Circ Res 80(1): 45-51.

45. Gavazzi G, Banfi B, Deffert C, Fiette L, Schappi M, Herrmann F and Krause KH (2006). "Decreased blood pressure in NOX1-deficient mice." FEBS Lett 580(2): 497-504.

46. Geiszt M, Kopp JB, Varnai P and Leto TL (2000). "Identification of renox, an NAD(P)H oxidase in kidney." Proc Natl Acad Sci U S A 97(14): 8010-4.

47. Gorlach A, Brandes RP, Nguyen K, Amidi M, Dehghani F and Busse R (2000). "A gp91phox containing NADPH oxidase selectively expressed in endothelial cells is a major source of oxygen radical generation in the arterial wall." Circ Res 87(1): 26-32.

48. Granger DN, Rutili G and McCord JM (1981). "Superoxide radicals in feline intestinal ischemia." Gastroenterology 81(1): 22-9.

49. Griendling KK and FitzGerald GA (2003). "Oxidative stress and cardiovascular injury: Part II: animal and human studies." Circulation 108(17): 2034-40.

50. Griendling KK, Sorescu D and Ushio-Fukai M (2000). "NAD(P)H oxidase: role in cardiovascular biology and disease." Circ Res 86(5): 494-501.

51. Groemping Y, Lapouge K, Smerdon SJ and Rittinger K (2003). "Molecular basis of phosphorylation-induced activation of the NADPH oxidase." Cell 113(3): 343-55.

52. Groemping Y and Rittinger K (2005). "Activation and assembly of the NADPH oxidase: a structural perspective." Biochem J 386(Pt 3): 401-16.

53. Gryglewski RJ, Palmer RM and Moncada S (1986). "Superoxide anion is involved in the breakdown of endothelium-derived vascular relaxing factor." Nature 320(6061): 454-6.

54. Guzik TJ, Mussa S, Gastaldi D, Sadowski J, Ratnatunga C, Pillai R and Channon KM (2002). "Mechanisms of increased vascular superoxide production in human diabetes mellitus: role of NAD(P)H oxidase and endothelial nitric oxide synthase." Circulation 105(14): 1656-62.

55. Hamilton CA, Brosnan MJ, Al-Benna S, Berg G and Dominiczak AF (2002). "NAD(P)H oxidase inhibition improves endothelial function in rat and human blood vessels." Hypertension 40(5): 755-62.

56. Hamilton CA, Brosnan MJ, McIntyre M, Graham D and Dominiczak AF (2001). "Superoxide excess in hypertension and aging: a common cause of endothelial dysfunction." Hypertension 37(2 Part 2): 529-34.

57. Han CH, Freeman JL, Lee T, Motalebi SA and Lambeth JD (1998). "Regulation of the neutrophil respiratory burst oxidase. Identification of an activation domain in p67(phox)." J Biol Chem 273(27): 16663-8.

58. Hanna IR, Hilenski LL, Dikalova A, Taniyama Y, Dikalov S, Lyle A, Quinn MT, Lassegue B and Griendling KK (2004). "Functional association of nox1 with p22phox in vascular smooth muscle cells." Free Radic Biol Med 37(10): 1542-9.

59. Harrison DG (1997). "Endothelial function and oxidant stress." Clin Cardiol 20(11 Suppl 2): II-11-7.

60. Harrison R (2002). "Structure and function of xanthine oxidoreductase: where are we now?" Free Radic Biol Med 33(6): 774-97.

61. Hink U, Li H, Mollnau H, Oelze M, Matheis E, Hartmann M, Skatchkov M, Thaiss F, Stahl RA, Warnholtz A, Meinertz T, Griendling K, Harrison DG, Forstermann U and Munzel T (2001). "Mechanisms underlying endothelial dysfunction in diabetes mellitus." Circ Res 88(2): E14-22.

62. Hong HJ, Hsiao G, Cheng TH and Yen MH (2001). "Supplemention with tetrahydrobiopterin suppresses the development of hypertension in spontaneously hypertensive rats." Hypertension 38(5): 1044-8.

63. Ikeda Y, Young LH, Scalia R, Ross CR and Lefer AM (2001). "PR-39, a proline/arginine-rich antimicrobial peptide, exerts cardioprotective effects in myocardial ischemia-reperfusion." Cardiovasc Res 49(1): 69-77.

64. Intengan HD and Schiffrin EL (2000). "Structure and mechanical properties of resistance arteries in hypertension: role of adhesion molecules and extracellular matrix determinants." Hypertension 36(3): 312-8.

65. Ischiropoulos H, Zhu L, Chen J, Tsai M, Martin JC, Smith CD and Beckman JS (1992). "Peroxynitrite-mediated tyrosine nitration catalyzed by superoxide dismutase." Arch Biochem Biophys 298(2): 431-7.

66. Jacobson GM, Dourron HM, Liu J, Carretero OA, Reddy DJ, Andrzejewski T and Pagano PJ (2003). "Novel NAD(P)H oxidase inhibitor suppresses angioplasty-induced superoxide and neointimal hyperplasia of rat carotid artery." Circ Res 92(6): 637-43.

67. Jialal I and Devaraj S (2003). "Antioxidants and atherosclerosis: don't throw out the baby with the bath water." Circulation 107(7): 926-8.

68. Jiang F, Drummond GR and Dusting GJ (2004). "Suppression of oxidative stress in the endothelium and vascular wall." Endothelium 11(2): 79-88.

69. Johnson DK, Schillinger KJ, Kwait DM, Hughes CV, McNamara EJ, Ishmael F, O'Donnell RW, Chang MM, Hogg MG, Dordick JS, Santhanam L, Ziegler LM and Holland JA (2002). "Inhibition of NADPH oxidase activation in endothelial cells by ortho-methoxy-substituted catechols." Endothelium 9(3): 191-203.

70. Jones SA, O'Donnell VB, Wood JD, Broughton JP, Hughes EJ and Jones OT (1996). "Expression of phagocyte NADPH oxidase components in human endothelial cells." Am J Physiol 271(4 Pt 2): H1626-34.

71. Judkins CP, Sobey CG, Dang TT, Miller AA, Dusting GJ and Drummond GR (2006). "NADPH-induced contractions of mouse aorta do not involve NADPH oxidase: a role for P2X receptors." J Pharmacol Exp Ther 317(2): 644-50.

72. Kalinina N, Agrotis A, Tararak E, Antropova Y, Kanellakis P, Ilyinskaya O, Quinn MT, Smirnov V and Bobik A (2002). "Cytochrome b558-dependent NAD(P)H oxidase-phox units in smooth muscle and macrophages of atherosclerotic lesions." Arterioscler Thromb Vasc Biol 22(12): 2037-43.

73. Kawahara T, Ritsick D, Cheng G and Lambeth JD (2005). "Point mutations in the proline-rich region of p22phox are dominant inhibitors of Nox1- and Nox2-dependent reactive oxygen generation." J Biol Chem 280(36): 31859-69.

74. Kerr S, Brosnan MJ, McIntyre M, Reid JL, Dominiczak AF and Hamilton CA (1999). "Superoxide anion production is increased in a model of genetic hypertension: role of the endothelium." Hypertension 33(6): 1353-8.

75. Kojda G and Harrison D (1999). "Interactions between NO and reactive oxygen species: pathophysiological importance in atherosclerosis, hypertension, diabetes and heart failure." Cardiovasc Res 43(3): 562-71.

76. Kojima S, Nomura T, Icho T, Kajiwara Y, Kitabatake K and Kubota K (1993). "Inhibitory effect of neopterin on NADPH-dependent superoxide-generating oxidase of rat peritoneal macrophages." FEBS Lett 329(1-2): 125-8.

77. Krotz F, Sohn HY and Pohl U (2004). "Reactive oxygen species: players in the platelet game." Arterioscler Thromb Vasc Biol 24(11): 1988-96.

78. Laemmli UK (1970). "Cleavage of structural proteins during the assembly of the head of bacteriophage T4." Nature 227(5259): 680-5.

79. Lambeth JD (2002). "Nox/Duox family of nicotinamide adenine dinucleotide (phosphate) oxidases." Curr Opin Hematol 9(1): 11-7.

80. Lambeth JD (2004). "NOX enzymes and the biology of reactive oxygen." Nat Rev Immunol 4(3): 181-9.

81. Landmesser U, Cai H, Dikalov S, McCann L, Hwang J, Jo H, Holland SM and Harrison DG (2002). "Role of p47(phox) in vascular oxidative stress and hypertension caused by angiotensin II." Hypertension 40(4): 511-5.

82. Landmesser U, Dikalov S, Price SR, McCann L, Fukai T, Holland SM, Mitch WE and Harrison DG (2003). "Oxidation of tetrahydrobiopterin leads to uncoupling of endothelial cell nitric oxide synthase in hypertension." J Clin Invest 111(8): 1201-9.

83. Langenstroer P and Pieper GM (1992). "Regulation of spontaneous EDRF release in diabetic rat aorta by oxygen free radicals." Am J Physiol 263(1 Pt 2): H257-65.

84. Lassegue B and Clempus RE (2003). "Vascular NAD(P)H oxidases: specific features, expression, and regulation." Am J Physiol Regul Integr Comp Physiol 285(2): R277-97.

85. Lassegue B, Sorescu D, Szocs K, Yin Q, Akers M, Zhang Y, Grant SL, Lambeth JD and Griendling KK (2001). "Novel gp91(phox) homologues in vascular smooth muscle cells: nox1 mediates angiotensin II-induced superoxide formation and redox-sensitive signaling pathways." Circ Res 88(9): 888-94.

86. Laursen JB, Somers M, Kurz S, McCann L, Warnholtz A, Freeman BA, Tarpey M, Fukai T and Harrison DG (2001). "Endothelial regulation of vasomotion in apoE-deficient mice: implications for interactions between peroxynitrite and tetrahydrobiopterin." Circulation 103(9): 1282-8.

87. Lavigne MC, Malech HL, Holland SM and Leto TL (2001). "Genetic demonstration of p47phox-dependent superoxide anion production in murine vascular smooth muscle cells." Circulation 104(1): 79-84.

88. Li JM and Shah AM (2002). "Intracellular localization and preassembly of the NADPH oxidase complex in cultured endothelial cells." J Biol Chem 277(22): 19952-60.

89. Li JM and Shah AM (2003). "Mechanism of endothelial cell NADPH oxidase activation by angiotensin II. Role of the p47phox subunit." J Biol Chem 278(14): 12094-100.

90. Li WG, Miller FJ, Jr., Zhang HJ, Spitz DR, Oberley LW and Weintraub NL (2001). "H(2)O(2)-induced O(2) production by a non-phagocytic NAD(P)H oxidase causes oxidant injury." J Biol Chem 276(31): 29251-6.

91. Lowry OH, Rosebrough NJ, Farr AL and Randall RJ (1951). "Protein measurement with the Folin phenol reagent." J Biol Chem 193(1): 265-75.

92. Majander A, Finel M and Wikstrom M (1994). "Diphenyleneiodonium inhibits reduction of iron-sulfur clusters in the mitochondrial NADH-ubiquinone oxidoreductase (Complex I)." J Biol Chem 269(33): 21037-42.

93. Martyn KD, Frederick LM, von Loehneysen K, Dinauer MC and Knaus UG (2006). "Functional analysis of Nox4 reveals unique characteristics compared to other NADPH oxidases." Cell Signal 18(1): 69-82.

94. Maru Y, Nishino T and Kakinuma K (2005). "Expression of Nox genes in rat organs, mouse oocytes, and sea urchin eggs." DNA Seq 16(2): 83-8.

95. Matsuno K, Yamada H, Iwata K, Jin D, Katsuyama M, Matsuki M, Takai S, Yamanishi K, Miyazaki M, Matsubara H and Yabe-Nishimura C (2005). "Nox1 is involved in angiotensin II-mediated hypertension: a study in Nox1-deficient mice." Circulation 112(17): 2677-85.

96. McCord JM (1985). "Oxygen-derived free radicals in postischemic tissue injury." N Engl J Med 312(3): 159-63.

97. Melov S, Doctrow SR, Schneider JA, Haberson J, Patel M, Coskun PE, Huffman K, Wallace DC and Malfroy B (2001). "Lifespan extension and rescue of spongiform encephalopathy in superoxide dismutase 2 nullizygous mice treated with superoxide dismutase-catalase mimetics." J Neurosci 21(21): 8348-53.

98. Meyer JW, Holland JA, Ziegler LM, Chang MM, Beebe G and Schmitt ME (1999). "Identification of a functional leukocyte-type NADPH oxidase in human endothelial cells:a potential atherogenic source of reactive oxygen species." Endothelium 7(1): 11-22.

99. Miller FJ, Jr., Gutterman DD, Rios CD, Heistad DD and Davidson BL (1998). "Superoxide production in vascular smooth muscle contributes to oxidative stress and impaired relaxation in atherosclerosis." Circ Res 82(12): 1298-305.

100. Milstien S and Katusic Z (1999). "Oxidation of tetrahydrobiopterin by peroxynitrite: implications for vascular endothelial function." Biochem Biophys Res Commun 263(3): 681-4.

101. Miyamoto Y, Akaike T, Yoshida M, Goto S, Horie H and Maeda H (1996). "Potentiation of nitric oxide-mediated vasorelaxation by xanthine oxidase inhibitors." Proc Soc Exp Biol Med 211(4): 366-73.

102. Mollnau H, Wendt M, Szocs K, Lassegue B, Schulz E, Oelze M, Li H, Bodenschatz M, August M, Kleschyov AL, Tsilimingas N, Walter U, Forstermann U, Meinertz T, Griendling K and Munzel T (2002). "Effects of angiotensin II infusion on the expression and function of NAD(P)H oxidase and components of nitric oxide/cGMP signaling." Circ Res 90(4): E58-65.

103. Moorhouse PC, Grootveld M, Halliwell B, Quinlan JG and Gutteridge JM (1987). "Allopurinol and oxypurinol are hydroxyl radical scavengers." FEBS Lett 213(1): 23-8.

104. Moreno JC, Bikker H, Kempers MJ, van Trotsenburg AS, Baas F, de Vijlder JJ, Vulsma T and Ris-Stalpers C (2002). "Inactivating mutations in the gene for thyroid oxidase 2 (THOX2) and congenital hypothyroidism." N Engl J Med 347(2): 95-102.

105. Mueller CF, Laude K, McNally JS and Harrison DG (2005). "ATVB in focus: redox mechanisms in blood vessels." Arterioscler Thromb Vasc Biol 25(2): 274-8.

106. Mugge A, Elwell JH, Peterson TE, Hofmeyer TG, Heistad DD and Harrison DG (1991). "Chronic treatment with polyethylene-glycolated superoxide dismutase partially restores endothelium-dependent vascular relaxations in cholesterol-fed rabbits." Circ Res 69(5): 1293-300.

107. Munzel T, Afanas'ev IB, Kleschyov AL and Harrison DG (2002). "Detection of superoxide in vascular tissue." Arterioscler Thromb Vasc Biol 22(11): 1761-8.

108. Nakazono K, Watanabe N, Matsuno K, Sasaki J, Sato T and Inoue M (1991). "Does superoxide underlie the pathogenesis of hypertension?" Proc Natl Acad Sci U S A 88(22): 10045-8.

109. Nishida S, Yoshida LS, Shimoyama T, Nunoi H, Kobayashi T and Tsunawaki S (2005). "Fungal metabolite gliotoxin targets flavocytochrome b558 in the activation of the human neutrophil NADPH oxidase." Infect Immun 73(1): 235-44.

110. O'Donnell VB and Freeman BA (2001). "Interactions between nitric oxide and lipid oxidation pathways: implications for vascular disease." Circ Res 88(1): 12-21.

111. Oelze M, Warnholtz A, Faulhaber J, Wenzel P, Kleschyov AL, Coldewey M, Hink U, Pongs O, Fleming I, Wassmann S, Meinertz T, Ehmke H, Daiber A and Munzel T (2006). "NADPH Oxidase Accounts for Enhanced Superoxide Production and Impaired Endothelium-Dependent Smooth Muscle Relaxation in BK{beta}1-/- Mice." Arterioscler Thromb Vasc Biol.

112. Ohara Y, Peterson TE and Harrison DG (1993). "Hypercholesterolemia increases endothelial superoxide anion production." J Clin Invest 91(6): 2546-51.

113. Paffenholz R, Bergstrom RA, Pasutto F, Wabnitz P, Munroe RJ, Jagla W, Heinzmann U, Marquardt A, Bareiss A, Laufs J, Russ A, Stumm G, Schimenti JC and Bergstrom DE (2004). "Vestibular defects in head-tilt mice result from mutations in Nox3, encoding an NADPH oxidase." Genes Dev 18(5): 486-91.

114. Pagano PJ, Chanock SJ, Siwik DA, Colucci WS and Clark JK (1998). "Angiotensin II induces p67phox mRNA expression and NADPH oxidase superoxide generation in rabbit aortic adventitial fibroblasts." Hypertension 32(2): 331-7.

115. Park JB, Touyz RM, Chen X and Schiffrin EL (2002). "Chronic treatment with a superoxide dismutase mimetic prevents vascular remodeling and progression of hypertension in salt-loaded stroke-prone spontaneously hypertensive rats." Am J Hypertens 15(1 Pt 1): 78-84.

116. Parks DA, Williams TK and Beckman JS (1988). "Conversion of xanthine dehydrogenase to oxidase in ischemic rat intestine: a reevaluation." Am J Physiol 254(5 Pt 1): G768-74.

117. Patterson C, Ruef J, Madamanchi NR, Barry-Lane P, Hu Z, Horaist C, Ballinger CA, Brasier AR, Bode C and Runge MS (1999). "Stimulation of a vascular smooth muscle cell NAD(P)H oxidase by thrombin. Evidence that p47(phox) may participate in forming this oxidase in vitro and in vivo." J Biol Chem 274(28): 19814-22.

118. Payne JA, Reckelhoff JF and Khalil RA (2003). "Role of oxidative stress in age-related reduction of NO-cGMP-mediated vascular relaxation in SHR." Am J Physiol Regul Integr Comp Physiol 285(3): R542-51.

119. Peterson GL (1977). "A simplification of the protein assay method of Lowry et al. which is more generally applicable." Anal Biochem 83(2): 346-56.

120. Pieper GM (1997). "Acute amelioration of diabetic endothelial dysfunction with a derivative of the nitric oxide synthase cofactor, tetrahydrobiopterin." J Cardiovasc Pharmacol 29(1): 8-15.

121. Pieper GM, Langenstroer P and Siebeneich W (1997). "Diabetic-induced endothelial dysfunction in rat aorta: role of hydroxyl radicals." Cardiovasc Res 34(1): 145-56.

122. Pleskova M, Beck KF, Behrens MH, Huwiler A, Fichtlscherer B, Wingerter O, Brandes RP, Mulsch A and Pfeilschifter J (2006). "Nitric oxide down-regulates the expression of the catalytic NADPH oxidase subunit Nox1 in rat renal mesangial cells." Faseb J 20(1): 139-41.

123. Podmore ID, Griffiths HR, Herbert KE, Mistry N, Mistry P and Lunec J (1998). "Vitamin C exhibits pro-oxidant properties." Nature 392(6676): 559.

124. Pou S, Pou WS, Bredt DS, Snyder SH and Rosen GM (1992). "Generation of superoxide by purified brain nitric oxide synthase." J Biol Chem 267(34): 24173-6.

125. Rajagopalan S, Kurz S, Munzel T, Tarpey M, Freeman BA, Griendling KK and Harrison DG (1996). "Angiotensin II-mediated hypertension in the rat increases vascular superoxide production via membrane NADH/NADPH oxidase activation. Contribution to alterations of vasomotor tone." J Clin Invest 97(8): 1916-23.

126. Rajagopalan S, Meng XP, Ramasamy S, Harrison DG and Galis ZS (1996). "Reactive oxygen species produced by macrophage-derived foam cells regulate the activity of vascular matrix metalloproteinases in vitro. Implications for atherosclerotic plaque stability." J Clin Invest 98(11): 2572-9.

127. Rey FE, Cifuentes ME, Kiarash A, Quinn MT and Pagano PJ (2001). "Novel competitive inhibitor of NAD(P)H oxidase assembly attenuates vascular O(2)(-) and systolic blood pressure in mice." Circ Res 89(5): 408-14.

128. Rey FE, Li XC, Carretero OA, Garvin JL and Pagano PJ (2002). "Perivascular superoxide anion contributes to impairment of endothelium-dependent relaxation: role of gp91(phox)." Circulation 106(19): 2497-502.

129. Rey FE and Pagano PJ (2002). "The reactive adventitia: fibroblast oxidase in vascular function." Arterioscler Thromb Vasc Biol 22(12): 1962-71.

130. Rhee SG (2006). "Cell signaling. H2O2, a necessary evil for cell signaling." Science 312(5782): 1882-3.

131. Riganti C, Costamagna C, Bosia A and Ghigo D (2005). "The NADPH oxidase inhibitor apocynin (acetovanillone) induces oxidative stress." Toxicol Appl Pharmacol.

132. Rodriguez-Iturbe B, Zhan CD, Quiroz Y, Sindhu RK and Vaziri ND (2003). "Antioxidant-rich diet relieves hypertension and reduces renal immune infiltration in spontaneously hypertensive rats." Hypertension 41(2): 341-6.

133. Romeis B (1989). Mikroskopische Technik. Munich, Urban und Schwarzenberg.

134. Rothe G and Valet G (1990). "Flow cytometric analysis of respiratory burst activity in phagocytes with hydroethidine and 2',7'-dichlorofluorescin." J Leukoc Biol 47(5): 440-8.

135. Schmidt HH and Walter U (1994). "NO at work." Cell 78(6): 919-25.

136. Shi J, Ross CR, Leto TL and Blecha F (1996). "PR-39, a proline-rich antibacterial peptide that inhibits phagocyte NADPH oxidase activity by binding to Src homology 3 domains of p47 phox." Proc Natl Acad Sci U S A 93(12): 6014-8.

137. Shinozaki K, Nishio Y, Okamura T, Yoshida Y, Maegawa H, Kojima H, Masada M, Toda N, Kikkawa R and Kashiwagi A (2000). "Oral administration of tetrahydrobiopterin prevents endothelial dysfunction and vascular oxidative stress in the aortas of insulin-resistant rats." Circ Res 87(7): 566-73.

138. Shiose A, Kuroda J, Tsuruya K, Hirai M, Hirakata H, Naito S, Hattori M, Sakaki Y and Sumimoto H (2001). "A novel superoxide-producing NAD(P)H oxidase in kidney." J Biol Chem 276(2): 1417-23.

139. Simons JM, Hart BA, Ip Vai Ching TR, Van Dijk H and Labadie RP (1990). "Metabolic activation of natural phenols into selective oxidative burst agonists by activated human neutrophils." Free Radic Biol Med 8(3): 251-8.

140. Singh U and Jialal I (2006). "Oxidative stress and atherosclerosis." Pathophysiology 13(3): 129-42.

141. Sorescu D, Weiss D, Lassegue B, Clempus RE, Szocs K, Sorescu GP, Valppu L, Quinn MT, Lambeth JD, Vega JD, Taylor WR and Griendling KK (2002). "Superoxide production and expression of nox family proteins in human atherosclerosis." Circulation 105(12): 1429-35.

142. Stielow C, Catar RA, Muller G, Wingler K, Scheurer P, Schmidt HH and Morawietz H (2006). "Novel Nox inhibitor of oxLDL-induced reactive oxygen species formation in human endothelial cells." Biochem Biophys Res Commun 344(1): 200-5.

143. Stocker R and Keaney JF, Jr. (2004). "Role of oxidative modifications in atherosclerosis." Physiol Rev 84(4): 1381-478.

144. Stolk J, Hiltermann TJ, Dijkman JH and Verhoeven AJ (1994). "Characteristics of the inhibition of NADPH oxidase activation in neutrophils by apocynin, a methoxy-substituted catechol." Am J Respir Cell Mol Biol 11(1): 95-102.

145. Suh YA, Arnold RS, Lassegue B, Shi J, Xu X, Sorescu D, Chung AB, Griendling KK and Lambeth JD (1999). "Cell transformation by the superoxide-generating oxidase Mox1." Nature 401(6748): 79-82.

146. Suzuki H, Swei A, Zweifach BW and Schmid-Schonbein GW (1995). "In vivo evidence for microvascular oxidative stress in spontaneously hypertensive rats. Hydroethidine microfluorography." Hypertension 25(5): 1083-9.

147. Tanaka K, Fujimoto Y, Suzuki M, Suzuki Y, Ohtake T, Saito H and Kohgo Y (2001). "PI3-kinase p85alpha is a target molecule of proline-rich antimicrobial peptide to suppress proliferation of ras-transformed cells." Jpn J Cancer Res 92(9): 959-67.

148. Taniyama Y and Griendling KK (2003). "Reactive oxygen species in the vasculature: molecular and cellular mechanisms." Hypertension 42(6): 1075-81.

149. Tegtmeier F WU, Schinzel R, Wingler K, Scheurer P, Schmidt HHHW (2005). Compounds containing a N-heteroaryl moiety linked to fused ring moieties for the inhibition of NAD(P)H oxidases and platelet activation. EP 1 598 354 A1.

150. Ten Freyhaus H, Huntgeburth M, Wingler K, Schnitker J, Baumer AT, Vantler M, Bekhite MM, Wartenberg M, Sauer H and Rosenkranz S (2006). "Novel Nox inhibitor VAS2870 attenuates PDGF-dependent smooth muscle cell chemotaxis, but not proliferation." Cardiovasc Res 71(2): 331-41.

151. Thomson L, Trujillo M, Telleri R and Radi R (1995). "Kinetics of cytochrome c2+ oxidation by peroxynitrite: implications for superoxide measurements in nitric oxide-producing biological systems." Arch Biochem Biophys 319(2): 491-7.

152. Touyz RM (2004). "Reactive oxygen species, vascular oxidative stress, and redox signaling in hypertension: what is the clinical significance?" Hypertension 44(3): 248-52.

153. Touyz RM, Chen X, Tabet F, Yao G, He G, Quinn MT, Pagano PJ and Schiffrin EL (2002). "Expression of a functionally active gp91phox-containing neutrophil-type NAD(P)H oxidase in smooth muscle cells from human resistance arteries: regulation by angiotensin II." Circ Res 90(11): 1205-13.

154. Touyz RM, Mercure C, He Y, Javeshghani D, Yao G, Callera GE, Yogi A, Lochard N and Reudelhuber TL (2005). "Angiotensin II-dependent chronic hypertension and cardiac hypertrophy are unaffected by gp91phox-containing NADPH oxidase." Hypertension 45(4): 530-7.

155. Tsunawaki S, Yoshida LS, Nishida S, Kobayashi T and Shimoyama T (2004). "Fungal metabolite gliotoxin inhibits assembly of the human respiratory burst NADPH oxidase." Infect Immun 72(6): 3373-82.

156. Ulker S, McKeown PP and Bayraktutan U (2003). "Vitamins reverse endothelial dysfunction through regulation of eNOS and NAD(P)H oxidase activities." Hypertension 41(3): 534-9.

157. Ulker S, McMaster D, McKeown PP and Bayraktutan U (2003). "Impaired activities of antioxidant enzymes elicit endothelial dysfunction in spontaneous hypertensive rats despite enhanced vascular nitric oxide generation." Cardiovasc Res 59(2): 488-500.

158. Vaziri ND, Ni Z and Oveisi F (1998). "Upregulation of renal and vascular nitric oxide synthase in young spontaneously hypertensive rats." Hypertension 31(6): 1248-54.

159. Vejrazka M, Micek R and Stipek S (2005). "Apocynin inhibits NADPH oxidase in phagocytes but stimulates ROS production in non-phagocytic cells." Biochim Biophys Acta 1722(2): 143-7.

160. Vignais PV (2002). "The superoxide-generating NADPH oxidase: structural aspects and activation mechanism." Cell Mol Life Sci 59(9): 1428-59.

161. Virdis A, Neves MF, Amiri F, Touyz RM and Schiffrin EL (2004). "Role of NAD(P)H oxidase on vascular alterations in angiotensin II-infused mice." J Hypertens 22(3): 535-42.

162. Viswanad B, Srinivasan K, Kaul CL and Ramarao P (2006). "Effect of tempol on altered angiotensin II and acetylcholine-mediated vascular responses in thoracic aorta isolated from rats with insulin resistance." Pharmacol Res 53(3): 209-15.

163. Wang HD, Xu S, Johns DG, Du Y, Quinn MT, Cayatte AJ and Cohen RA (2001). "Role of NADPH oxidase in the vascular hypertrophic and oxidative stress response to angiotensin II in mice." Circ Res 88(9): 947-53.

164. Wassmann S, Laufs U, Muller K, Konkol C, Ahlbory K, Baumer AT, Linz W, Bohm M and Nickenig G (2002). "Cellular antioxidant effects of atorvastatin in vitro and in vivo." Arterioscler Thromb Vasc Biol 22(2): 300-5.

165. Wendt MC, Daiber A, Kleschyov AL, Mulsch A, Sydow K, Schulz E, Chen K, Keaney JF, Jr., Lassegue B, Walter U, Griendling KK and Munzel T (2005). "Differential effects of diabetes on the expression of the gp91phox homologues nox1 and nox4." Free Radic Biol Med 39(3): 381-91.

166. White CR, Darley-Usmar V, Berrington WR, McAdams M, Gore JZ, Thompson JA, Parks DA, Tarpey MM and Freeman BA (1996). "Circulating plasma xanthine oxidase contributes to vascular dysfunction in hypercholesterolemic rabbits." Proc Natl Acad Sci U S A 93(16): 8745-9.

167. Wilcox JN, Subramanian RR, Sundell CL, Tracey WR, Pollock JS, Harrison DG and Marsden PA (1997). "Expression of multiple isoforms of nitric oxide synthase in normal and atherosclerotic vessels." Arterioscler Thromb Vasc Biol 17(11): 2479-88.

168. Wingler K, Wunsch S, Kreutz R, Rothermund L, Paul M and Schmidt HH (2001). "Upregulation of the vascular NAD(P)H-oxidase isoforms Nox1 and Nox4 by the renin-angiotensin system in vitro and in vivo." Free Radic Biol Med 31(11): 1456-64.

169. Zalba G, Beaumont FJ, San Jose G, Fortuno A, Fortuno MA and Diez J (2001). "Is the balance between nitric oxide and superoxide altered in spontaneously hypertensive rats with endothelial dysfunction?" Nephrol Dial Transplant 16 Suppl 1: 2-5.

170. Zalba G, Beaumont FJ, San Jose G, Fortuno A, Fortuno MA, Etayo JC and Diez J (2000). "Vascular NADH/NADPH oxidase is involved in enhanced superoxide production in spontaneously hypertensive rats." Hypertension 35(5): 1055-61.

171. Zalba G, San Jose G, Beaumont FJ, Fortuno MA, Fortuno A and Diez J (2001). "Polymorphisms and promoter overactivity of the p22(phox) gene in vascular smooth muscle cells from spontaneously hypertensive rats." Circ Res 88(2): 217-22.

172. Zhao H, Kalivendi S, Zhang H, Joseph J, Nithipatikom K, Vasquez-Vivar J and Kalyanaraman B (2003). "Superoxide reacts with hydroethidine but forms a fluorescent product that is distinctly different from ethidium: potential implications in intracellular fluorescence detection of superoxide." Free Radic Biol Med 34(11): 1359-68.

173. Zou MH, Shi C and Cohen RA (2002). "Oxidation of the zinc-thiolate complex and uncoupling of endothelial nitric oxide synthase by peroxynitrite." J Clin Invest 109(6): 817-26.

10 ACKNOWLEDGEMENTS

I owe immensely to many people who have made it possible for me to come this far and finally finish this work culminating into a thesis. Expressing my gratitude to the following people in my mother tongues seems sensible.

Meinem Betreuer **Herrn Prof. Dr. H.H.H.W Schmidt** danke ich herzlich für seine Unterstützung und ständige Bereitschaft, meine Projekte zu diskutieren, was stets neue Sichtweisen und Denkansätze hervorbrachte. Weiterhin schätzte ich überaus die Unabhängigkeit, die er mir gewährte, und die Förderung meiner wissenschaftlichen und persönlichen Weiterentwicklung.

Herrn Prof. Dr. Dr. J. Krieglstein danke ich sehr für die Übernahme des Koreferates und die Möglichkeit zur Diskussion meiner Ergebnisse.

Dr. Knut Beuerlein schulde ich große Dankbarkeit sowohl auf wissenschaftlicher als auch persönlicher Ebene. Methodisch machte er mich mit der Histologie und der Immunhistochemie vertraut und fungierte auch bei dem „wissenschaftlichen Arbeiten“ als Vorbild. Unzählige Diskussionen, für die er stets zur Verfügung stand, bereicherten meinen Erfahrungsschatz.
Ähnliches gilt für **Dr. Thomas Eucker**, der mich die Prinzipien der Molekularbiologie lehrte. Die anregenden Diskussionen auf dem Gebiet der Musik und der psychoaktiven Substanzen sollen hier nicht unerwähnt bleiben, da sie meinen Horizont erweiterten. Knut, Thomas: Danke für Eure Geduld und Euer Vertrauen in mich, ohne das ich wohl nicht so weit gekommen wäre!

Den weltbesten TAs **Petra Kronich** und **Helmut Müller** danke ich sowohl für die professionelle Unterstützung meiner Projekte als auch für das angenehme und freundliche Arbeitsklima, das ich während meines Doktorandendaseins sehr genossen habe. Für leider zu kurze Zeit gesellte sich noch **Bärbel Fühler** dazu, die Petra und Helmut in Professionalität und Freundlichkeit in nichts nach stand.

Dr. Sanchaita Sonar danke ich sehr für ihre Freundschaft und stetige Hilfsbereitschaft während unserer gemeinsamen Doktorandenzeit. Viele Gespräche bereicherten mein Leben und meinen Englischwortschatz.

Dr. Arun Kumar und **Dr. Ashraf Taye** danke ich für viele fruchtbare, wissenschaftliche Diskussionen und für ihre Freundschaft, die hoffentlich über alle Ländergrenzen lange erhalten bleibt.

Allen weiteren Kollegen aus der Schmidt-Arbeitsgruppe, besonders **Dr.med cand. Daniel Janowitz** und **Dr. Pavel Nedvetsky (und Familie)**, danke ich für die Kameradschaft und tollen Erlebnisse einer gemeinsamen Zeit, an die ich mich gerne zurückerinnere.

Ich danke weiterhin **Dr. Kirstin Wingler**, die mir bei vielen wissenschaftlichen Fragen sehr gute Hilfestellungen gab und ausserdem die Substanz VAS2870 zur Verfügung stellte.

Außerdem möchte ich allen Mitarbeitern des Rudolf-Buchheim-Instituts danken. Hervorzuheben ist hier **Herr Prof. Dr. Florian Dreyer**, der mir die Fertigstellung der Doktorarbeit mit viel Geduld ermöglichte und ausserdem, wie auch **Herr Prof. Dr. Hansjörg Teschemacher**, ein wertvoller Gesprächspartner bezüglich Pharmakologie und Lehre war.
Heike Schubert und **Ulrike Moll**, dem „office-team“ des RBI, danke ich für die Organisation und Hilfe bei den vielen nicht-wissenschaftlichen Angelegenheiten, die während der Erstellung einer Dissertation anfallen.

Dem **Sonderforschungsbereich SFB 547 „Kardiopulmonales Gefäßsystem“** danke ich für die finanzielle Unterstützung meiner Arbeit.

Schliesslich schulde ich einen besonderen Dank meiner Frau **Alexandra**, die mit mir die Höhen und Tiefen einer Doktorarbeit durchlitt und mir dabei stets ein einfühlsamer und aufbauender Partner war. Genauso möchte ich dem Rest meiner **Familie und meinen Freunden** für die liebe Unterstützung in diesem Lebensabschnitt danken. Aus meinem Freundeskreis möchte ich besonders **Michael Basseler**, der mir ein wertvoller Freund in Gießen wurde und sowohl sportlich als auch mental zum Gelingen dieser Arbeit beitrug, als auch **Dr. Lea-Ann Dailey**, die die finale Durchsicht dieser Arbeit leistete, hervorheben.

11 CURRICULUM VITAE

Personal data

Name:	Sven Wind	
Date of birth:	May 9, 1977	
Place of birth:	Dillenburg	Nationality: German
Martial status:	Married	

Dissertation

Since 02/2003	Dissertation under the supervision of Prof. Dr. Harald HHW Schmidt at Rudolf-Buchheim-Institute of Pharmacology, Justus-Liebig-University, Giessen

University education

1997-2001	Study of Pharmaceutical Sciences, Philipps-University, Marburg/Lahn
2001-2002	Practical training at the Department of Pharmaceutics and Pharmaceutical Chemistry, University of Utah, Salt Lake City (USA)
2002	Practical training at Reventlow-Apotheke, Hamburg
12/2002	license to practice as a pharmacist („Approbation zum Apotheker“)

Community service

1996-1997 Ottfried-Preussler-Schule (school for physically and mentaly handicaped children)

School education

1983-1987 Comprehensive School, Manderbach

1987-1996 Wilhelm-von-Oranien-Gymnasium, Dillenburg

Professional activities

Member of Deutsche Pharmazeutische Gesellschaft (DPhG)

Publications

Reviews

Wind S, Kumar AHS (**2005**). “Apocynin: Mother Nature’s gift to combat oxidative stress” Phcog Mag 1(4): 136-39

Contributions to conferences

Wind S, Kronich P, Müller H, Schmidt HHHW (**2004**). “Nitric oxide signaling components and NAD(P)H oxidase isoforms as *in vitro* targets of purple grape products in vascular cells“ Naunyn-Schmiedebergs Arch Pharmacol 369(Suppl 1): R98 (Mainz, Germany).

Taye A, **Wind S**, Hein L, Schmidt HHHW (**2004**). "Differential effects of angiotensin II receptors AT_{1A} and AT_2 on vasomotor activity and Nox expression in aorta from AT_{1A} or AT_2 receptor-deficient mice." Naunyn-Schmiedebergs Arch Pharmacol 369(Suppl 1): R97 (Mainz, Germany).

Wind S, Kronich P, Müller H, Schmidt HHHW (**2004**). "Downregulation of Nox4 as potential protective mechanism of purple grape products in vascular cells". 2nd international conference on NADPH oxidases (Atlanta, USA).

Taye A**, Wind S**, Schmidt HHHW (**2004**). "Downregulation of vascular Nox1/4 in AT1a receptor-deficient mice leads to reduced nitrative stress and enhanced endothelium-dependent relaxation". 2nd international conference on NADPH oxidases (Atlanta, USA).

Taye A**, Wind S**, Hein L, Schmidt HHHW (**2004**). "Divergent effects of AT_1 and AT_2 receptors on vascular function involve Nox-dependent oxidative stress and NO-dependent guanylyl cyclase". 70th Annual Meeting of the German Cardiac Society (Mannheim, Germany).

Taye A**, Wind S**, Hein L, Schmidt HHHW (**2004**) "Divergent effects of AT_{1A} and AT_2 receptors on NO signaling." 9. NO-Forum der deutschsprachigen Länder (Mainz, Germany)

Wind S, Taye A, Beuerlein K, Eucker T, Kronich P, Kumar AHS, Geyer H, Wingler K and Schmidt HHHW (**2006**) "Oxidative stress and endothelial dysfunction in aged spontaneously hypertensive rats can be reversed by inhibition of NADPH oxidase." Naunyn Schmiedebergs Arch Pharmacol. 372(Suppl 1): 92 (Mainz, Germany)

Wind S, Taye A, Beuerlein K, Eucker T, Janowitz D, Schmidt HHHW (**2006**) „Novel NADPH oxidase inhibitor reverses endothelial dysfunction in a model of essential hypertension" DPhG Doktorandentagung (Nürnberg-Heroldsberg, Germany)

12 ERKLÄRUNG

Ich versichere, dass ich meine Dissertation

„Pharmacological and biochemical studies on the contribution of NADPH oxidases to oxidative stress in the aorta of spontaneously hypertensive rats”

selbständig, ohne unerlaubte Hilfe angefertigt und mich dabei keiner anderen als der von mir ausdrücklich bezeichneten Quellen und Hilfen bedient habe.

Die Dissertation wurde in der jetzigen oder einer ähnlichen Form noch bei keiner anderen Hochschule eingereicht und hat noch keinen sonstigen Prüfungszwecken gedient.

Marburg, den _____ _____

Sven Wind